

UNIVERSIDADE DE LISBOA
FACULDADE DE CIÊNCIAS
DEPARTAMENTO DE FÍSICA



Ciências
ULisboa

Development of Cellulose-Based Hydrogels for Personal Care Applications

Beatriz dos Santos Simões

Mestrado em Engenharia Biomédica e Biofísica

Dissertação orientada por:
Professora Doutora Brígida Ferreira
Professor Doutor Arménio Serra

Resumo

Os produtos de higiene pessoal, essenciais na sociedade atual servem propósitos relacionados com limpeza, embelezamento e cuidados com a aparência do utilizador. Os polímeros superabsorventes (SAPs) desenvolvidos primeiramente no Japão em 1979 revolucionaram o setor destes produtos, introduzindo novos materiais no sector. Os SAPs são capazes de absorver mais de 1000 vezes o seu peso seco e reter elevadas quantidades de fluídos. Assim, tornaram-se indispensáveis em produtos de higiene absorventes, como fraldas, produtos de higiene feminina e produtos de incontinência, onde é necessário a existência de materiais que permitam a retenção eficaz de grandes quantidades de fluído e, ao mesmo tempo, previnam o derrame e ofereçam conforto ao utilizador.

Atualmente, os SAPs disponíveis no mercado são, na sua maioria, derivados de petróleo e, portanto, não são biodegradáveis, nem renováveis. Os produtos de higiene descartáveis representam entre 2 e 7% dos resíduos sólidos urbanos na Europa e a maioria destes produtos têm como destino de fim de vida útil, aterros ou incineradores. Para além disso, estes materiais levam centenas de anos para se degradar completamente, agravam as emissões de poluentes e o acúmulo de resíduos a longo prazo. Assim, estes produtos de higiene de uso único acarretam um grande impacto ambiental e contribuem significativamente para a pegada ambiental do Humano. Além dos problemas ambientais, os componentes químicos presentes nos SAPs convencionais também despertam preocupações em relação à saúde humana. Substâncias como o ácido acrílico, a acrilamida e seus derivados, conhecidas pela sua potencial toxicidade podem estar amplamente presentes e, quando em contato prolongado com a pele, como é o caso de fraldas e materiais absorventes, estas substâncias podem provocar irritações cutâneas e toxicidade a longo prazo. A crescente conscientização dos impactos ambientais e de saúde relacionados com a utilização de polímeros superabsorventes não biodegradáveis em produtos de cuidados pessoais tem levado a uma procura por alternativas mais sustentáveis e biodegradáveis.

Neste sentido, a celulose, o biopolímero mais abundante na natureza, emerge como uma alternativa promissora para a produção de hidrogéis superabsorventes. A celulose é uma substância natural renovável, presente em plantas, árvores e outras fontes vegetais, que representa uma solução sustentável para o desenvolvimento de materiais com menor impacto ambiental. Além de ser abundante, a celulose apresenta propriedades intrínsecas propícias para a formulação de hidrogéis, como a hidrofilicidade, biocompatibilidade e biodegradabilidade. Estas propriedades tornam-a uma excelente opção para substituir os SAPs derivados de petróleo, contribuindo para a redução da pegada ambiental e dos riscos para a saúde humana associados aos itens de higiene descartáveis.

Este estudo focou-se no desenvolvimento de hidrogéis à base de celulose para aplicação em produtos de higiene pessoal, especialmente em fraldas. O objetivo é tirar proveito das propriedades intrínsecas da celulose e produzir um material superabsorvente que combine eficácia na absorção de fluídos com sustentabilidade ambiental. Foram produzidos hidrogéis através da copolimerização da celulose com monómeros de tipo acrilatos e foi realizado um estudo de otimização do desempenho desses hidrogéis através da investigação vários parâmetros que influenciam diretamente a capacidade de absorção dos

hidrogéis, propriedade crucial quando se fala de produtos superabsorventes. Entre os parâmetros estudados encontra-se o agente de reticulação, o método de secagem, a densidade de reticulação, a proporção de monômeros e a proporção entre a celulose e os monômeros.

Para a caracterização final, os hidrogéis com propriedades de retenção de água mais promissoras foram preparados em diferentes formas para simular condições reais. No entanto, observou-se que também este parâmetro tem efeito na capacidade absorção dos hidrogéis. Hidrogéis partidos manualmente atingiram um equilíbrio entre máxima capacidade de absorção e cinética de inchaço mais rápida, embora não tenham superado a capacidade de inchaço em água (70 g/g) de hidrogéis quando cortados em formas circulares de 2 cm de diâmetro, que alcançou um valor de 102 g/g.

Após a otimização de todos esses parâmetros, as formulações consideradas mais promissoras foram submetidas a uma caracterização detalhada das suas propriedades térmicas, capacidade de inchaço (em água destilada, urina sintética, e soluções tampão de pH 4 e pH 8), capacidade de retenção de líquidos, capacidade de absorção sob pressão e capacidade de retenção após centrifugação. As propriedades de biocompatibilidade dos hidrogéis também foram avaliadas de forma a garantir a sua segurança e adequação ao uso em produtos de cuidados pessoais. Como controle positivo, foi utilizado material absorvente isolado de fraldas descartáveis comercialmente disponíveis e as suas propriedades comparadas com as dos hidrogéis produzidos.

Os resultados indicam que os hidrogéis desenvolvidos demonstraram notáveis capacidades de absorção atingindo valores de retenção promissoras tanto em água destilada (69,9 g/g) como em urina sintética (14,0 g/g). Essa formulação também superou os resultados dos SAPs de fraldas descartáveis em termos de capacidade de retenção de líquidos, após uma avaliação do seu desempenho ao longo de um período de 8 horas. Além disso, nos testes de retenção centrífuga e absorção sob pressão os hidrogéis produzidos atingiram 12,5 g/g e 6,1 g/g, respectivamente. Embora estes resultados ainda não superem os SAPs de fraldas descartáveis, exceto em relação à capacidade de retenção, a pequena diferença observada nos testes de inchamento em urina sintética entre os hidrogéis (14,0 g/g) e os SAPs das fraldas (20,7 g/g) sugerem que os hidrogéis de celulose têm um grande potencial para substituir os SAPs convencionais. Os hidrogéis produzidos obtiveram resultados de capacidade de inchaço superiores a outros superabsorventes à base de celulose reportados na literatura, bem como, materiais superabsorventes de fraldas comercialmente disponíveis.

Em relação às propriedades térmicas, os hidrogéis produzidos apresentaram menor peso residual a 600 °C e maior estabilidade térmica, com temperaturas T_{95} e T_{90} mais altas em comparação ao material absorvente das fraldas. Os elevados níveis de resíduos dos materiais absorventes das fraldas indicam a presença de componentes inorgânicos e não combustíveis, que colocam desafios ambientais a nível de gestão e reciclagem destes materiais.

Adicionalmente, os testes de citotoxicidade realizados confirmaram que os hidrogéis além de se ter destacado nas propriedades de retenção de fluídos, também são biocompatíveis, uma vez que a viabilidade celular foi superior a 75%, sendo assim classificada como não citotóxica de acordo com a norma ISO 10993-5:1999. Em contrapartida, os SAPs de fraldas descartáveis demonstraram uma viabilidade celular inferior a 75% no ensaio MTS, o que levanta preocupações quanto à compatibilidade com a pele e à segurança do uso prolongado desses materiais.

Com base nos resultados obtidos, o estudo provou que os hidrogéis à base de celulose são uma alternativa promissora aos polímeros superabsorventes convencionalmente utilizados em fraldas e produtos de higiene pessoal. No entanto, ainda existem desafios a serem superados, nomeadamente em termos de propriedades de inchaço, para que os hidrogéis à base de celulose atendam às exigências de absorção e retenção exigidas para a aplicação mencionada. As suas propriedades de biocompatibilidade

demonstraram-se promissoras, uma vez que os hidrogéis produzidos com celulose superaram os SAPs convencionais derivados de petróleo, que, além de não serem biodegradáveis, apresentaram toxicidade celular. Em suma, os avanços conseguidos provaram que os hidrogéis de celulose têm um grande potencial para substituir os SAPs não biodegradáveis, apresentando-se como uma solução mais sustentável e segura não só para o meio ambiente como também a saúde humana. Assim sendo, uma otimização contínua das propriedades dos hidrogéis à base de celulose, poderá trazer inúmeras vantagens e, futuramente, revolucionar a indústria de produtos de higiene pessoal.

Palavras chave: Hidrogéis à base de celulose, Biodegradável, Polímeros superabsorventes, Produtos de Higiene Pessoal, Sustentabilidade

Abstract

The environmental and health impacts of non-biodegradable superabsorbent polymers (SAPs) in personal care products have become a growing concern, since the majority of these are synthetic-based polymers. Although these SAPs can absorb more 1000 times their dry weight, their non-biodegradability and potential health risks, especially derived from prolonged contact, rise environmental and health concerns. This study aims the development cellulose-based hydrogels by taking advantage of biocompatibility, biodegradability, and hydrophilicity properties of cellulose. Cellulose was copolymerized with alternative monomers and an investigation on several parameters that influence absorption capacity was carried out in order to obtain greater absorption capacities. The parameters included cellulose degree of substitution (DS), crosslinking density, monomers ratio, cellulose:monomers ratio, drying method, hydrogel preparation method, and fluid salinity. The most promising hydrogels demonstrated remarkable absorption capacities for synthetic urine (14.0 g/g), as well as, holding centrifuge retention (12.5 g/g), and underload capacities (6.2 g/g). Also, their non-cytotoxic nature showed potential, with produced hydrogels outperforming traditional diaper absorbent materials in biocompatibility. These hydrogels present a sustainable alternative to conventional SAPs, promoting reduced health risks while advancing the development of biodegradable personal care products. Furthermore, continuous improvements of these hydrogels properties could revolutionize the industry of hygiene products.

Keywords: Cellulose-based hydrogels, Biodegradable, Personal Care Products, Superabsorbent polymers, Sustainability

Acknowledgments

Firstly, I would like to dedicate this dissertation to my parents and brother. Thank you for your unconditional support. Your constant presence and encouragement have been indispensable throughout all my life. Also, I want to thank you for your constant encouragement in pursuing my dreams and life goals.

I would also like to thank Professor Brígida Ferreira for all her help and advice during my masters journey, in particular, during the dissertation. Further, I would like to express my greater gratitude to Professor Arménio Serra and the PolySys Investigation Group for the warm welcome during my stay in Coimbra and always showing availability to assist me. These past months have turned me into a more capable and prepared person to tackle future challenges in my professional path.

A special thanks to Rafael Rebelo for working with me throughout the entire project, continuously striving for improvement. I would also like to thank Sofia Saraiva and Teresa Costa for making my days in the laboratory lighter and more fun, as well as for always being there to listen when things weren't going so well in the research.

I cannot forget to thank my friends, especially João Sequinho and Juliana Azevedo, for accompanying me up to this point, making my university journey so much more enjoyable, and being there in difficult times. Thank you for always showing me the true meaning of friendship.

Last but not least, I want to thank my boyfriend, Nuno, for always standing by me with love and support and believing in me, even when I doubted myself. Also, without you, Coimbra would not be Coimbra. Thank you for always making everything better.

Table of Contents

Resumo	iii
Abstract	vii
Acknowledgments	ix
List of Figures	xv
List of Tables	xix
List of Acronyms/Abbreviations	xxi
1 Introduction	1
1.1 Context and Motivation	1
1.2 Objective	1
1.3 Scope and Significance of the Study	2
2 State of the Art	3
2.1 Personal Care Products	3
2.1.1 Types of Personal Care Products	4
2.1.2 Absorbent Hygiene Products	4
2.1.3 Superabsorbent Materials in Personal Care Products	7
2.1.3.1 Hydrogels	7
2.1.3.2 Types of Hydrogels	8
2.1.3.3 Hydrogels properties	9
2.1.4 Impacts of Personal Care Products	10
2.1.4.1 Health Impact	10
2.1.4.2 Environmental Impact	11
2.2 Natural-based Superabsorbents Polymers	11
2.2.1 Cellulose and Cellulose-based Absorbents	11
2.2.1.1 Cellulose Structure and Properties	13
2.2.1.2 Synthesis of Cellulose-based Hydrogels	14
2.2.1.3 Applications of Cellulose-based Hydrogels	17
2.3 Suitability of Cellulose-based Hydrogels for Personal Care Products	17

3	Materials and Methods	19
3.1	Materials	19
3.2	Preparation and modification of cellulose for hydrogel applications	19
3.2.1	Cellulose pulp pretreatment	19
3.2.2	Cellulose dissolution	20
3.2.3	Cellulose modification	20
3.3	Isolation of SAPs from commercial diapers	21
3.4	Preparation of cellulose-based hydrogels	21
3.5	Characterization techniques of hydrogels	22
3.5.1	Fourier transformed infrared spectroscopy (FTIR)	22
3.5.2	Nuclear Magnetic Resonance Spectroscopy	22
3.5.3	Morphology	22
3.5.4	Thermal properties	22
3.5.5	Gel Fraction	23
3.5.6	Free Swelling Capacity	23
3.5.7	Swelling – Synthetic Urine and pH Buffers	23
3.5.8	Water/Synthetic Urine Retention Capacity	23
3.5.9	Synthetic Urine Centrifuge Retention Capacity	24
3.5.10	Absorbency Under Load (AUL)	24
3.5.11	Biodegradability	25
3.5.12	Cytotoxicity	25
3.5.13	Statistical Analysis	25
4	Results and Discussion	27
4.1	Cellulose Derivatives Preparation and Characterization	27
4.2	Cellulose-Based Hydrogels Preparation	30
4.2.1	Most common monomers for superabsorbents hydrogels	30
4.2.2	Alternative monomers for superabsorbents hydrogels	33
4.2.2.1	Crosslinker Effect	37
4.2.2.2	Drying Method Effect	40
4.2.2.3	Monomers Ratio Effect in Cellulose-Based Hydrogels	41
4.2.2.4	Cellulose Degree of Substitution Effect	43
4.2.2.5	Crosslinker Quantity Effect in Cellulose-Based Hydrogels	45
4.2.2.6	Initiator Quantity Effect in Cellulose-Based Hydrogels	46
4.2.2.7	Cellulose:Monomers Ratio Effect	47
4.3	Most Promising Cellulose-Based Hydrogels	49
4.3.1	Detailed Characterization of Cellulose-Based Hydrogels	49
4.3.1.1	Thermal Properties	51
4.3.1.2	Swelling and Holding Properties	53
4.3.1.3	Biodegradability	57
4.3.1.4	Biocompatibility	57
5	Conclusion	59
5.1	Final Remarks	59
5.2	Future Work	60

5.3 Work Limitations	60
Bibliography	61
Appendices	73
A Method of Preparation of Hydrogels	75
B Determination of Degree of Substitution	76

List of Figures

2.1	Timeline of the use of PCPs from Ancient Egyptian to Modern Society (Adapted from: [8])	3
2.2	Different types of personal care products (Adapted from: [8])	4
2.3	Modern disposable diaper diagram and composition (Adapted from: [1], [3])	5
2.4	Modern standard pad diagram and composition (Adapted from:[1], [3])	6
2.5	Modern incontinence diaper diagram and composition (Adapted from:[1], [3])	7
2.6	Classification of hydrogels (Adapted from: [19])	8
2.7	Major pathways of formation of cellulose (Adapted from: [54])	13
2.8	Molecular structure of cellulose (Adapted from: [59])	13
2.9	Chemical structure of cellulose and some of its derivatives (Adapted from: [64])	14
2.10	Applications of cellulose-based hydrogels (Adapted from: [83])	17
3.1	Process of cellulose sulfuric acid hydrolysis: (a) cellulose pulp hydrolyzed in sulfuric acid at 450 rpm for 36 hours, and (b) experimental setup for the filtration procedure.	20
3.2	Protocol of cellulose modification for further biomedical applications.	21
3.3	(a) Open configuration of a commercially available diaper. (b) Cross-sectional view of the absorbent core, demonstrating the heterogeneous distribution of SAPs. (c) Isolated SAPs extracted from the absorbent core, prepared for detailed characterization.	21
3.4	Schematic representation for AUL tests (Adapted from: [84]).	24
4.1	Particle size distribution of cellulose after sulfuric acid hydrolysis.	27
4.2	Formation of AHP-cellulose using cellulose dissolved in a 7 wt% NaOH and 12 wt% urea aqueous solution (Adapted from: [88]).	28
4.3	¹ H NMR spectra of cellulose derivatives prepared with (a) five, (b) four, and (c) three equivalents of AGE. All the spectra were obtained in deuterium oxide, and the peak of solvent used as reference.	29
4.4	FTIR spectra of (a) cellulose powder and (b) cellulose derivative prepared with five equivalents of AGE.	29
4.5	Chemical structure of (a) acrylamide [102], (b) acrylic acid [103], (c) potassium acrylate [104] and (d) N,N'-methylenebisacrylamide [105].	31
4.6	FTIR spectra of (a) cellulose powder, (b) Cell_Lyo, (c) Cell_5_DH (d) Cell_AAK:AAm_C0.5_DH, (e) Cell_AAK_C0.5_DH, and (f) SAPs extracted from commercially available diapers.	32

4.7	Homopolymers and cellulose copolymerized hydrogels with AA, AAm, and AAK (a) water swelling kinetics and (b) gel fraction. Gels with $\varnothing=20$ mm were open air dried after solvent exchange with ethanol. Mass measurements were taken at 15 min, 30 min, and at equilibrium. For the legend see Table 4.3.	33
4.8	Chemical structure of (a) AMPS [114], (b) SPM [115], (c) PAHEMA [116] and (d) BMEP [117].	34
4.9	Swelling behavior and post-test disintegration of cellulose-co-AMPS hydrogels in which (a) represents the dynamic swelling behavior of cellulose-co-AMPS hydrogels under experimental conditions and (b) their disintegration post-test.	34
4.10	Chemical structure of META [119].	35
4.11	(a) Water swelling kinetics and (b) gel fraction of cellulose-based hydrogels varying monomers ratios. Samples with $\varnothing=20$ mm of gels and dried in the oven. The free swelling absorbency was taken at 15 min, 30 min and at maximum swelling capacity. Legend in Table 4.5.	36
4.12	^1H NMR spectra obtained from the formulations (a) Cell_S1:P1:M2, (b) Cell_S1:P2:M1, (c) Cell_P1:M1 and (d) Cell. All spectra were collected in deuterium oxide.	36
4.13	Results from (a) water swelling kinetics and (b) gel fraction from influence of the crosslinker study. Hydrogels were cut ($\varnothing=20$ mm) and oven dried before submitted to swelling tests. Legend presented in Table 4.6.	37
4.14	(a) Water swelling kinetics and (b) gel fraction of alternative homopolymer hydrogels. Samples with $\varnothing=20$ mm of gels were collected and the drying method chosen was oven drying. The free swelling absorbency was taken at 15 min, 30 min and at maximum swelling capacity. For legend see Table 4.7.	38
4.15	Hydrogels produced from copolymerizing the alternative monomers. (a) Water absorbency and (b) gel fraction. The test was conducted with $\varnothing=20$ mm gels oven dried. Also, as previous methodology, the absorbency was measured at 15 min, 30 min, and 24 hours. The legend is presented in Table 4.8.	39
4.16	The drying method investigation was carried out with the three approaches (OD, Et, and Met) mentioned. To determined the effect of drying method (a) swelling kinetics in water (at 15 min, 30 min, 24 hours) and (b) gel content of gels ($\varnothing=20$ mm) were collected. Gels of cellulose copolmerized with SPM were prepared with 0.5%.wt of crosslinking agent, whereas homopolymers from SPM had 5%.wt of BAAM.	40
4.17	SEM images of cross-section of oven dried hydrogels: (a) cellulose hydrogel (control sample) (b) Cell_P1:M1, and air dried after solvent exchange with ethanol: (c) cellulose hydrogel and (d) Cell_P1:M1.	41
4.18	Influence of monomers ratio in (a) water swelling kinetics and (b) gel content. The assay was performed with hydrogels ($\varnothing=20$ mm) dried in open air with solvent exchange with ethanol. For legend see Table 4.9	42
4.19	FTIR spectra of (a) cellulose powder, (b) Cell_5, (c) Cell_5_H (d) SPM hydrogel, (e) PAHEMA hydrogel, (f) META hydrogel and (g) Cell_S1:P1:M1 hydrogel.	43
4.20	Cellulose-based hydrogels absorption behavior and (g) gel content with DS ranging from 0.76 to 1.21. Samples of $\varnothing=20$ mm were submitted to swelling tests. See legend in Table 4.10.	44

4.21	(a) Water absorption capacity of cellulose-based hydrogels ($\varnothing = 20$ mm) at 15 min, 30 min, and at 24 hours and (b) gel fraction with BAAM quantity varying from 0.1 to 0.5 wt.%. Legend in Table 4.11.	46
4.22	Influence of initiator dosage of hydrogels ($\varnothing = 20$ mm) in (a) water retention capacity at 15 min, 30 min and 24 hours and (b) gel content. Legend in Table 4.12.	47
4.23	Hydrogels ($\varnothing = 20$ mm) with different cellulose:monomers ratio (a) water retention capacity at 15 min, 30 min and 24 hours and (b) gel content. For legend see Table 4.13	48
4.24	Swelling behavior of Cell_S2:P1:M1_10:90 hydrogel over time. Three preparation methods were compared: cryogenic fracture (CF), grinding in a coffee grinder (CG), and coarsely hand breaking (HB). The swelling ratio was measured at different time intervals up to maximum swelling.	50
4.25	SEM images of hydrogel surfaces prepared under different conditions: (a) hydrogels cut into 20 mm circular samples, (b) cryogenically fractured hydrogels, (c) hydrogels ground in a coffee grinder, and (d) manually broken hydrogels.	51
4.26	(a) TGA (b) DTG curves of samples in order to evaluate the thermal stability.	52
4.27	Swelling kinetics of most promising hydrogels for personal care products, as well as control samples, in (a) deionized water, (b) synthetic urine, (c) pH 4 buffer solution, and (d) pH 8 buffer solution. Legend in Table 4.14.	54
4.28	(a) Deionized water and (b) synthetic urine retention capacity of most promising samples and controls over an 8-hour period. Legend in Table 4.14.	55
4.29	Free swelling capacity (FSC), absorbency under load (AUL), and centrifuge retention capacity (CRC) of most promising hydrogels and controls in synthetic urine. Legend in Table 4.14.	56
4.30	Preliminary biodegradability tests showed visible hydrogel adhesion to the soil. This result prevented the measurement of the hydrogels biodegradability over a period of three weeks.	57
4.31	NHDF fibroblast viability in response to hydrogels and diaper samples over 3 and 7 days (MTS Assay). Legend in Table 4.14.	58
A.1	Various hydrogel preparation methods for characterization purposes included: (a) cutting hydrogels into 20 mm diameter discs, (b) cryogenically fracturing the hydrogels, (c) grinding the hydrogels using a coffee grinder, and (d) manually breaking the hydrogels into coarse pieces.	75
B.1	Determination of degree of substitution through ^1H NMR method. Spectra of cellulose derivative prepared with 4 equivalents of AGE is used in this example.	76

List of Tables

2.1	Characteristics of natural superabsorbent materials	12
2.2	Properties and usage of some of the cellulose derivatives (Adapted from: [64]).	15
4.1	Cellulose derivatives conditions and DS.	28
4.2	Conditions, maximum swelling and gel fraction obtain from cellulose homopolymers prepared with three different DS.	30
4.3	Formulation and synthesis conditions for homopolymers and cellulose copolymerized hydrogels with AA, AAm, and AAK. All hydrogels were prepared with 1 wt.% of initiator.	31
4.4	Formulation and conditions of cellulose-based hydrogels copolymerized with AMPS. All hydrogels were prepared with 1 wt.% of BMEP and initiator.	34
4.5	The composition of the hydrogels investigated to analyze the effects of varying monomers concentrations. All hydrogels were prepared with 1 wt.% BMEP and initiator.	35
4.6	Formulation of hydrogels to conduct the crosslinker effect study.	37
4.7	Parameters for producing homopolymers from the alternative monomers. Hydrogels were produced using 1 wt.% of initiator.	38
4.8	Formulation and synthesis conditions for copolymerization of alternative monomers. . .	39
4.9	Composition and formulation conditions of the hydrogels produced to analyze the effects of varying monomers concentrations. All hydrogels used 1 wt.% of BAAM as crosslinker and wt.% of initiator.	42
4.10	Formulations and conditions of hydrogels for degree of substitution effect study. Hydrogels were produced with 1 wt.% of both BAAM and initiator.	44
4.11	Hydrogels formulations produced to assess the crosslinker agent quantity effect. The initiator quantity was set at 1 wt.%.	45
4.12	Formulation and reaction conditions used in the investigation of initiator dosage effects. Hydrogels were produced with 0.5 wt.% of BAAM.	46
4.13	Formulation and reaction conditions implemented for the study of cellulose: monomers ratio. Both crosslinker agent and initiator quantities were set at 0.5 wt.%.	48
4.14	Formulation and reaction conditions of cellulose-based hydrogels considered the most promising for personal care products and negative control.	49
4.15	Thermal properties of samples assessed by TGA.	52

List of Acronyms/Abbreviations

3D - Three-dimensional

AA - Acrylic Acid

AAm - Acrylamide

AA_{Na} - Sodium Acrylate

AAK - Potassium Acrylate

ADL - Acquisition and Distribution Layer

AGE - Allyl Glycidyl Ether

AGU - Anhydroglucose Units

AHP - Absorbent Hygiene Product

AHP-cellulose - 3-allyloxy-2-hydroxy-propyl cellulose

AIBN - 2,2-azo-isobutyronitrile

AMPS - 2-Acrylamido-2-methyl-1-propanesulfonic Acid

ANOVA - Analysis of Variance

AUL - Absorbency Under Load

BAAm - N,N'-Methylenebisacrylamide

BEKP - Bleached Eucalyptus Kraft Pulp

BMEP - Bis[2-(Methacryloyloxy)ethyl] Phosphate

CBH - Cellulose-Based Hydrogel

CRC - Centrifuge Retention Capacity

DMAc - N,N-dimethylacetamide

DMSO - Dimethyl Sulfoxide

DP - Degree of Polymerization

DS - Degree of Substitution

FSC - Free Swelling Capacity

FTIR - Fourier Transformed Infrared Spectroscopy

GF - Gel Fraction

HMP - 2-Hydroxy-2-methylpropiophenone

KPS - Potassium Persulfate

MCC - Microcrystalline Cellulose

META - 2-(Methacryloyloxy)ethyl Trimethylammonium Chloride

NaCl - Sodium Chloride

NaOH - Sodium Hydroxide

NMMO - N-methylmorpholine-N-oxide

NMR - Nuclear Magnetic Resonance Spectroscopy

PAAM - Polyacrylamide

PAA - Poly(acrylic Acid)

PAHEMA - Phosphoric Acid 2-Hydroxyethyl Methacrylate Ester

PCP - Personal Care Product

PEG - Poly(ethylene Glycol)

PHEMA - Poly(2-hydroxyethyl Methacrylate)

PNIPAM - Poly(N-isopropyl Acrylamide)

PVA - Poly(vinyl Alcohol)

SAP - Superabsorbent Polymer

SD - Standard Deviations

SEM - Scanning Electron Microscope

SPM - 3-Sulfopropyl Methacrylate

TBAF - Tetrabutylammonium Fluoride

TEMED - Tetramethylene-diamine

TGA - Thermogravimetric Analysis

UV - Ultraviolet

Chapter 1

Introduction

In this first chapter, the context, motivation, and objectives behind this dissertation will be highlighted. Additionally, a scope and significance of this study will be described.

1.1 Context and Motivation

There is a growing awareness of the environmental consequences of single-use products, particularly absorbent hygiene products (AHPs) [1] such as baby diapers, feminine hygiene products, and adult incontinence products [2]. These items are essential to absorb human fluids in different stages of life and their use continues to increase, becoming indispensable in developed societies [3].

Superabsorbent polymers (SAPs) are a common ingredients in personal hygiene products being disposable diaper their largest consumer [4]. It is estimated that a baby uses around 4000 diapers, most of which are discarded in landfills contributing to environmental accumulation [5]. Furthermore, the SAPs currently on the market are mainly derived from synthetic polymers based on acrylic acid and/or acrylamide [6]. Despite their excellent water absorption and retention capabilities, these polymers are neither bio-based nor biodegradable, [2], [5] exacerbating their environmental impact [5].

In contrast, cellulose, the most abundant biopolymer on Earth as it can be found in trees, plants, fruits, vegetables, and biowaste [7] offers a sustainable alternative since it is a biodegradable, biocompatible, renewable, and hydrophilic polymer [2], [4]. Hence, cellulose-based superabsorbents could present a greener solution to mitigate the environmental and health consequences associated with traditional SAPs [5].

1.2 Objective

The aim of this study is the development of cellulose-based hydrogels by taking advantage of the bioproperties of cellulose such as safety, biocompatibility, biodegradability, and high hydrophilicity. The cellulose will be copolymerized with other polymers to produce hydrogels and enhance their water/urine/body fluids absorption capacity, salts and pH resistance, physical, mechanical, degradability and non-cytotoxicity properties. Additionally, the comparison between prepared hydrogels and a diaper isolated hydrogel will be assessed.

1.3 Scope and Significance of the Study

In this work cellulose-based hydrogels with effective absorption capacity, focusing on their potential to replace the commonly used SAPs in AHPs, particularly in diapers, will be developed. Cellulose-based hydrogels possess several advantages such as:

- alignment with global sustainability objectives;
- provide a more sustainable alternative to conventional SAPs, which lack of biodegradability and biocompatibility properties;
- contribute to the reduction of the human footprint, by reducing the waste generated by AHPs;
- lead to advances in the production of biodegradable materials suitable for personal care products.

Thus, it becomes imperative the development of greener and sustainable products, as cellulose-based ones.

Chapter 2

State of the Art

In the second chapter, an overview of the current developments of hydrogels for personal care products is presented.

2.1 Personal Care Products

The first appearance of personal care products (PCPs) dates to the dawn of human societies. Over the centuries, these products have acquired a significant role in our daily routines by contributing to our health, appearance, and hygiene [8].

Starting in Ancient Egypt, cosmetics were an indicator of wealth, and it was believed that it pleased the gods. Other cultures such as the ancient Greeks also used PCPs as a symbol of wealth and beauty. The use of PCPs continued to grow until the 19th century, when Queen Victoria declared her aversion to cosmetics. It was not until the end of the Second World War and the emergence of the Internet that PCPs began to regain their importance in our lives [8]. Figure 2.1 shows the timeline of personal care products.



Figure 2.1: Timeline of the use of PCPs from Ancient Egyptian to Modern Society (Adapted from: [8])

In the earliest days, PCPs were derived from plants and animals, but these products evolved and diversified, incorporating scientific innovations and societal trends [8] and becoming available in several forms. Nowadays, PCPs serve many purposes regarding personal hygiene, cleaning, beautifying, and grooming [8], [9], [10], [11]. Some PCPs on the market, like lip balms, diaper rash ointments, sun blockers, and mouthwash, may contain traces of pharmaceuticals. Although pharmaceuticals are included in their composition, they are still termed PCPs as the definition covers both cosmetics and medicines used for aesthetic and therapeutic purposes [9], [12].

2.1.1 Types of Personal Care Products

PCPs are consumer products conceived for external use on the human body and include a remarkably range of products for hair and body care which include cleansing, moisturizing, and conditioning. Figure 2.2 presents some of the main types of PCPs available [8].

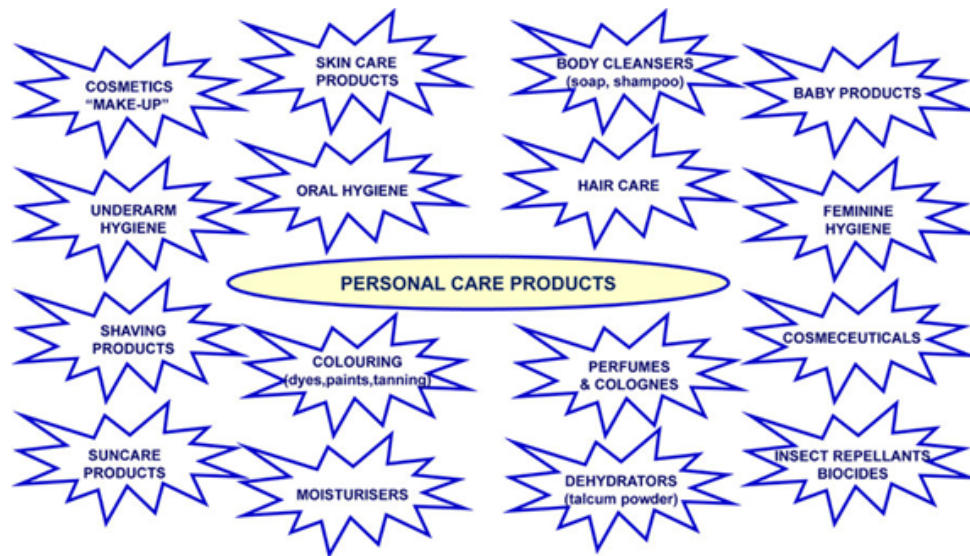


Figure 2.2: Different types of personal care products (Adapted from: [8])

The beginning of the 20th century brought a change with the introduction of absorbent hygiene products. It all started with the invention of a diaper, which was made from wood pulp bandages [2]. Their commercialization significantly enhanced the well-being and skin condition for many people. Presently, AHPs encompass three main categories: baby diapers, feminine hygiene products, and adult incontinence products [2], [4], [8], [13]. These commodities are designed to absorb body fluids such as urine, menstrual fluids, and faeces (in the case of diapers) while providing comfort to their users [2], [4], [13].

2.1.2 Absorbent Hygiene Products

Absorbent hygiene products can differ in size, shape, and quality for multiple purposes and genders, but they all share a common function: maximize fluid retention. Absorbing body fluids efficiently is achieved through a mechanism for water absorption similar across all these products [2], [4]. The four main functional layers meticulously engineered to enhance the overall performance of these products are: the topsheet or facing, acquisition and distribution layer (ADL), absorbent core and backsheet or outer cover [1].

- *Topsheet*: It is the layer in contact with the user's skin, and therefore its material needs to be soft and dry to prevent skin irritation. Fluids are not retained in this layer because its main purpose is

to transfer the fluid quickly to the next layer so that the contact time between the fluid and the skin is minimal.

- **ADL:** The fluids are briefly retained in this layer. A capillary action spreads it over a broader region in this layer, facilitating absorption by the core (next layer). This layer is important during critical times since it permits the succeeding layer to progressively absorb the fluids. In AHPs with high superabsorbents content and low fluff pulp levels must possess an ADL with improved spread performance, whereas AHPs with high fluff and/or low SAP levels can function without a separate ADL due to their superior capillary qualities.
- **Absorbent core:** This is the most important component and is responsible for the major purpose of AHPs: to absorb and retain human fluids. The absorbent layer in some of the most current 'ultra-thin' feminine hygiene products is made via airlaid technology, which consists of a prefabricated multi-layered structure composed of SAP, fluff pulp, or other capillary fibers.
- **Backsheet:** This layer plays a role in preventing leakage and it is typically composed of low gauge polyethylene film that can be breathable or non-breathable. Some products additionally contain a soft nonwoven cover or a breathable film to maintain a good skin condition [1], [2].

Although the typical setting of AHPs is similar, their content and composition are slightly different depending on the final aim of it [14].

• **Baby Diapers**

In the 1930s, the cloth-based disposable sanitary towels and diapers were introduced in Sweden. Prior, diapers were made of cotton or muslin and wrapped around the baby and secured. Also, they could be washed and reused [2]. Later, in 1961, Procter and Gamble invented the modern disposable diaper made with a non-woven top sheet and a cellulose filling core [3].

Diapers have been continuously enhanced when it comes to their performance, comfort, fit, design, and convenience [13], [15]. These days, baby diapers are made up of the four layers mentioned above. Their absorbent core is usually made of fluff pulp and SAP to absorb and retain large quantities of the baby's fluids. Figure 2.3 illustrates a diagram of a modern disposable diaper and its composition [1], [2], [3].

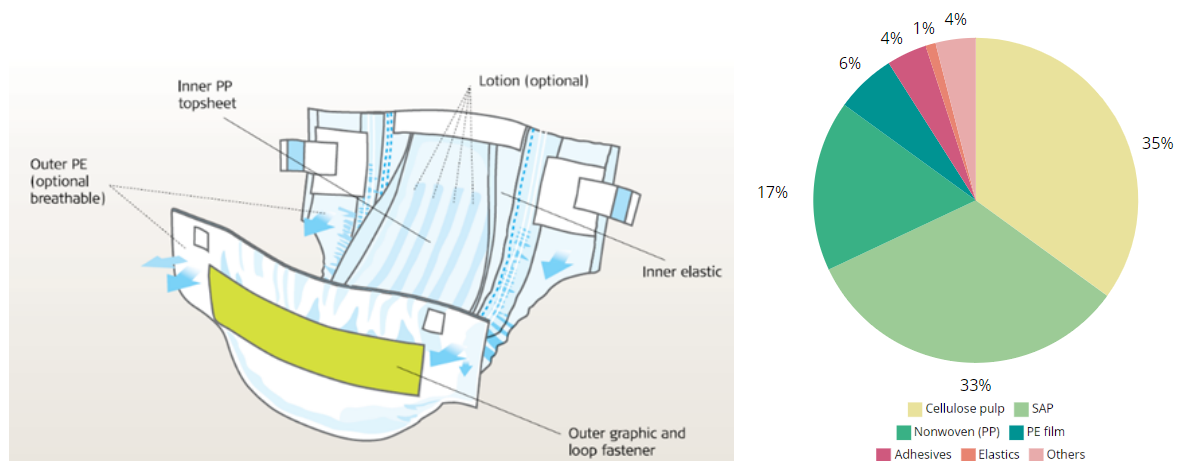


Figure 2.3: Modern disposable diaper diagram and composition (Adapted from: [1], [3])

• ***Feminine Hygiene Products***

As previously mentioned, the disposable pads began to be commercialized in the early 1890s, but only gained its respective importance during First World War, when nurses began wearing the wooden pulp bandages to hold back their flow. The progress in sanitary pads were influenced by evolution in baby diapers such as using hotmelt adhesives and superabsorbent polymers, to become thinner, more absorbent, and more comfortable [1] .

Sanitary pads also include a layer known as release paper in addition to the four previously mentioned layers. This layer covers the adhesive on the backsheet, which is removed before the pad is attached to the users underwear. Figure 2.4 shows the schematic view of a standard sanitary pad and its composition [1], [2], [3].

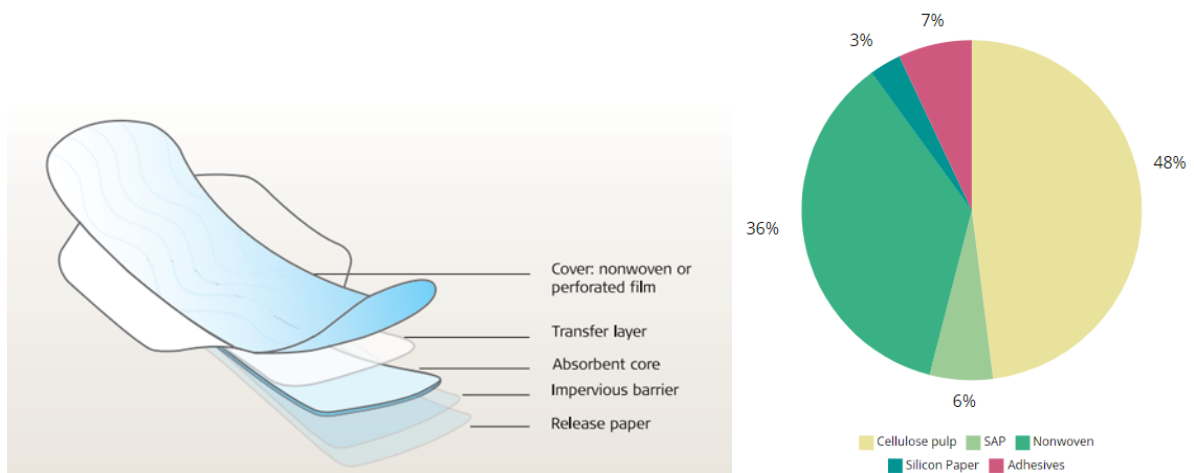


Figure 2.4: Modern standard pad diagram and composition (Adapted from:[1], [3])

• ***Adult Incontinence Products***

The most recent addition to the AHP industry is adult incontinence products. Their application was first seen in Europe in the late 1960s, and they were developed using technologies adopted from baby diapers and feminine sanitary products. Originally, these products were used in medical environment like nursing homes and hospitals, where they provided significant improvements in terms of comfort, hygiene, infection prevention, and cost efficiency [3].

There are multiple solutions available to suit different forms of incontinence, disability, and lifestyle needs. Small pantyliners, pads and light pants, two-part systems (pad and pant), complete briefs, and belted briefs are also available. Figure 2.5 exhibits a diagram of the modern adult incontinence diaper and its constitution [1], [2], [3].

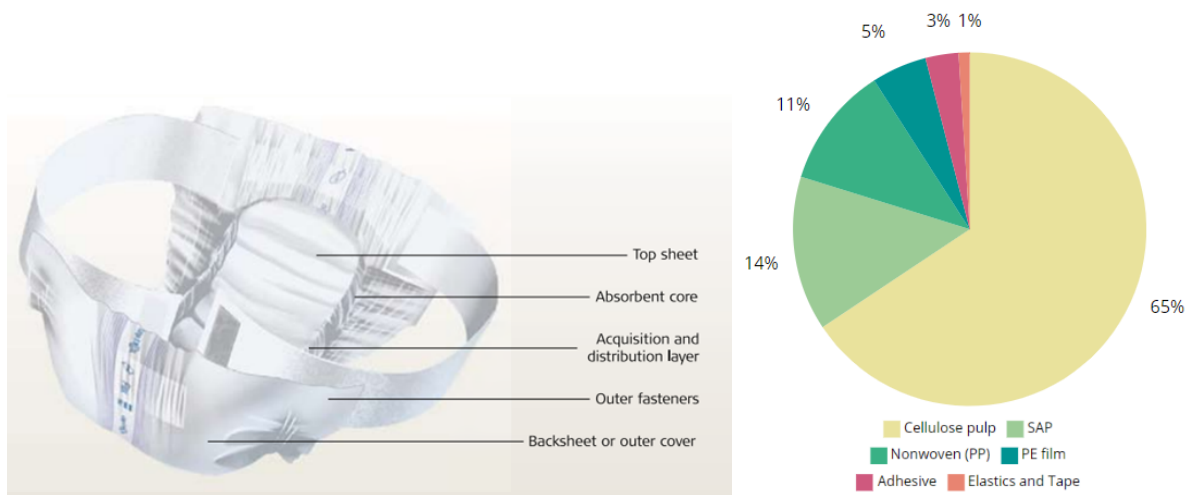


Figure 2.5: Modern incontinence diaper diagram and composition (Adapted from:[1], [3])

2.1.3 Superabsorbent Materials in Personal Care Products

Regarding the absorbent component, cellulose has been used ever since when AHPs were discovered. Its abundance of hydrophilic hydroxyl groups enables it to be easily wetted by water and aqueous solutions [13]. In 1979, superabsorbent materials appeared in Japan and completely innovated the AHPs field by bringing new materials such as acrylate-based ones [2], [15]. Before superabsorbent materials, much more absorbent fluff pulp was required to absorb the same amount of urine. Diapers were thicker, weighed more, and could retain significantly less urine. The traditional absorbent materials such as cloth, cotton, paper wadding and cellulose fiber had low efficiency and allow leakage [2], [4].

Superabsorbent polymers have a three-dimensional (3D) hydrophilic structure that allows them to absorb and retain large amounts of aqueous solution in their networks and can absorb more than 1000 times their dry weight in liquids [2], [4], [16], [17] without dissolving [18]. As a result, these polymers have revolutionized the personal care products industry by absorbing and retaining large quantities of liquid even under pressure and ensuring that diapers and sanitary pads work effectively and that the skin remains dry and healthy [2], [15], [16].

2.1.3.1 Hydrogels

Hydrogels are crosslinked polymer chains with 3D network configurations, which can absorb significant volumes of fluid. Because of the high water content, flexible structure, and porosity of hydrogels, they resemble real tissues [19]. The first hydrogels were made by scientists Wichterle and Lim. The authors were able to produce a synthetic poly-2-hydroxyethyl methacrylate hydrogel and used it as a filling material for eye enucleation and contact lenses [20]. Since then, hydrogels have been arranged for over the 60 years to be implantable, injectable and sprayable for various organs and tissues. Currently, hydrogels are largely employed in industries like agriculture, biomaterials, the food industry, medication delivery, tissue engineering, and regenerative medicine. However, with continued technical improvements in hydrogel fabrication, it is expected that their uses may spread into even more fields in the future [19], [21].

2.1.3.2 Types of Hydrogels

Hydrogels can be divided into different categories, as shown in Figure 2.6. They are categorized according to the source and composition of the polymers, the crosslinking method, the configuration, the ability to respond to stimuli, their properties and ionic charge [19], [20], [21].

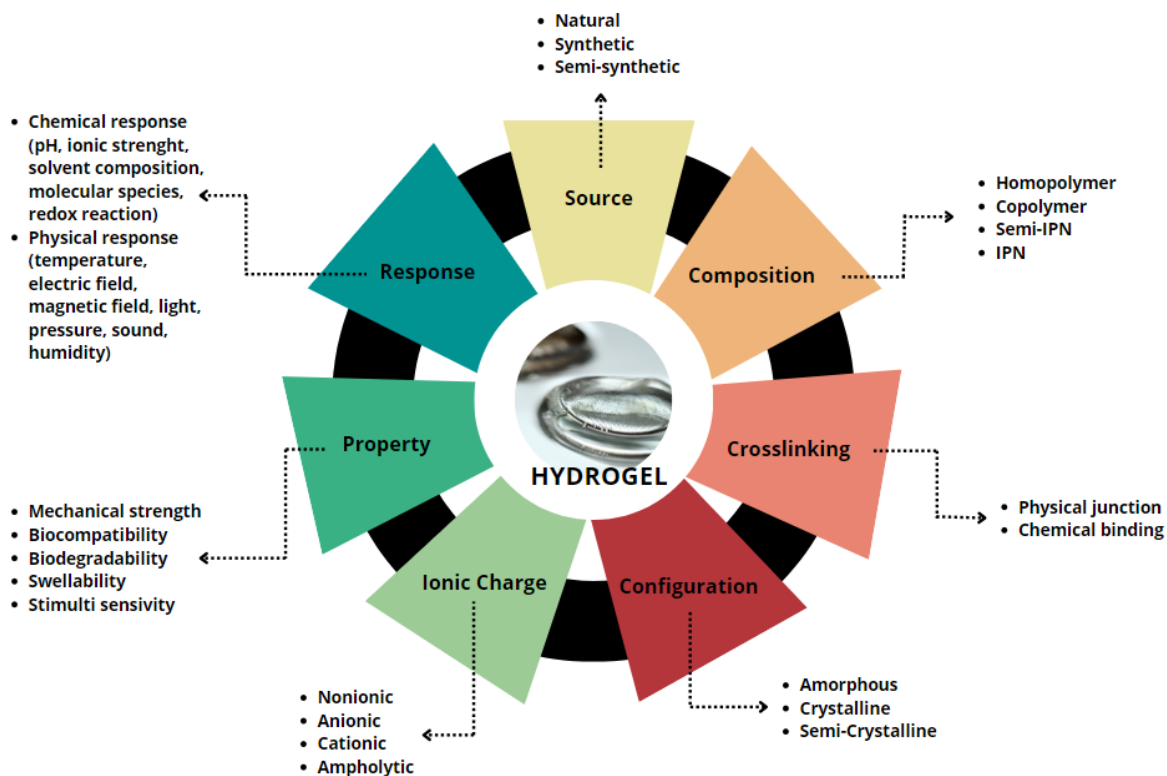


Figure 2.6: Classification of hydrogels (Adapted from: [19])

Natural polymers encompass polysaccharides (chitin, chitosan, cellulose, starch, gums, alginate, and carrageenan), biological polymers (nucleic acid and deoxyribonucleic acid), polyamides (collagen), polyphenols (lignin), organic polyesters, inorganic polyesters, and polyanhydrides (poly sebacic acid) while synthetic hydrogels are derived from polymers like poly(vinyl alcohol) (PVA), poly(ethylene glycol) (PEG), polyacrylamide (PAAM), poly(2-hydroxyethyl methacrylate) (PHEMA), poly(N-isopropyl acrylamide) (PNIPAM), poly(acrylic acid) (PAA) and their derivatives [19], [20]. The combination of synthetic and natural hydrogels results in semi-synthetic hydrogels that exhibit improved mechanical and biological properties [22].

Based on their crosslinking method, hydrogels are classified as chemical hydrogels or physical hydrogels [19], [20]. The degree of crosslinking is one of the main properties that affect hydrogels swelling, with highly crosslinked components having a lower swelling ratio since the polymer structure becomes more compressed, restricting the network extent [23]. The polymers involved in hydrogels can be homopolymers, copolymers, semi-interpenetrating networks or interpenetrating networks [19], [21]. Moreover, based on their configuration, hydrogels can be designated as amorphous, crystalline, or semi-crystalline [19] and labeled as cationic, anionic, or neutral hydrogels depending on their ionic charge [19], [20], [21].

Hydrogels are capable to respond to different stimuli, which can be chemical (pH, ionic strength, solvent composition, molecular species and redox reaction) or physical (temperature, electric field, magnetic field, light, pressure, sound and humidity) [19], [21]. Furthermore, hydrogels exhibit a variety of

characteristics and can be categorized into two main types: conventional hydrogels and smart hydrogels. Conventional hydrogels undergo minor changes, such as swelling, in response to external environmental factors and generally possess low mechanical strength. On the other hand, smart hydrogels are highly responsive to subtle variations in external conditions, swiftly adapting their physical attributes, including mechanical strength, swellability, and sensitivity to stimuli [19].

2.1.3.3 Hydrogels properties

The properties of hydrogels such as swelling, biological and mechanical properties are influenced by their structure which depends on the production method and chemical composition [23], [24].

- **Swelling Properties**

Swelling refers to the ability of hydrogels to retain large amounts of fluids without disintegrating. The swelling response of hydrogels in various environments, such as pH levels, and ionic strength, is crucial for determining their suitability for different applications. The process consists of three major steps [19], [20], [23]:

1. *Diffusion*: Water molecules are diffused into the hydrogel network [20], [25] and hydrate most of the polar hydrophilic groups [26].
2. *Polymer chain loosening*: Water molecules will act as proton donors and receptors and polymer chains which contain electronegative elements (O, N and F) interact with hydrogen atoms [17], [20], [25].
3. *Hydrogel network expansion*: The loosened polymer chains subsequently extend, causing the hydrogel network to swell [20], [25].

The presence of hydrophilic groups, such as hydroxyl, carboxyl, amine, and sulfate groups, within the polymer network chains of hydrogels facilitates their expansion. Water molecules are attracted to these hydrophilic and polar groups, establishing a primary water bond. The groups also engage with the water molecules and create secondary bonds. The phenomenon of swelling is based on osmotic pressure due to the existence of unequal distribution of ions in the polymer network and in the aqueous environment. When hydrogels are put in water, the osmotic pressure encourages the expansion of the polymeric network and the hydrogels begin to expand, reaching the swelling equilibrium when the osmotic forces and the elastic forces of the polymeric chains are equivalent [23].

- **Mechanical Properties**

Hydrogel mechanical characteristics are important in establishing the viability of these materials for different applications [27]. The molecular weight of the polymer and the crosslinking density influence the degree of bonding between the polymer chains and therefore have an impact on the mechanical properties of the materials [28]. While natural hydrogels possess weak mechanical properties and are difficult to manage due to their batch-to-batch fluctuation [29], synthetic hydrogels exhibit better mechanical strength [20], [21]. Nonetheless, desired mechanical properties of hydrogels can be achieved by incorporating specific polymers, co-monomers, and crosslinkers, as well as by adjusting the degree of crosslinking resulting in stronger hydrogels. However, an excessively high degree of crosslinking can lead to low elongation and elasticity, making the hydrogels more brittle [20].

- **Biological Properties**

The biological properties of hydrogels are assessed by their biocompatibility and biodegradability. Biocompatibility concerns the capacity of hydrogels to interact within a biological environment without being harmful to the host [20], [23] and it is especially important when considering the interaction between synthetic polymer-based hydrogels and human tissue [20]. Natural hydrogels particularly those made from polysaccharides, are biocompatible and non-toxic due to their resemblance to the extracellular matrix and ability to interact with cells, tissues, and biological fluids [24]. Meanwhile, inflammation disorders, mechanical damage, and immunological rejections are frequently associated as potential side effects of synthetic materials [23]. Biodegradability refers to the ability of organisms to break down hydrogels into non-toxic by-products through degradation processes. This important property for the biomedical field is influenced by the system moieties as well as the process of manufacturing [20]. Natural polymers reveal a better biological interaction compared to synthetic hydrogels and are environmentally friendly, since they are degradable by several bacteria and fungi present in air, water and soil [30]. The good biodegradability and biocompatibility of natural polymers makes them ideal for the production of hydrogels aiming biomedical applications [20], [31].

2.1.4 Impacts of Personal Care Products

Nowadays, the high accumulation of PCPs in the environment and the potential toxicity of their constituents are a significant concern in environmental science and public health. Even at minimal concentrations, the PCPs components have the capacity to trigger diverse physiological effects in the environment [32].

2.1.4.1 Health Impact

The use of diapers can lead to a range of health issues due to chemical exposure [33]. Diaper rash is a prevalent condition linked to diapers, particularly in children [4]. Furthermore, diapers have been found to contain dioxin, a highly toxic substance associated with cancer and leading to developmental delays, weakened immunity, hormonal disruption and skin disorders [33]. Toxic amounts of dioxins have also been reported in some rayon viscose tampons [2]. Sodium polyacrylate, phthalates and heavy metals are other chemicals found in diapers that can lead to health side effects [4]. Moreover, the use of tampons and other devices like menstrual cups, cervical caps, contraceptive sponges, intrauterine devices, diaphragms, and pessaries have been linked to a serious condition called *Staphylococcal* toxic shock syndrome [34]. Another adverse effect on human health is the release of volatile organic compounds from disposable diapers [4] and sanitary pads [35].

While absorbent hygiene products may come with certain health concerns, they have revolutionized the lives of countless individuals, whether they are users themselves or caregivers. These products contribute to an enhanced quality of life through features such as dryness, cleanliness, leakage prevention, comfort, and skin health having a profoundly positive impact by providing security, comfort, discretion, and odor control. Moreover, they empower users to maintain their dignity and confidence, enabling them to participate in various activities, including leaving their homes, working, engaging in social interactions, and enjoying a fulfilling life [36].

2.1.4.2 Environmental Impact

Hygiene products are mainly single-use products that generate a large amount of waste representing 2-7% of municipal solid waste produced in Europe. The usual end-of-life approach for these products are landfills or incinerators with actual disposable diapers taking approximately 500 years to decompose, in the case of landfilling. [3], [37], [38], [39]. The inadequate waste management of AHPs results in the emission of non-biogenic CO₂ and the landfilling of persistent pollutants [38], [40]. Further, SAPs are the primary contributor to the global warming potential in diaper manufacture [41]. These superabsorbent materials are commonly produced by combining synthetic polymers, which exacerbates environmental issues due to its origin and lack of natural biodegradability [41].

The environmental impact of these products can be mitigated by applying eco-design principles and innovative strategies, such as reducing their mass, strengthening their sustainability and facilitating their end-of-life options [3], [38]. In terms of reducing mass, SAPs have significantly contributed to lowering the weight of diapers due to the replacement of fluff pulp by polymers with superior absorption properties. This replacement improves children's comfort and also reduces the volume of waste that has to be processed or disposed [39]. Another option is to replace conventional petroleum-based SAPs with bio-based materials, taking advantage of their biodegradability, biocompatibility and non-toxicity properties [42]. This is an environmentally friendly solution for personal care products, helping to reduce dependence on fossil fuels and greenhouse gas emissions. Additionally, biodegradable materials can be recirculated in composting facilities. Regarding treating and recycling used, there are various ecologically acceptable choices, such as recycling, biodegradation, composting, anaerobic digestion, dark fermentation and pyrolysis [39]. Studies have shown that the recovery and reuse of SAP has potential benefits, given the growing impacts of the disposable hygiene products industry and the growing interest in impact mitigation [41]. Even still, there are still barriers to overcome, as separate collecting and subsequent processing of diapers is only authorized in certain countries. In addition, the differing compositions amongst diapers from different producers makes it difficult to sorting them [39].

2.2 Natural-based Superabsorbents Polymers

The superabsorbents polymers commercially available are synthetic, produced from petroleum-based monomers such as acrylic acid, methacrylic acid, and acrylamide, and their derivatives [43], [44]. The synthetic hydrogels are often found in personal care items [2], [45] although they account with certain drawbacks, such as the environmental contamination, health risks mentioned above, as well as their non-renewability [43]. The problems associated with synthetic hydrogels have led to a growing demand for bio-based superabsorbents that are eco-friendlier and more sustainable [13]. Table 2.1 summarizes the properties and applications of some of the most used natural-based superabsorbents.

2.2.1 Cellulose and Cellulose-based Absorbents

In 1838, French scientist Anselme Payen identified a resilient fibrous substance that endures after the treatment of multiple plant tissues with acids and ammonia, as well as subsequent extraction using water, alcohol, and ether. Through elemental analysis the molecular formula was determined as $(C_6H_{10}O_5)_n$. Later in 1839, the term "cellulose" was first used in a report of the French academy on the work of Payen [51]. Cellulose has been used for about 150 years [51] and it is the most abundant natural polymer on Earth, as it is one of the main components of the cell walls of most plants [7], [52], [53] given its capacity to maintain a semi-crystalline state of aggregation in an aquatic environment [54]. On average,

Table 2.1: Characteristics of natural superabsorbent materials

Category	Type	Origins	Properties and Characteristics	Applications	Refs
Protein	Collagen & Gelatin	Collagen is present in articular & bone tissues while gelatin is a heterogeneous mixture of polypeptides derived from collagens.	Easy isolation & solubilization, low cost, biocompatible, weak antigenicity, biodegradable & high water absorptency under load.	Hygiene products, food & pharmaceutical industries, medical field & agriculture.	[2], [46]
	Silk Fibroin	Produced by insects such as orbweaving spiders & silk worms.	Biocompatible, bioabsorbable, tuneable degradation, good mechanical properties, thermally stable, easy chemical modification & abundant.	Personal care products, tissue engineering, drug delivery & agriculture.	[2], [47]
Polysaccharide	Alginate	Brown algae.	Biocompatible, immunogenic, low cost & gel-formating property.	Drug release, tissue engineering & food industry.	[26], [48]
	Chitosan	Exoskeleton of animals & cell walls of fungi.	Biocompatible, immunostimulant, lower mechanical properties & reduced cytotoxicity, good swelling rate & mucoadhesive properties.	Drug delivery, wound dressing, tissue engineering cell encapsulation & water treatment.	[26], [46]
	Starch	Green plants (mainly potatoes & corn).	Abundant, biocompatible, good mechanical resistance & plasticity.	Drug delivery, telecommunication cable production, cosmetic creams, agriculture & adhesive, food, petroleum & paper industries	[26], [49]
	Carrageenan	Red algae.	Biocompatible, low immunogenicity & cytotoxicity, easy functionalization & tuneable physicochemical properties, water-retention a gel-forming properties.	Drug delivery, tissue engineering wound healing & food industry.	[26], [50]
	Cellulose	Cell wall of terrestrial plants, algae & bacteria.	Biocompatibility, thermal & chemical stability & high hydrophilicity.	Drug delivery, tissue & wound engineering dressing paper & textile industries. Personal hygiene products.	[26], [30]

plant matter contains about 33% cellulose organisms [53], although the concentration varies depending on the type of plant [55]. Figure 2.7 represents the major pathways of cellulose synthesis.

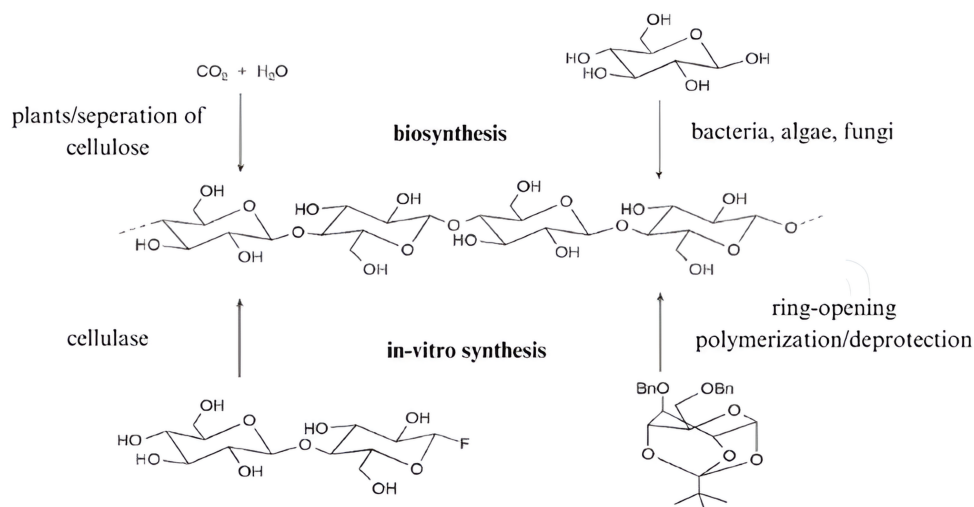


Figure 2.7: Major pathways of formation of cellulose (Adapted from: [54])

Among polysaccharides, cellulose possess both hydrophilicity and robust mechanical properties. These properties are attributed to the multiplicity of hydroxyl groups present, which preferentially form hydrogen bonds with water (in amorphous domains) or with the hydroxyl groups of neighboring polymer chains (in crystalline domains) [56]. Moreover, cellulose, being a natural polymer, presents low toxicity and excellent biodegradability and biocompatibility properties. In this manner, hydrogels produced from cellulose present high adsorption due to his multiple hydroxyl groups and superior mechanical, biocompatibility and biodegradability properties suitable for biomedical applications [57].

2.2.1.1 Cellulose Structure and Properties

Cellulose is made up of two anhydroglucose units (AGU) linked to each other by an oxygen covalently attached to C1 of one glucose ring and to C4 of the adjacent ring, called $\beta(1-4)$ glycosidic bond [58]. As illustrated in Figure 2.8, one end of the chain is terminated with a D-glucose unit, while the other end is terminated with a C4-OH group, referred to as the non-reducing end. The terminating group at the opposite end of the chain is a C1-OH group, known as the reducing end, which includes an acetal structure [54].

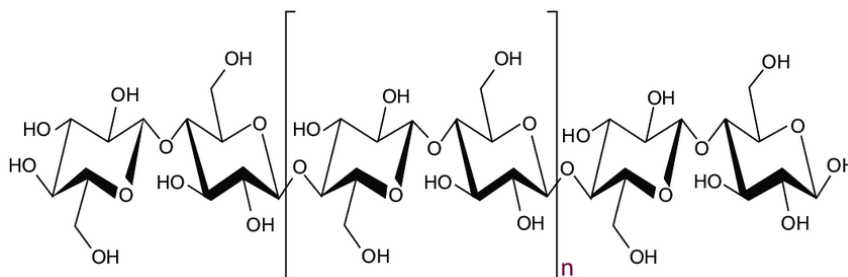


Figure 2.8: Molecular structure of cellulose (Adapted from: [59])

The hydroxyl groups found in cellulose macromolecules are involved in several intra- and intermolecular hydrogen bonds and cause parallel arrangement of multiple cellulose chains, forming elementary fibrils, which aggregate into the lowest well-defined morphological entity, namely microfibrils that lead to different ordered crystalline configurations [58], [60]. The crystalline packing is especially important when dealing with physical properties manipulation. Therefore, intra- and intermolecular hydrogen bonds are responsible for the high crystallinity, rigidity, and consequently the insolubility (in water and most organic solvents) of cellulose [58]. The cellulose limited solubility in water and organic solvents impose a challenge for the synthesis of hydrogels from cellulose and its derivatives [61]. Over the years, several solvent systems for the cellulose have been studied, such as ionic liquids, LiOH/urea, NaOH/urea, NaOH/thiourea[7], NaOH/CS₂ (viscose process), N-methylmorpholine-N-oxide(NMMO, liocell process), Li/N,N-dimethylacetamide (DMAc), and tetrabutylammonium fluoride/dimethyl sulfoxide (TBAF/DMSO) [62] to cleave the strong bonds between the cellulose chains [63]. Among these, the NaOH/urea solvent system stands out due to its ease of preparation, cost-effectiveness, practicality, and capacity to enhance cellulose dissolution rates at low temperatures [7]. Within this system, alkali species hydrate and intertwine with cellulose chains to form a hydrogen-bonded network at reduced temperatures. Concurrently, urea hydrates self-assemble onto this networks surface, culminating in a transparent, stable solution [63].

As mentioned, this compound has been used from ancient times by humans in various ways and therefore are currently several cellulose derivatives (Figure 2.9). Most of these derivatives which are presented in Table 2.2 are mainly obtained by chemical or physical modification [54], [64].

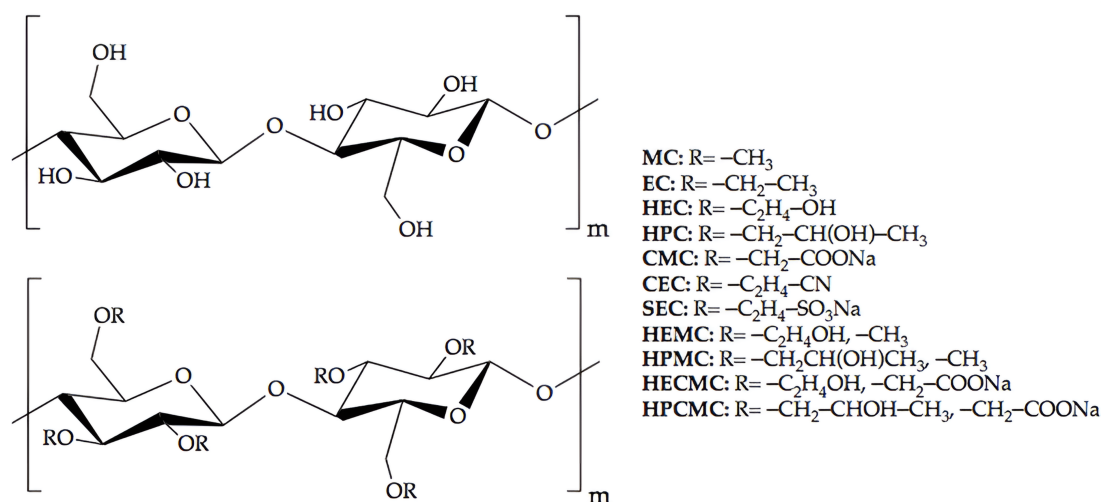


Figure 2.9: Chemical structure of cellulose and some of its derivatives (Adapted from: [64])

2.2.1.2 Synthesis of Cellulose-based Hydrogels

Hydrogels can be fabricated by different methods, through the crosslinking of stable polymeric networks which can occur after the polymer chain is synthesized, or with the growth of the polymer chain. In this manner, the synthesization of hydrogels begins with monomers, pre-polymers, and polymers [19]. The two main methods of crosslinking to produce hydrogels are physical and chemical [7], even though chemical synthesis methods are the most commonly used to manufacture cellulose-based superabsorbent hydrogels [2].

Table 2.2: Properties and usage of some of the cellulose derivatives (Adapted from: [64]).

Name	Properties	Usage	Refs
Phosphate cellulose	-	Enrichment agents, ion exchangers.	[65]
Nitrocellulose	Crystalline crosslinking.	Coatings, adhesives, cosmetics, food packaging, centrifugation & tube materials.	[66]
Cellulose acetate	Biodegradable, renewable, non-corrosive, non-toxic & biocompatible.	Nanocomposites for biomedical applications & equipment.	[67]
Methylcellulose	High water retention, thermo-gelation, macro-phase separation & syneresis.	Slow-release preparation.	[68]
Ethylcellulose	Thermoplastic, water insoluble, nonionic, thermally stable & hydrophobicity.	Controlled release formulations, coating agents.	[69], [70]
Carboxymethyl cellulose	Hydrophilic, bioadhesive, non-toxic, pH sensitive, thermally stable.	Hindering crystallization or degradation of the drug. Enhancing the frequency of drug release.	[69], [71]
Hydroxyethyl cellulose	Suspension, adhesion, emulsification, dispersion & moisture.	Food stabilizers, thickeners, adhesives, pharmaceutical excipients, stabilizers, film coating agents.	[30]
Hydroxypropyl cellulose	Biodegradable & biocompatible, self-repairing abilities, shape memory, unique hydrophilic/hydrophobic change.	Thermo-responsive hydrogels.	[72]
Hydroxypropyl methylcellulose	Viscous soluble fiber, high viscosity, gelling.	Thickener, emulsifier, stabilizer, gelling agents, antioxidants & hypoglycemics.	[73], [74]
Hydroxyethyl methylcellulose	Water solubility, thermally stable & gel properties.	Hypoglycemics, antioxidant, coatings, medical dressings.	[74], [75]

1. *Physical Crosslinking*

In physically crosslinked hydrogels, also referred to as pseudo-hydrogels or thermally reversible hydrogels, the polymeric network is established through a combination of Van der Waals forces, hydrogen bonds, ionic bonds, and hydrophobic interactions [64]. Despite their potential suitability for biomedical applications owing to the absence of chemical crosslinking agents, and thus, avoiding potential cytotoxicity from unreacted chemical crosslinker [76], physically crosslinked hydrogels are reversible, in nature [64] and thus present mechanical instability. Consequently, they may naturally dissolve over time [77] and could undergo degradation in an unpredictable manner [30]. Cellulose-based hydrogels (CBHs) synthesized via physical crosslinking methodologies, including freeze-thaw cycles, phase-inversion, heating and cooling, pH shifting, mixing polyanions and polycations, or mixing a polyelectrolyte solution with an oppositely charged multivalent ion [78] often exhibit poor mechanical strength [79]. Nevertheless, physically crosslinked hydrogels find major use in adsorption applications due to their large porosity, which boosts the possibility of pollutant adsorption. Additionally, these hydrogels display minimal pH

sensitivity, simple regeneration, and can sustain their adsorption capability without undergoing degradation arising from interactions with crosslinkers inherent in chemical processes. [79].

2. *Chemical Crosslinking*

On the other hand, chemically crosslinked hydrogels have permanent junctions, which makes them suitable for long-term use [77]. The process is not spontaneous [77] and the hydroxyl groups of cellulose can be covalently linked to the amine, carboxyl, or amide group of the added crosslinking agents [80]. The chemical crosslinking of CBHs are described in literature as being achieved through various methods: (1) grafting; (2) the use of crosslinking agents; (3) radical polymerization; (4) enzyme crosslinking, where enzymes catalyze the formation of covalent bonds between polymer chains; and (5) radiation polymerization to create robust, high stable crosslinked hydrogels [61]. The most widely implemented crosslinkers for cellulose are citric acid, epichlorohydrin, aldehydes and aldehyde-based reagents, urea derivatives, carbodiimides, and multifunctional carboxylic acids [4], [80]. These crosslinkers facilitate the formation of covalent bonds with the hydroxyl groups present in cellulose and/or react with functional groups within the cellulose molecules to create a crosslinked network [79]. Most of the CBHs are synthesized using chain growth polymerization process [79] which is an effective methods for producing superabsorbent hydrogels because it offers improved regulation over the polymerization heat, and reduced cost [2].

Typical polymerization methods for the synthesis of hydrogels are stated below. Free radical polymerization is an established technique for synthesizing CBHs using solution polymerization. It is known for its ease application under different reaction conditions, an extensive range of temperatures and wavelengths that could be used, and low costs. The process typically involves three stages: initiation, propagation, and termination [79]. In this process, cellulose macromolecules generate free radicals through initiators [2] such as benzoyl peroxide, 2,2-azo-isobutyronitrile (AIBN), ammonium peroxydisulphate (APS), potassium persulfate (KPS) and tetramethylene-diamine (TEMED) in the presence of certain light, pressure, temperature, and radiation (gamma, ultraviolet, electron beam [79], [81] or microwave radiation [2]) [79]. In the propagation phase, the radicals react with monomers to form a polymer chain and finally in termination the growth of the polymer chain is halted [79]. Other polymerization technique called suspension polymerization can be employed. In this case, the dispersed phase is aqueous, while the continuous phase is organic. Conventionally, the monomer is dissolved within the dispersed phase and surfactants ensure homogeneous monomer and other aqueous reagents dispersion throughout the continuous phase. Despite the capacity of this method to yield particles of desired sizes, the uses of organic solvents such as n-hexane and toluene presents challenges in purification [82]. Grafting involves the addition of monomeric units to the backbone of the cellulose polymer and has been utilized to change material properties, demonstrating enhancements by incorporating additional beneficial properties from specific monomers [7].

3. *Double Crosslinking*

Physical and chemical crosslinking have already been implemented together. Zhao *et al.* have proposed a strategy using sequential chemical crosslinking and physical crosslinking to form double-crosslinked cellulose hydrogels based on cellulose, alkali hydroxide and urea aqueous solutions. The authors reported transparent, foldable, elastic hydrogels and quick recovery properties. This new class of polysaccharide hydrogels presented a cellulose hydrogel with high strength and toughness with potential applications in artificial blood vessels and skin, tissue engineering materials, and catalyst carriers [64].

2.2.1.3 Applications of Cellulose-based Hydrogels

Cellulose-based hydrogels are being widely implemented in biomedical, drug delivery systems, and personal health care sectors but also in agriculture and horticulture, water treatment industries (Figure 2.10) [30] since cellulose is a highly abundant, biocompatible, biodegradable polymer and it also has high mechanical strength [80].

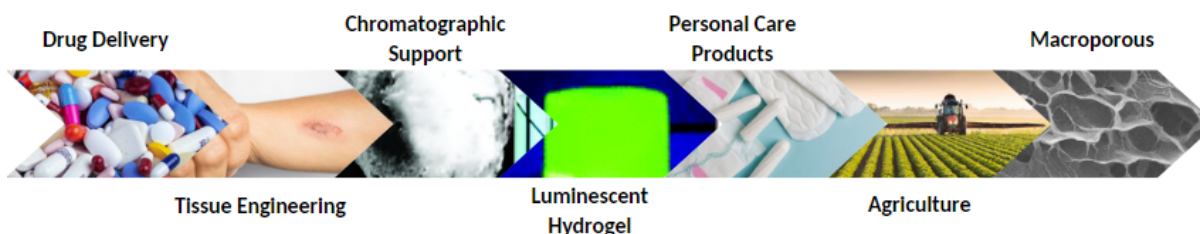


Figure 2.10: Applications of cellulose-based hydrogels (Adapted from: [83])

Although biodegradable health care products consist in a more sustainable option than commercially available ones, they have not either been industrialized or been commercially available and most of the cellulose-based hydrogels used in health products consists in an envelope of nonwoven tissue, a plastic cover material, and an absorbent fluff of wood pulp cellulose. Despite the advances, the commercialization of cellulose-based superabsorbents is still a challenge mainly due to their swelling and mechanical performance, and also the price compared with the conventional SAPs [2].

2.3 Suitability of Cellulose-based Hydrogels for Personal Care Products

In recent years, bio-based polymers represent a small but growing segment of the global hygiene products market driven by the increasing global demand for bio-based materials. The increasing attention for environmental issues called the attention for the development of natural absorbent materials with high absorption capacity, biodegradability and biocompatibility [2].

Among these bio-based materials, cellulose stands out as a particularly promising candidate for the primary source of hydrogels used in personal care products [4]. Its excellent hydrophilic, biocompatibility, and biodegradability properties represent a competitive advantage over synthetic polymers currently employed in these products [2], [30]. Nonetheless, the desired properties for the application can be achieved by functionalizing cellulose with active compounds [61]. As the consumer preference for sustainable products increases the future of cellulose-based hydrogels in the hygiene products market is expected to rise significantly [2].

Chapter 3

Materials and Methods

Chapter 3 focuses on specifying the materials used, as well as describing the tasks and main procedures. In addition, the characterization methods employed to evaluate the properties of the hydrogels are presented.

3.1 Materials

The industrial cellulose pulp, bleached eucalyptus kraft pulp (BEKP, DP \approx 1175), was supplied by Biotek (Altri, SGPS, SA, Portugal) and used without additional purification. Commercial diapers were purchased from Mercadona (Figueira da Foz, Portugal). Urea ((NH₂)₂CO, 99%) was acquired from ChemLab (Belgium), sodium hydroxide (NaOH, 99%) was bought from JGMS (Portugal) and sodium chloride (NaCl) was purchased in a local hypermarket Continente (Coimbra, Portugal). Allyl glycidyl ether (AGE, 99+%), 2-hydroxy-2-methylpropiophenone (HMP, 96+%), 2-(methacryloyloxy)ethyl trimethylammonium chloride (META, 80% in water), and acrylic acid (AA, 99+%) were obtained from TCI (Belgium).

Bis[2-(methacryloyloxy)ethyl] phosphate (BMEP, 98+%), 2-acrylamido-2-methyl-1-propanesulfonic acid (AMPS, 99%), phosphoric acid 2-hydroxyethyl methacrylate ester (PAHEMA, 90%), potassium phosphate dibasic (K₂HPO₄), potassium hydroxide (KOH, 84+%), and 3-sulfopropyl methacrylate (SPM, 98%), were all supplied by Sigma-Aldrich (Germany). Potassium dihydrogen phosphate (KH₂PO₄, 99.5+%) was obtained from Honeywell Fluka (Portugal). Deuterium oxide (D₂O, 99.9%) and sodium phosphate dibasic were acquired from Eurisotop (CotecNet, France) and Thermo Scientific (Portugal), respectively. N,N'-methylenebisacrylamide (BAAm, 98%) and ammonium chloride (NH₄Cl, 99.5%) were provided by Riedel-de Haën (Germany). Acrylamide (AAm, 98.5%) and sodium sulfite (Na₂SO₃, 98+%) were sourced from Acros Organics (Belgium). Deionized water was obtained by reverse osmosis system.

All reagents were used as received, except for META, which was purified by passing through aluminum oxide (Al₂O₃, 99%) before its use, supplied by Thermo Scientific (Portugal).

3.2 Preparation and modification of cellulose for hydrogel applications

3.2.1 Cellulose pulp pretreatment

The industrial cellulose pulp was submitted to a sulfuric acid hydrolysis to decrease the degree of polymerization (DP) of the cellulose chains [84], [85]. Briefly, a determined cellulose sample (150 g)

was mechanically defibrillated using a coffee grinder until obtain a cotton-like material. Then, ground pulp was added to a 3 l of diisopropilic ether with 10.5 mL of sulfuric acid and was mechanically stirred during 36 h at 450 rpm, at room temperature, as illustrated in Figure 3.1 - A. The suspended cellulose was vacuum filtered, added to a 0.5% KOH/ethanol solution for neutralization, washed with ethanol twice, and dried in an oven at 50°C for further usage. The filtration apparatus employed is represented in Figure 3.1 - B. A granulometry analysis was conducted on the cellulose powder and the final DP was calculated by intrinsic viscosity method $[\eta]$ at 25 ± 0.5 °C, using Mark Houwink equations [86].

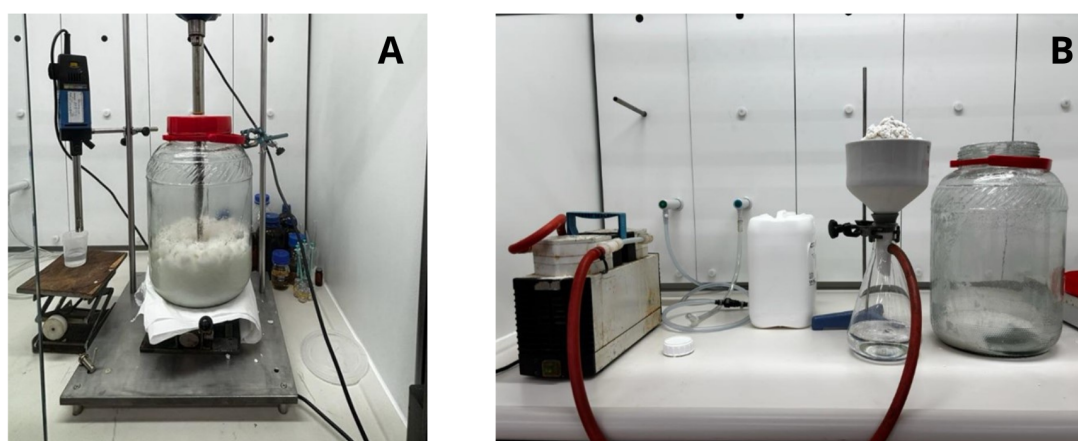


Figure 3.1: Process of cellulose sulfuric acid hydrolysis: (a) cellulose pulp hydrolyzed in sulfuric acid at 450 rpm for 36 hours, and (b) experimental setup for the filtration procedure.

3.2.2 Cellulose dissolution

Qi *et al.* reported that cellulose can be dissolved in a precooled 7 wt.% NaOH/12 wt.% urea aqueous solution [87]. A sample of the cellulose powder (6 g) was slowly added into a NaOH/urea/H₂O solution precooled at ≈ 5 °C and stirred until a homogeneous suspension is accomplished. Then, the suspension was frozen at ≈ -18.0 °C and thawed under vigorous magnetic stirring, to achieve a yellowish cellulose solution.

3.2.3 Cellulose modification

The modification of cellulose was carried out according to the procedure developed by Qi *et al.* [88] (Figure 3.2). Cellulose solution was added to a three-neck round bottom flask equipped with a dropping funnel and the system was sealed and purged with nitrogen for 15 min. Then, AGE was dropwise into cellulose solution. Various amounts of AGE were added to this solution, with molar ratios of AGU:AGE ranging between 1:3 and 1:5. The reaction continued for 24 hours at 30 °C, under nitrogen atmosphere. The reaction solution was precipitated and washed with previously cooled acetone. The acetone was decanted, and 50 mL of distilled water was added, stirred until redissolved and, purified using dialysis membranes (MWCO: 3,500 Da) against distilled water for three days until a neutral pH was reached. The pH was monitored with indicator paper, and the distilled water was replaced frequently. The final product was lyophilized, stored at approximately -18°C and protected from light.

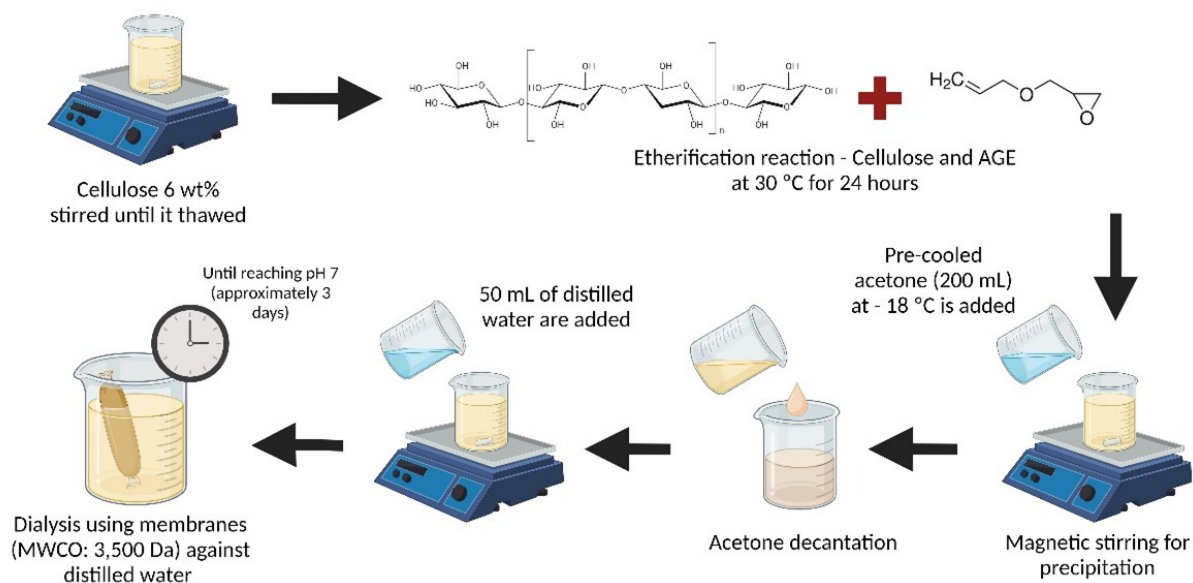


Figure 3.2: Protocol of cellulose modification for further biomedical applications.

3.3 Isolation of SAPs from commercial diapers

The absorbent interior of the diapers was accessed by carefully cutting along the sides with a scalpel. The absorbent core was then extracted, and the SAPs were isolated by sieving (Figure 3.3). As a result, a SAP sample from commercial diapers was obtained and utilized in subsequent experimental procedures as a positive control sample.

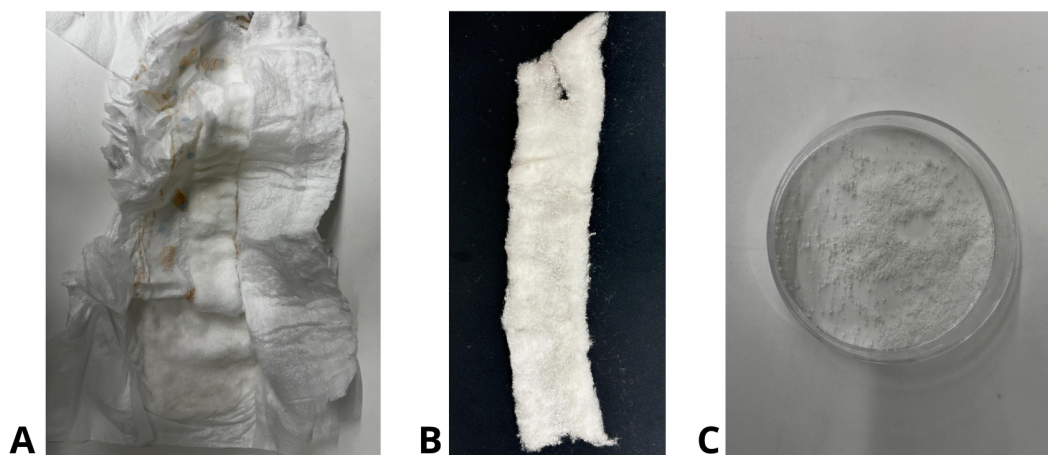


Figure 3.3: (a) Open configuration of a commercially available diaper. (b) Cross-sectional view of the absorbent core, demonstrating the heterogeneous distribution of SAPs. (c) Isolated SAPs extracted from the absorbent core, prepared for detailed characterization.

3.4 Preparation of cellulose-based hydrogels

The cellulose-based hydrogels copolymerized with synthetic monomers were obtained through the following procedure. Monomers employed are mentioned in Chapter 4. Freeze-dried cellulose was dissolved in distilled water (10 mL) and stirred until complete dissolution. Following this, the required monomers and the crosslinking agent were added to the mixture, and after full dissolution, a UV-light ini-

tiator (2-hydroxy-2-methylpropiophenone) was added. The resulting solution was subsequently placed into a petri dish and subjected to ultraviolet radiation for 4 hours. After polymerization, hydrogels were dried using three different methods: (1) oven dried, at 50 °C; or underwent a solvent exchange with (2) ethanol, and (3) methanol, and consequently air-dried for 24h at room temperature. Then, for characterization purposes, hydrogels were prepared using four different conditions: (1) cut into circular shape (diam: 20 mm), (2) cryogenic fracture, (3) ground in a coffee grinder, and (4) coarsely hand-broken (see Appendix A.1). Several different monomers were tested for the preparation of cellulose-based hydrogels. Additionally, different monomers:cellulose, AGE:AGU ratios, and the percentages of crosslinking agent and initiator were investigated and are specified in Table alongside the different investigated topics.

3.5 Characterization techniques of hydrogels

The hydrogels prepared in this study underwent multiple characterization techniques to properly evaluate their properties. In this section, the techniques and characterization methods employed to assess the properties of hydrogels are described.

3.5.1 Fourier transformed infrared spectroscopy (FTIR)

The hydrogels underwent analysis via FTIR using a Nicolet™ iS20 Spectrometer (Thermo Scientific) equipped with a Smart iTX - Diamond ATR accessory. The analysis was conducted with a resolution of 4 cm⁻¹ and 64 accumulations. The spectra were obtained within the range of 4000–600 cm⁻¹, at room temperature, and subjected to smoothing and analysis using Curve Manager software (ACD/Labs), version 6.00.

3.5.2 Nuclear Magnetic Resonance Spectroscopy

Avance III HD 400 MHz spectrometer (Bruker, Germany) was used to acquired nuclear magnetic resonance (NMR) spectra, at a temperature of 25 °C. The equipment was fitted with a 5 mm TIX triple resonance detection probe.

3.5.3 Morphology

The hydrogels were firstly freeze-dried in liquid nitrogen and fractured to avoid potential plastic deformation. The pre-gold coated samples were then observed using a field emission scanning electron microscope (SEM), ZEISS MERLIN (Compact/VPCcompact, Gemini II, Germany), with an accelerating voltage of 1.0 kV.

3.5.4 Thermal properties

Thermogravimetric analysis (TGA) was employed to investigate the thermal stability of the hydrogels. A NETZSCH TG 209F1 Libra (Netzsch, Germany) instrument was utilized, operating at a heating rate of 10 °C/min within a temperature range of 25 °C to 600 °C under a nitrogen purge flow of 250 mL/min.

3.5.5 Gel Fraction

The gel fraction (GF) is a metric that determines the stability and efficacy of gels. For hydrogel samples (disks with a diameter of 2 cm), the GF assessment was carried out with the following procedure. Samples were initially dried out and weighed (W_1), and subsequently submerged in distilled water for 48 hours to remove any unreacted materials. The crosslinked gel was obtained by removing the samples and drying them until a constant weight was achieved (W_{dry}). The GF was calculated as [44], [89]:

$$Gel\ Fraction\ (\%) = \frac{W_{dry}}{W_1} * 100 \quad (3.1)$$

3.5.6 Free Swelling Capacity

Free swelling capacity (FSC) was evaluated by gravimetry method. The samples were dried until they reached a constant weight (W_{dry}). These samples were then submerged in 50 mL of deionized water and weighed at specific time intervals (W_t) to observe the swelling behavior. Equilibrium swelling measurements were taken after 24 hours. All measurements were acquired at room temperature. Excess surface water was carefully wiped off with absorbent paper to obtain accurate mass determinations. The degree of swelling was estimated based on the ratio between the mass of the swollen gel and the dry gel, using the following formula [44], [89], [90]:

$$Swelling\ Ratio\ (g/g) = \frac{W_t - W_{dry}}{W_{dry}} \quad (3.2)$$

where W_t represents the weight of the sample at a specific swelling time t , and W_{dry} represents the original dry weight of the sample.

3.5.7 Swelling – Synthetic Urine and pH Buffers

Hydrogels were subjected to swelling tests in synthetic urine and buffer solutions at pH 4 and pH 8. Similar to free swelling capacity, the swelling ratio was calculated using Equation 3.2. The synthetic urine was prepared by dissolving 25 g of urea, 9 g of sodium chloride, 2.5 g of sodium phosphate, 3 g of ammonium chloride, and 3 g of sodium sulfite in 750 mL of deionized water. The final volume was set to 1 L [84]. The buffers were prepared according to AAT Bioquest [91] procedures.

3.5.8 Water/Synthetic Urine Retention Capacity

The holding capacity of the hydrogels was evaluated over an 8-hour period following the same procedure for synthetic urine and water. The initial swollen mass of hydrogels was taken at equilibrium after hydrogels were submerged in the respective fluid. Mass measures were then taken at various time intervals (at room temperature). The mass loss was given by equation 3.3 [90].

$$Retention\ Capacity\ (\%) = \frac{W_t}{W_e} * 100 \quad (3.3)$$

where W_t represents the mass of the hydrogel at a specific time interval, and W_e is the initial mass of the hydrogel at equilibrium in water/synthetic urine.

3.5.9 Synthetic Urine Centrifuge Retention Capacity

Centrifuge retention capacity (CRC) refers to the ability of hydrogels to retain fluids after being saturated and centrifuged under controlled conditions [92]. The procedure was adapted from ISO 17190-6:2020 Urine-absorbing aids for incontinence — Polyacrylate superabsorbent powders Part 6: Test method for determination of the fluid retention capacity in saline solution by gravimetric measurement following centrifugation. A determined quantity of swollen SAPs (100 mg) in synthetic urine was centrifuge subjecting the sample at a g-force of about 250G (1400 rpm), for 3 min. The excess of fluid was removed, and the samples were reweighed. The CRC was calculated according to [44]:

$$CRC (g/g) = \frac{W_c - W_{dry}}{W_{dry}} \quad (3.4)$$

where W_c is the weight of the swollen hydrogel after centrifugation, and W_{dry} is the initial weight of the dry hydrogel.

3.5.10 Absorbency Under Load (AUL)

The method intended to evaluate the water absorption capacity of cellulose-based hydrogels under a specific applied load [92]. In the procedure, a 60 mm glass filter plate was positioned in a tray, and a 60 mm diameter filter paper was set on the plate. The tests were conducted with synthetic urine, ensuring that the fluid completely covered the filter paper and reached the upper surface of the filter plate, as illustrated in Figure 3.4. A pre-weighted dried sample was coarsely hand-broken (W_{dry}) and placed on the wet filter paper, and a cylindrical beaker was employed to apply a load of 50 g/cm² to the sample. After an hour, the sample was reweighed to determine the amount of fluid absorbed (W_{abs}). The absorbency under load was subsequently calculated using the following equation [84], [92]:

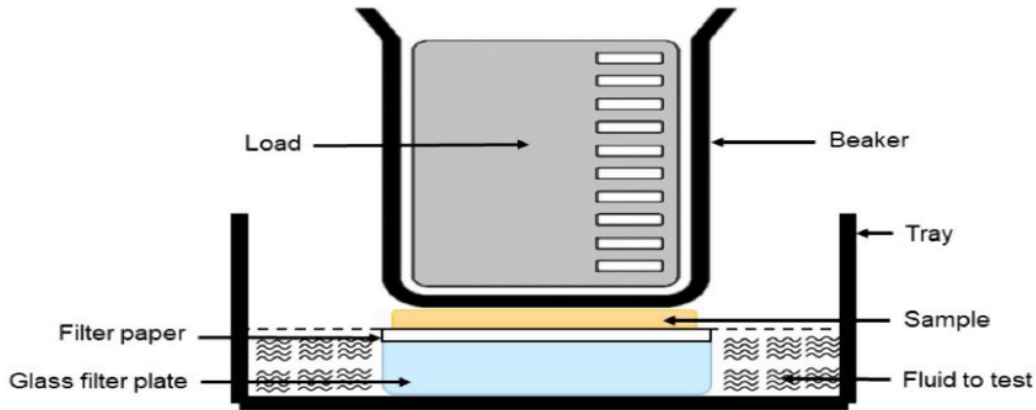


Figure 3.4: Schematic representation for AUL tests (Adapted from: [84]).

$$AUL (g/g) = \frac{W_{abs} - W_{dry}}{W_{dry}} \quad (3.5)$$

3.5.11 Biodegradability

A preliminary experiment was conducted over a 30-day period to evaluate the biodegradation behavior. Initially, the dried samples were weighted W_{dry} and subsequently buried under soil at a depth of 10 cm within a container. The soil was watered with distilled water and the experiment was kept at room temperature during the time interval. Upon retrieval, the samples were carefully extracted, washed with distilled water, and dried out at 50 °C until a consistent weight was attained. The final weight is measured W_{b} , and the biodegradability was determined by calculating the percentage of weight loss. The rate of degradation (%) of the specimens is estimated with equation 3.6:

$$\text{Degradation (\%)} = \frac{W_{\text{dry}} - W_{\text{b}}}{W_{\text{dry}}} * 100 \quad (3.6)$$

3.5.12 Cytotoxicity

The hydrogels were sterilized for 45 minutes with UV-light irradiation beforehand for in vitro assays. To evaluate the in vitro impact of hydrogels on cell viability and proliferation, NHDF fibroblast cells were dispersed on the surface of each sample at a density of 1×10^5 per well. Cell-seeded hydrogels were kept at 37°C and 5% CO₂ for 3 and 7 days. Colorimetric CellTiter 96®Aqueous One Solution Cell Proliferation Assay (MTS assay, Promega, USA) was employed to determine the cell viability of the fibroblasts on the hydrogels after the incubation time points, in accordance with the instructions provided by the manufacturer. Briefly, cell-seeded mats were incubated at 37 °C for 3 hours after the complete culture medium in each well was replaced with 450 μL serum-free culture medium and 50 μL MTS reagent. Then, 100 μL (in triplicate) of solution from each well was placed into a 96-well plate, and the absorbance at the wavelength of 490 nm was determined via a spectrophotometric microplate reader. Untreated NHDF cells, i.e., cells seeded directly over the surface of the wells, without hydrogels, were used as controls. Cell viability was calculated as the percentage of survival relative to the untreated NHDF cells, which were considered to have 100% viability.

3.5.13 Statistical Analysis

All quantitative data were obtained from three independent experiments. Values on this study were reported as mean ± standard deviations (SD). Significant differences among each experimental group were determined through one-way analysis of variance (ANOVA), followed by Tukey's multiple comparisons test. A *p* value lower than 0.05 (**** *p*<0.0001) was considered as being statistically significant. Data analysis was performed in GraphPad Prism version 10.4 XML Project (GraphPad Software Inc., La Jolla, CA, USA).

Chapter 4

Results and Discussion

In this chapter, the results from the prepared hydrogels will be presented and discussed. In addition, the chemical, thermal and morphological characterization of the hydrogels considered to have the most relevant properties for personal care products will be presented.

4.1 Cellulose Derivatives Preparation and Characterization

The NaOH/Urea/H₂O solvent system confines the maximum molecular weight of cellulose chains to less than 10⁵ g/mol, which translates to a DP of 617 [84]. In that sense, through chemical hydrolysis, the DP of cellulose fiber was calculated and confirmed to reduce from ≈ 1175 to ≈ 280 . A particle size analysis of cellulose was carried out to assess the particle size following chemical hydrolysis. Figure 4.1 reveals the histogram of particle size distribution. Approximately 90% of the cellulose material was able to pass through the 45 μm sieve which suggests that the resulting powder is very homogenous in particle size. Both DP and particle size are in line with those from microcrystalline cellulose (MCC), like Avicel® and other commercialized MCC grades. Also, cellulose powders achieved by other hydrolysis techniques resulted in similar DP values [84], [85].

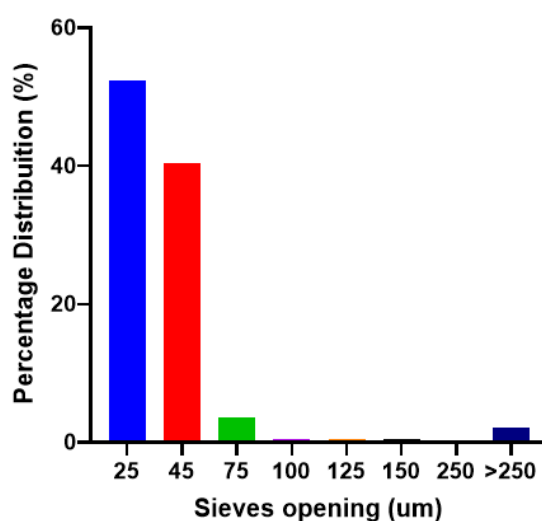


Figure 4.1: Particle size distribution of cellulose after sulfuric acid hydrolysis.

Qi *et al.* reported that cellulose can react directly with AGE in a precooled NaOH/Urea/H₂O aqueous solution because the basicity of the solvent is sufficient to start the etherification [88]. Cellulose was successfully modified with AGU:AGE ratios ranging from 1:3 to 1:5, as depicted schematically in Figure 4.2 [88]. During the reaction conditions for the synthesis of 3-allyloxy-2-hydroxy-propyl cellulose (AHP-cellulose), the solution remained translucent and homogeneous as the reaction proceeded.

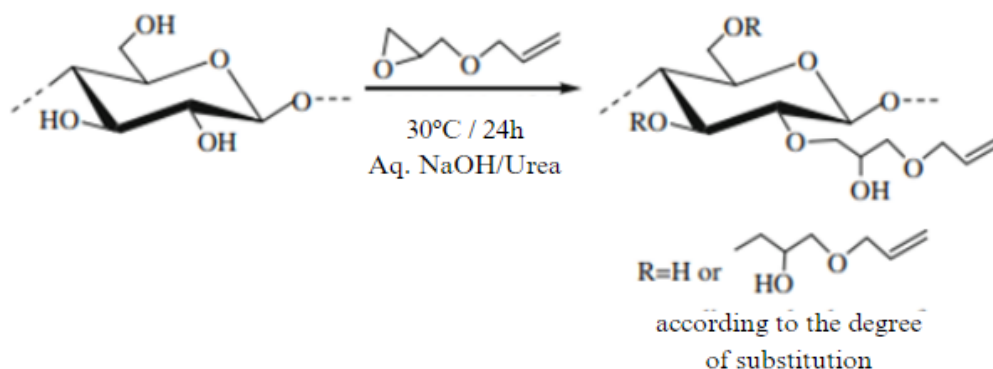


Figure 4.2: Formation of AHP-cellulose using cellulose dissolved in a 7 wt% NaOH and 12 wt% urea aqueous solution (Adapted from: [88]).

Cellulose derivatives were characterized with ¹H NMR (Figure 4.3) to verify the existence of ethylenic protons and determine the degree of substitution (DS). The DS (Table 4.1) was calculated by dividing the integration area of the H11 and H12 peaks by the area of the anomeric proton (H1) (see Appendix B.1) [93]. The signals between 5.3 and 6.1 ppm in Figure 4.3 confirm the existence of ethylenic protons (H11 and H12) in the cellulose derivatives. The peak detected between 4.4 and 4.6 ppm corresponds to the α -anomeric proton of the glucose residues (H1). Lastly, peaks identified within 3.1 to 4.1 ppm were assigned to the remaining protons. Figure 4.3 and Table 4.1 shows that the substitution degree increases with higher amount of AGE. These findings suggest an increased number of -OH groups react with the AGE epoxy moiety, leading to a stronger conversion of double bonds.

Table 4.1: Cellulose derivatives conditions and DS.

Sample ^a	AGU:AGE Molar Ratio (wt. %)	DS ^b
Cell_3	1:3	0.76
Cell_4	1:4	0.96
Cell_5	1:5	1.21

^a Labeled according to Cell_*a*, with *a* indicating the number of AGE equivalents.

^b Determined by ¹H NMR method.

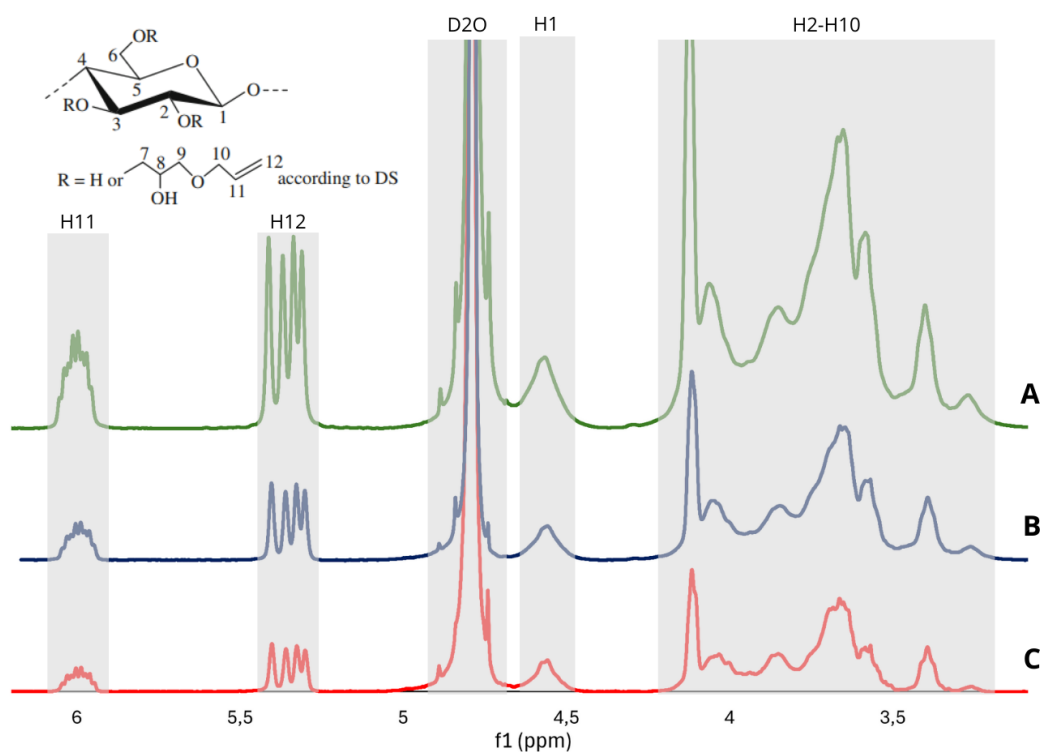


Figure 4.3: ^1H NMR spectra of cellulose derivatives prepared with (a) five, (b) four, and (c) three equivalents of AGE. All the spectra were obtained in deuterium oxide, and the peak of solvent used as reference.

Further confirmation of the synthesis of the cellulose derivatives was obtained by FTIR spectra (Figure 4.4). FTIR spectra of Cell_5 was used as model to confirm the modification. Cellulose powder and Cell_5 exhibit the characteristic band in the range of $3600\text{--}3200\text{ cm}^{-1}$, which corresponds to the stretching vibration of the hydroxyl groups in the O-H bonds [84]. The presence of a peak at 1645 cm^{-1} in the cellulose derivatives and absence in the cellulose powder, can be attributed to the stretching of C=C bonds [88], confirming that cellulose was successfully modified with AGE.

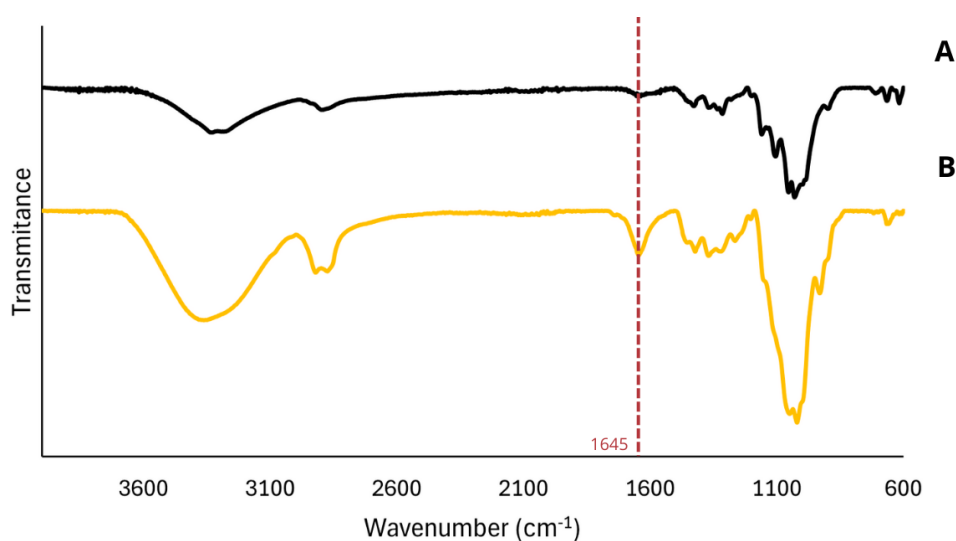


Figure 4.4: FTIR spectra of (a) cellulose powder and (b) cellulose derivative prepared with five equivalents of AGE.

4.2 Cellulose-Based Hydrogels Preparation

To assess the suitability of cellulose hydrogels, cellulose homopolymers hydrogels were prepared using AHP-cellulose as macromonomers. Table 4.2 shows that hydrogels with lower degrees of modification have higher swelling values. This higher swelling capacity is linked with a small decrease in gel fraction suggesting that although lower modification increases water absorption capacity, the polymer network formed is less crosslinked, as expected. Nevertheless, cellulose hydrogels presented gel fraction values over 90%, indicating a very stable polymer network [94], [95].

Table 4.2: Conditions, maximum swelling and gel fraction obtain from cellulose homopolymers prepared with three different DS.

Sample ^a	Crosslinker (wt.%) ^b	Initiator (wt.%)	Maximum Swelling (g/g)	Gel Fraction (wt.%)
Cell_3	0.5	1	11,0	91,5
Cell_4	0.5	1	8,5	94,9
Cell_5	0.5	1	8,4	97,7

^a Labeled according Cell_*a*, with *a* representing the number of AGE equivalents of cellulose.

^bBAAm used as crosslinker.

In hygiene absorbent products, like diapers, superabsorbent materials should absorb and hold significant quantities of fluid while also preventing leakage [2], [4]. In this case, the highest stated swelling value was 11.0 g/g, in sample Cell_3, which reflects low swelling capacities compared to the commercially available, which can reach swellings into the 64.2-102.1 g/g range [92]. In order to enhance cellulose-based hydrogels absorbency properties, a study was conducted by copolymerizing cellulose with other monomers.

4.2.1 Most common monomers for superabsorbents hydrogels

Acrylic acid (AA), acrylamide (AAM) and their derivatives (Figure 4.5) are synthetic monomers extensively used in the manufacture of superabsorbent hydrogels [43], [44], [96], [97]. These monomers possess in their structure hydrophilic groups such as -COOH, -SO₃H, -NH₂, and -OH, which contribute significantly to their swelling capacity [97].

AAM is the main monomer used in the production of superabsorbents hydrogels. AAM-based hydrogels exhibit sensitivity to both physical and chemical stimuli. Although, the acrylamide-based hydrogels have superior swelling features [97], the monomer is known for its carcinogenic nature [98]. In this manner, in human applications, it becomes crucial to synthesize hydrogels with a minimal quantity of residual monomers and undesirable side reaction products [95] since reactants used in synthesis could originate hazardous and poisonous by-products [23], [95].

AA is another monomer often crosslinked to result in hydrogels with a high water absorption capacity [97]. Acrylic acid, also known as propene acid, has a carboxyl group, which can ionize in water, forming carboxylate anions (-COO⁻). During the ionization process the hydrophilicity of the polymer increases which enhances its ability to absorb and retain large amounts of water. Additionally, acrylic acid produces pH sensitive hydrogels with greater swelling properties at pHs higher than its pKa (pKa = 4.25) [99]. The neutralization of AA forms sodium/potassium acrylate (AANa/AAK) [100]. This monomer has sodium/potassium ions (Na⁺/K⁺) which enhance the affinity for water and results in higher swelling capacity [101].

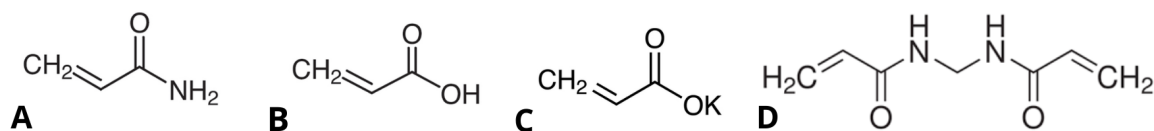


Figure 4.5: Chemical structure of (a) acrylamide [102], (b) acrylic acid [103], (c) potassium acrylate [104] and (d) N,N'-methylenebisacrylamide [105].

In this work, the swelling capabilities of synthetic monomers were investigated by co-polymerizing acrylamide, acrylic acid and potassium acrylate (prepared with 75% neutralization). Moreover, cellulose-based hydrogels copolymerized with AAK and AAm were prepared to evaluate the effect of cellulose on swelling capacity and gel content. The crosslinking agent selected was N,N'-methylenebisacrylamide (BAAm) owing to its common application in the production of superabsorbent hydrogels [106], [107]. All the conditions and formulas are specified in Table 4.3.

Table 4.3: Formulation and synthesis conditions for homopolymers and cellulose copolymerized hydrogels with AA, AAm, and AAK. All hydrogels were prepared with 1 wt.% of initiator.

Sample ^a	CellM ^b	Cell:Mon Ratio (wt.%) ^c	Monomers (wt.%)			BAAm (wt.%)
			AA	AAm	AAK	
AA_C1.0	-	0:100	100	0	0	1
AAm_C1.0	-	0:100	0	100	0	1
AAm:AA_C1.0	-	0:100	50	50	0	1
AA_C0.5	-	0:100	100	0	0	0.5
AAm_C0.5	-	0:100	0	100	0	0.5
AAm:AA_C0.5	-	0:100	50	50	0	0.5
AAK_C0.5	-	0:100	0	0	100	0.5
AAK:AAm_C0.5	-	0:100	0	50	50	0.5
Cell_AAK_C0.5	5	50:50	0	0	50	0.5
Cell_AAK:AAm_C0.5	5	50:50	25	0	25	0.5

^a Samples were named following the format *a_Cb*, where *a* represents the incorporated monomers and *b* indicates the quantity of crosslinking agent.

^b Number of AGE equivalents in the cellulose derivative.

^c Cellulose and monomers content ratio in prepared gel.

Figure 4.6 shows the FTIR spectra of cellulose powder, lyophilized (Lyo) cellulose, and dried hydrogels (DH) of cellulose homopolymer as well as hydrogels of cellulose copolymerized with acrylic acid AA and AAK. FTIR spectra confirm the copolymerization of cellulose with AAK and AAm. Asymmetric and symmetric stretching of the carboxylate groups (COO⁻) and C-N were identified in peaks at 1557 cm⁻¹ and 1402 cm⁻¹, respectively [108]. Comparing Cell_AAK:AAm_C0.5 with Cell_AAK_C0.5, the amide peak I (1650 cm⁻¹) increased following a rising trend of AAm content, revealing the presence of acrylamido groups in hydrogels [84].

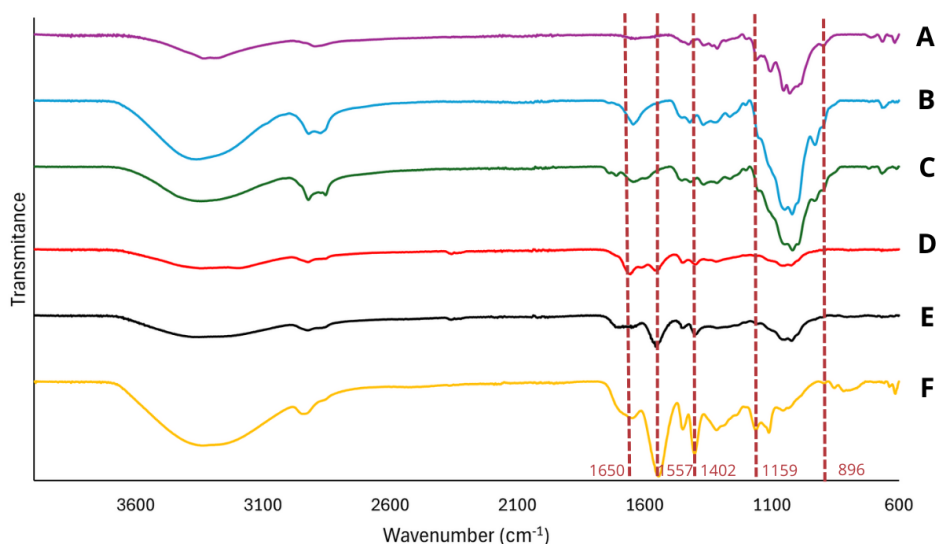


Figure 4.6: FTIR spectra of (a) cellulose powder, (b) Cell_Lyo, (c) Cell_5_DH (d) Cell_AAK:AAm_C0.5_DH, (e) Cell_AAK_C0.5_DH, and (f) SAPs extracted from commercially available diapers.

Additionally, it is noteworthy that the band at 1650 cm^{-1} corresponds to the double bonds of cellulose. In spectrum C it is observed that cellulose does not fully polymerized. The FTIR spectrum of SAPs isolated from diapers showed characteristic bands at 1650 cm^{-1} , 1557 cm^{-1} , and 1402 cm^{-1} , confirming the presence of a polyacrylate-type polymer in the diaper samples. The absence of band between 1159 cm^{-1} and 896 cm^{-1} confirmed that diapers SAPs do not contain cellulose in their composition.

The results of swelling absorbance and gel fraction (Figure 4.7) were in line with the existing literature [23], [109], showing that synthesized hydrogels with a lower percentage of crosslinker have a higher swelling ratio because the polymer structure becomes less compacted. Figure 4.7 - A demonstrated that AAm hydrogels showed a lower swelling property compared to other hydrogels. However, when AAm is copolymerized with AA to form hydrogels, the outcomes are superior. This enhancement can be attributed to the higher hydrophilicity of AA compared to AAm, which increases the capacity of hydrogels to absorb water [99].

The AAK_C0.5 and AAK:AAm_C0.5 achieved swelling values of 1920.2 g/g and 1408.2 g/g , respectively. These results are in accordance with what was mentioned previously, since potassium acrylate includes, in addition to a carboxyl group, a K^+ ion, which provides greater swelling capacity [101]. Yet the swelling values reduce dramatically to 10.9 g/g (Cell_AAK_C0.5) and 10.3 g/g (Cell_AAK:AAm_C0.5) when are copolymerized with cellulose suggesting a significant change in the polymer structure that limits its maximum swelling capacity.

The higher percentage of the gel fraction implies an increased number of covalent bonds, causing a larger density of crosslinks inside the hydrogel [94] and a very stable polymer networks [95]. The higher density of networks reduces its expansion capacity, which results in a lower swelling ratio [94] as is illustrated in Figure 4.7. On the other hand, a lower gel fraction reflects a decreased amount of monomer incorporation during polymerization [94], [95].

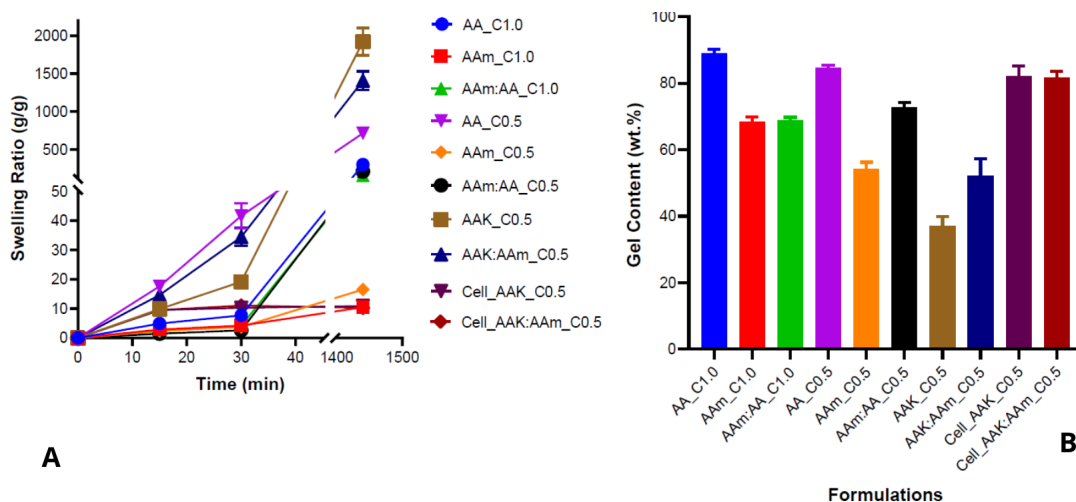


Figure 4.7: Homopolymers and cellulose copolymerized hydrogels with AA, AAm, and AAK (a) water swelling kinetics and (b) gel fraction. Gels with $\phi = 20$ mm were open air dried after solvent exchange with ethanol. Mass measurements were taken at 15 min, 30 min, and at equilibrium. For the legend see Table 4.3.

The results revealed gel fractions varying between 37.0 wt.% and 88.9 wt.% with low values representing low extension of polymerization which could be a risk to human health if monomers are still present since the repeated or prolonged exposure to these chemicals can lead to skin sensitization, allergic reaction, target organ damage, or irritation [23], [95]. Figure 4.7 - A highlights the high swelling features of both AAK_C0.5 and AAK:AAm_C0.5. Nevertheless, Figure 4.7 - B indicates that the gel fraction of these hydrogels are 37.0 wt.% and 52.3 wt.%, respectively. However, the incorporation of cellulose with these formulations significantly raise the gel fraction values to 82.3 wt.% and 81.6 wt.%, respectively. These findings align with the role of cellulose, with multiple reactive sites [110], allows the binding of monomers to a structural polymer chain. This contributes to an increased gel content, which supports the theory of a more effective integration of monomers into the gel network, hence reducing the presence of unreacted monomers.

4.2.2 Alternative monomers for superabsorbents hydrogels

Figure 4.10 present three unconventional synthetic monomers employed in personal care products. All three are hydrophilic monomers with an ionic nature that improves water absorption and retention capacity [23], [97].

The compound known as 2-acrylamido-2-methylpropane sulfonic acid (AMPS, Figure 4.8 - A) is highly soluble in water, thermally stable, resistant to hydrolysis, and retains stability across a broad pH range [111]. Not to mention, superabsorbent materials capable of achieving maximum swelling of 2618 g water/g dry hydrogel have been produced from 3-sulfopropyl methacrylate potassium salt (SPM, Figure 4.8 - B) [112]. The phosphate group present in phosphoric acid 2-hydroxyethyl methacrylate ester (PAHEMA, Figure 4.8 - C) and bis[2-(methacryloyloxy)ethyl] phosphate (BMEP, Figure 4.8 - D) is expected to increase the biodegradability of polymers. BMEP was selected as the crosslinking agent [113]. The solutions containing PAHEMA monomer were adjusted to a basic pH ($\text{pH} \approx 8$) with a NaOH 10M solution. Table 4.4 presents the formulations tested with these monomers.

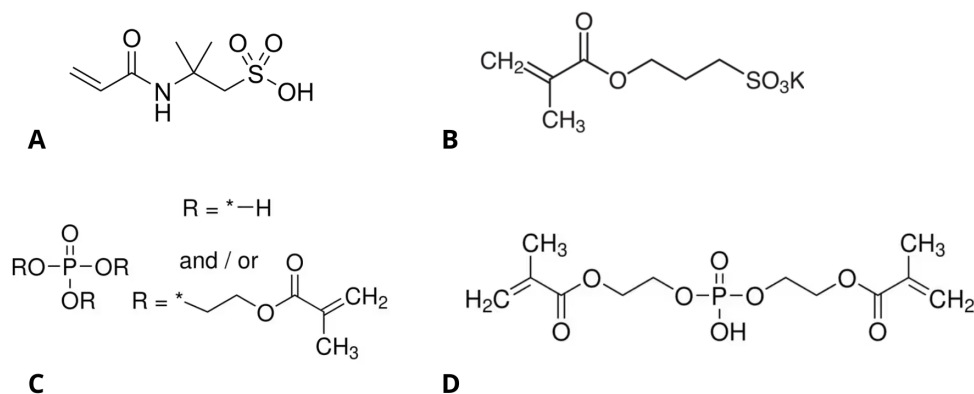


Figure 4.8: Chemical structure of (a) AMPS [114], (b) SPM [115], (c) PAHEMA [116] and (d) BMEP [117].

Table 4.4: Formulation and conditions of cellulose-based hydrogels copolymerized with AMPS. All hydrogels were prepared with 1 wt.% of BMEP and initiator.

Sample ^a	CellM ^b	Cell:Mon Ratio (wt.%) ^c	Monomers (wt.%)		
			SPM	PAHEMA	AMPS
Cell_A	5	50:50	0	0	50
Cell_S1:A1	5	50:50	25	0	25
Cell_S2:P1:A1	5	50:50	25	12.5	12.5
Cell_S1:P2:A1	5	50:50	12.5	25	12.5
Cell_S1:P1:A2	5	50:50	12.5	12.5	25
Cell_S1:P1:A1	5	50:50	16.7	16.7	16.7

^a Samples were named following the format Cell_*ab:ab* format, where *a* represents the monomers incorporated in hydrogels and *b* the ratio between the three monomers (S as SPM, P for PAHEMA, and A as in AMPS).

^b Number of AGE equivalents in the cellulose derivative.

^c Cellulose and monomers content ratio in prepared gel.

It was noticed that including the AMPS monomer led to hydrogels with substantial rigidity, which rendered it impossible to carry out the swelling behavior characterization. Figure 4.9 highlights the outputs obtained during the tests of these hydrogels, illustrating their tendency to disintegrate and fragment during the tests.

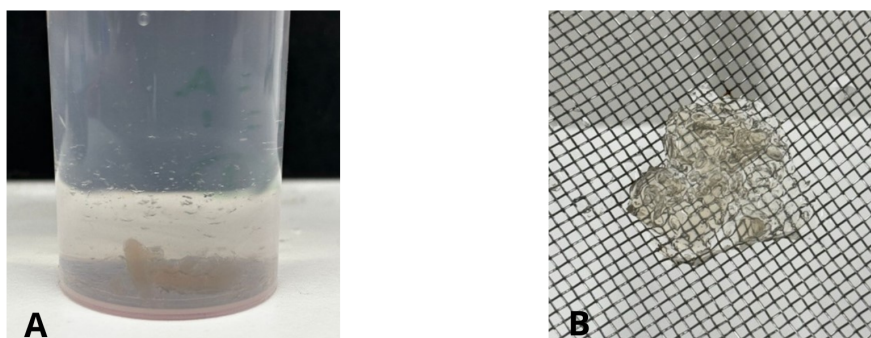


Figure 4.9: Swelling behavior and post-test disintegration of cellulose-co-AMPS hydrogels in which (a) represents the dynamic swelling behavior of cellulose-co-AMPS hydrogels under experimental conditions and (b) their disintegration post-test.

Given the challenges encountered, this monomer was discarded, and 2-(methacryloyloxy)ethyl trimethylammonium chloride (META, Figure 4.10) was explored as an alternative option. Besides being hydrophilic, the presence of a quaternary ammonium group in its structure can provide the superabsorbent material antimicrobial properties [118], which are highly beneficial for products designed for hygiene or medicinal purposes. Also, META cationic nature contrasting with the anionic nature of the other monomers can result in stronger electrostatic forces [20] and elevate the absorbency properties [19].

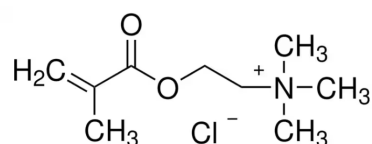


Figure 4.10: Chemical structure of META [119].

The monomer concentration in polymer formulation alters the crosslinking degree and the fraction of chain entanglements inside the hydrogels, and thus their viscoelastic characteristics and swelling degree [120]. In this way, the influence of the concentration the three monomers (SPM, PAHEMA and META) on the structure in cellulose-based hydrogels was carried out under the conditions stated in Table 4.5.

Table 4.5: The composition of the hydrogels investigated to analyze the effects of varying monomers concentrations. All hydrogels were prepared with 1 wt.% BMEP and initiator.

Sample ^a	CellM ^b	Cell:Mon Ratio (wt.%) ^c	Monomers (wt.%)		
			SPM	PAHEMA	META
Cell	5	0:100	0	0	0
Cell_S	5	50:50	50	0	0
Cell_P	5	50:50	0	50	0
Cell_M	5	50:50	0	0	50
Cell_S1:P1	5	50:50	25	25	0
Cell_P1:M1	5	50:50	0	25	25
Cell_S1:M1	5	50:50	25	0	25
Cell_S2:P1:M1	5	50:50	25	12.5	12.5
Cell_S1:P2:M1	5	50:50	12.5	25	12.5
Cell_S1:P1:M2	5	50:50	12.5	12.5	25
Cell_S1:P1:M1	5	50:50	16.7	16.7	16.7

^a Labeled according Cell_{ab}:ab format, with *a* indicating the monomers incorporated in hydrogels and *b* the ratio between the three monomers (S as SPM, P for PAHEMA, and M as in META).

^b Number of AGE equivalents in the cellulose derivative.

^c Cellulose and monomers content ratio in prepared gel.

Figure 4.11 shows (a) the water swelling kinetics and (b) gel fraction of gels prepared from the formulations of Table 4.5. The evaluation of the gel fraction showed that the observed gel content averaged 65.7%, which was lower than anticipated. Notably, the Cell_S formulation stood out among the others; however, the remaining swelling values are similar to those from cellulose control hydrogels, which led to the assumption that the crosslinking process was not effective.

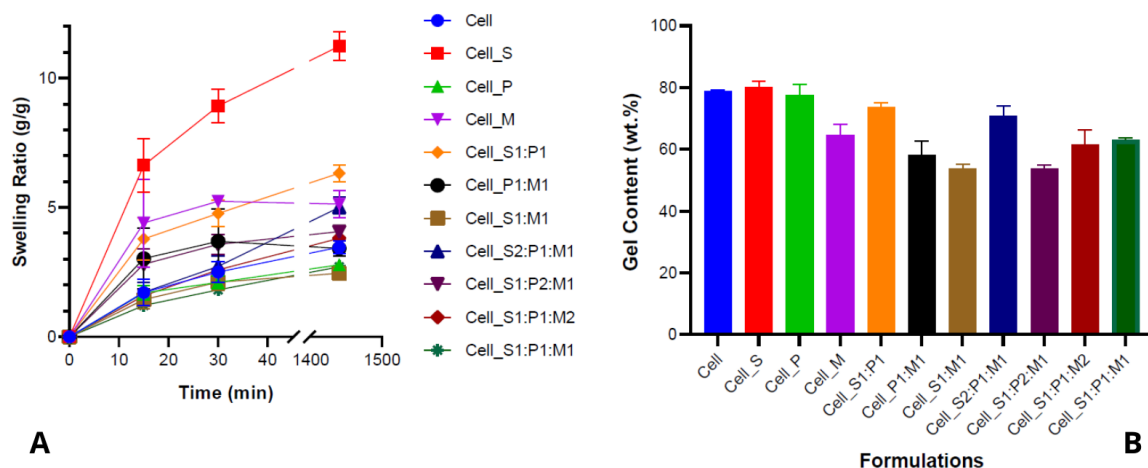


Figure 4.11: (a) Water swelling kinetics and (b) gel fraction of cellulose-based hydrogels varying monomers ratios. Samples with $\phi = 20$ mm of gels and dried in the oven. The free swelling absorbency was taken at 15 min, 30 min and at maximum swelling capacity. Legend in Table 4.5.

Subsequently, ^1H NMR (Figure 4.12) evaluation was performed into swelling water to determine the presence and/or absence of double bonds in the monomers and cellulose in order to determine the crosslinking process occurrence.

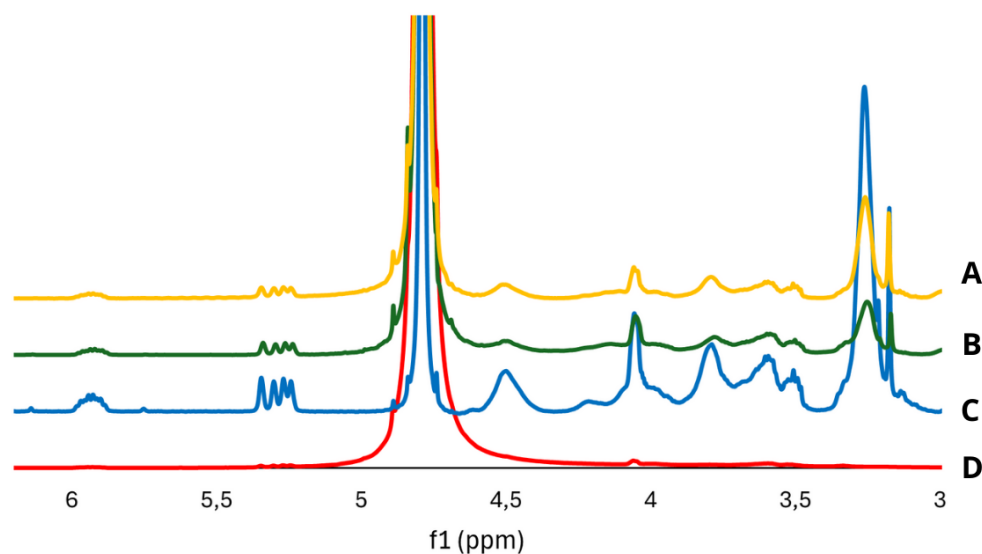


Figure 4.12: ^1H NMR spectra obtained from the formulations (a) Cell_S1:P1:M2, (b) Cell_S1:P2:M1, (c) Cell_P1:M1 and (d) Cell. All spectra were collected in deuterium oxide.

The ^1H NMR spectra were collected after extracting water from the hydrogel swelling tests, using deuterium oxide as solvent. All spectra displayed peaks corresponding to double bonds, as reported in the literature [88]. The double bonds of the monomers probably overlap with those of cellulose, making it difficult to distinguish between them and interpret the spectra. However, upon comparison it is clear that the presence of monomers proved that the polymerization process was inefficient.

4.2.2.1 Crosslinker Effect

Since both gel fraction and swelling capacities were lower than anticipated, BAAM was evaluated as a crosslinker to analyze its effectiveness in enhancing the polymerization and crosslinking of hydrogels. Cell_S was used as model sample once it presented the most promising results regarding swelling properties. Hydrogels synthesized using different crosslinker agents, as well as different percentages of BAAM, are outlined in Table 4.6.

Table 4.6: Formulation of hydrogels to conduct the crosslinker effect study.

Sample ^a	CellM ^b	Cell:SPM Ratio (wt.%) ^c	Crosslinker (wt.%)	Initiator (wt.%)
Cell_S_0.5BAAM	5	50:50	0.5	1
Cell_S_1.0BAAM	5	50:50	1	1
Cell_S_2.0BAAM	5	50:50	2	1
Cell_S_1.0BMEP	5	50:50	1	1

^a Samples were named following the format Cell_*a*_bc, where *a* represents the incorporated monomer (S as SPM), *b* the quantity of crosslinking agent, and *c* the crosslinker agent.

^b Number of AGE equivalents in the cellulose derivative.

^c Cellulose and SPM content ratio in prepared gel.

The influence of the crosslinker on the swelling behavior and gel content of the samples was evaluated and it is shown in Figure 4.13. The gels crosslinked with BMEP exhibited a swelling capacity reaching up to 11.3 g/g, in contrast to BAAM crosslinked gels, which did not surpass 8.1 g/g, with the same amount of crosslinker. However, Cell_S_1.0BAAM and Cell_S_1.0BMEP exhibited 82.6 wt.% and 80.2 wt.% of gel fraction, respectively. Lastly, all BAAM crosslinked gels reported over 77% of gel content. This supports that BAAM is more reactive, leading to a denser and more stable network.

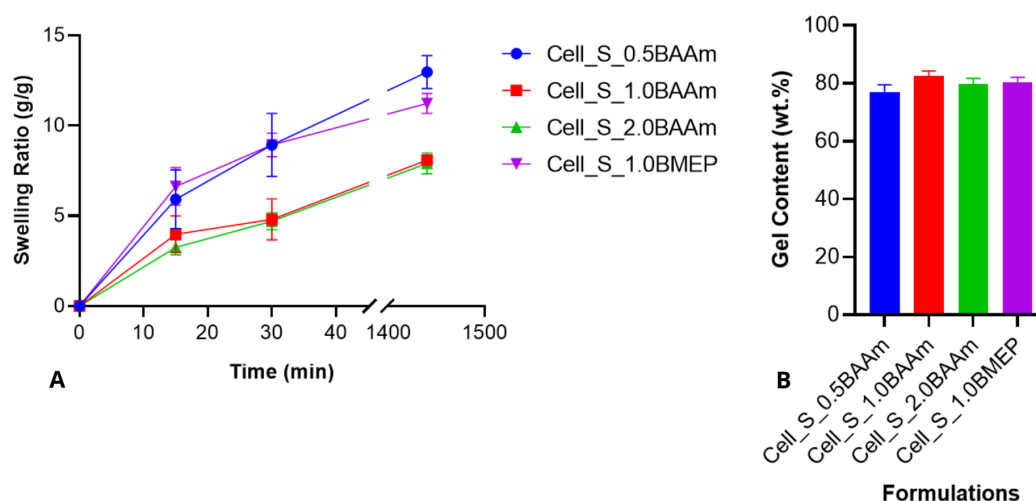


Figure 4.13: Results from (a) water swelling kinetics and (b) gel fraction from influence of the crosslinker study. Hydrogels were cut ($\phi=20$ mm) and oven dried before submitted to swelling tests. Legend presented in Table 4.6.

To further analyze the use of BAAM in hydrogels, homopolymer hydrogels were synthesized from these alternative monomers according to Table 4.7. As referred, these are not conventional monomers used in absorbents, so it was important to evaluate their capacity to prepare hydrogels and also their swelling capacity.

Table 4.7: Parameters for producing homopolymers from the alternative monomers. Hydrogels were produced using 1 wt.% of initiator.

Sample ^a	Cell:Mon Ratio (wt.%) ^b	Monomers (wt.%)			BAAm (wt.%)	Hydrogel
		SPM	PAHEMA	META		
S_C1	0:100	100	0	0	1	No
S_C3	0:100	100	0	0	3	Yes
S_C5	0:100	100	0	0	5	Yes
P_C1	0:100	0	100	0	1	No
P_C3	0:100	0	100	0	3	No
P_C5	0:100	0	100	0	5	Yes
M_C1	0:100	0	0	100	1	No
M_C3	0:100	0	0	100	3	Yes
M_C5	0:100	0	0	100	5	Yes

^a Samples were named following the format a_Cb , where a represents the incorporated monomers (S as SPM, P for PAHEMA, and M as in META) and b the quantity of crosslinking agent.

^b Cellulose and monomers content ratio in prepared gel.

Figure 4.14 displays the outcomes obtained from the swelling tests. Similar to the previous outputs, hydrogels with increasing concentrations of crosslinking agent showed lower swelling capacity and higher gel content results. The formulations with low concentrations of crosslinking agent were unable to produce hydrogels, probably because of a low crosslinking density. In the case of the PAHEMA monomer, the homopolymer hydrogel was only attained with a crosslinking agent concentration of 5%, while the other homopolymers hydrogels crosslinked could be obtained at over 3%. This is an interesting fact considering that gels with AAm or AA can be prepared with smaller amounts of crosslinker (less than 0.5% in some cases), which immediately indicated some issues regarding polymerization and crosslinking processes.

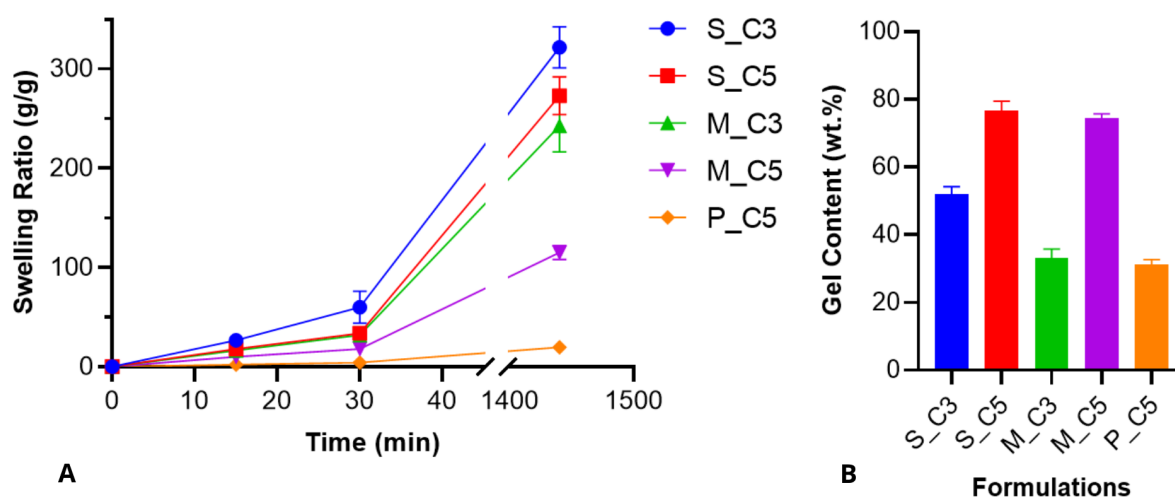


Figure 4.14: (a) Water swelling kinetics and (b) gel fraction of alternative homopolymer hydrogels. Samples with $\varnothing=20$ mm of gels were collected and the drying method chosen was oven drying. The free swelling absorbency was taken at 15 min, 30 min and at maximum swelling capacity. For legend see Table 4.7.

Regarding swelling capacity, except for PAHEMA, the hydrogels exhibited similar values than those generated with AAm and AA (Figure 4.7 - A), with SPM performing the highest values (321.5 g/g and 272.9 g/g) followed by META (242.6 g/g). PAHEMA, which has an estimated diester content of 25% (as stated by the technical sheet [116]) can function as a crosslinking agent too, which can compromise the

crosslinking of hydrogel, and can explain the low value of swelling obtained (19.6 g/g). Nevertheless, hydrogels produced from it can lead to reduced flexibility and lower polymer chain mobility in comparison to linear polymers, leading to decreased swelling capacities (Figure 4.14 - A) [23], [109]. It is worth mentioning that when using the same amount of crosslinking agent (5%), the P_C5 produced less than half of the gel fraction (31.1 wt.%) compared to S_C5 (76.7 wt.%) and M_C5 (74.3 wt.%) indicating the difficulty of these monomers to produce high conversion crosslinked polymer chains. In order to prevent and overcome such problems, the synergistic effect of the combinations of these monomers was also evaluated (Table 4.8).

Table 4.8: Formulation and synthesis conditions for copolymerization of alternative monomers.

Sample ^a	Cell:Mon Ratio (wt.%) ^b	Monomers Ratio (wt.%)			BAAm (wt.%)	Initiator (wt.%)
		SPM	PAHEMA	META		
S1:P1	0:100	0.5	0.5	0	5	1
P1:M1	0:100	0	0.5	0.5	5	1
S1:M1	0:100	0.5	0	0.5	5	1
S1:P1:M1	0:100	0.33	0.33	0.33	5	1

^aSamples were named following the format *ab:ab*, where *a* indicates the monomers included (S as SPM, P for PAHEMA, and M as in META) and *b* the ratio between them.

^b Cellulose and monomers content ratio in prepared gel

The results (Figure 4.15) demonstrated a significant negative synergistic effect. Homopolymers hydrogels produced swelling capacity values of up to 272.9 g/g (Figure 4.14 - A), whereas the combination of these monomers resulted in a maximum swelling capacity of 48.9 g/g. This fact can be related to the (co)polymerization process, where the conversion of monomers alter the network structure and reduce the overall ability of the hydrogel to absorb water [121]. In terms of the gel fraction, the results ranged between 59.5 wt.% and 75.5 wt.% (Figure 4.15 - B) which are consistent with the obtained in homopolymer hydrogels, and increasing the gel content in hydrogels where PAHEMA is present too, corroborating the proposed theory of copolymerization.

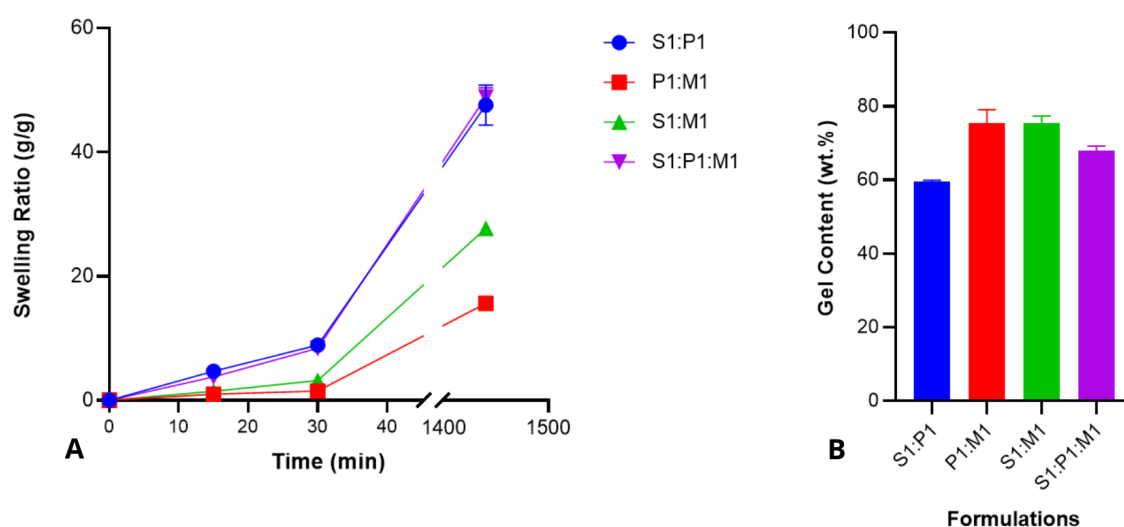


Figure 4.15: Hydrogels produced from copolymerizing the alternative monomers. (a) Water absorbency and (b) gel fraction. The test was conducted with $\varnothing = 20$ mm gels oven dried. Also, as previous methodology, the absorbency was measured at 15 min, 30 min, and 24 hours. The legend is presented in Table 4.8.

These results provide insights about the use of BAAM as a crosslinker agent in this work. Prepared hydrogels revealed high absorbance capacities (Figure 4.14), and also, when copolymerized with cellulose, hydrogels achieved high gel content fractions (Figure 4.13). Consequently, further studies were done with BAAM as a crosslinker agent.

4.2.2.2 Drying Method Effect

The drying process selected has a major effect on the morphology and porosity of cellulose-based absorbents [122]. Upon selecting BAAM as crosslinker, three distinct drying techniques were tested: (1) oven drying (OD) at 50 °C, air-drying after solvent exchange with (2) ethanol (Et), or (3) methanol (Met). Hornification process is an irreversible aggregation of cellulose fibers when dried at temperatures above 40-50°C that leads to reduced porosity and swelling capacity. Solvent exchange with ethanol and methanol was employed to mitigate this effect [123], [124]. To identify the most suitable drying method, the investigation assessed variations in the swelling capacity and gel fraction of hydrogels, both with and without cellulose (Figure 4.16).

The data revealed that the maximal swelling capacity of prepared hydrogels without cellulose remained constant regardless of the drying methods employed. However, when the SPM monomer was copolymerized with cellulose, oven drying resulted in significantly poorer outcomes, both in terms of water absorption capacity and gel fraction. Solvent exchange with methanol was more effective in maintaining water absorption for cellulose-based hydrogels, yielding the greatest results in terms of swelling (16.6 g/g) and gel fraction (84.2 wt.%). Following this, solvent exchange with ethanol showed a maximum swelling capacity of 15.0 g/g representing a 25% improvement relatively to oven drying (11.2 g/g).

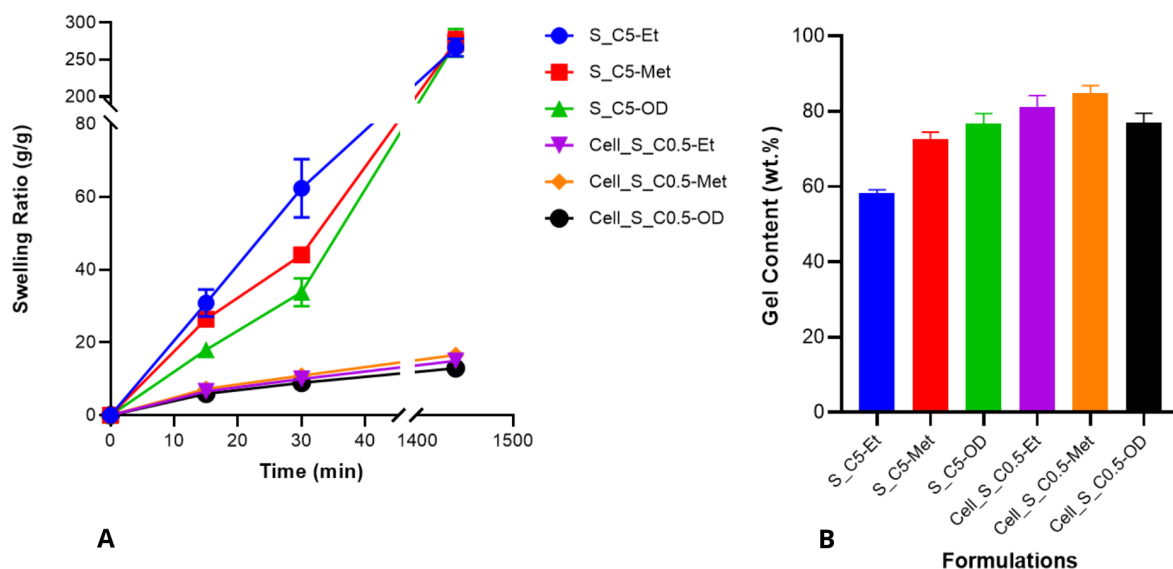


Figure 4.16: The drying method investigation was carried out with the three approaches (OD, Et, and Met) mentioned. To determine the effect of drying method (a) swelling kinetics in water (at 15 min, 30 min, 24 hours) and (b) gel content of gels ($\varnothing = 20$ mm) were collected. Gels of cellulose copolymerized with SPM were prepared with 0.5%.wt of crosslinking agent, whereas homopolymers from SPM had 5%.wt of BAAM.

The SEM images (Figure 4.17) compare the structures of cellulose-based hydrogels submitted to different drying methods—oven drying and air-drying after solvent exchange with ethanol. The oven-dried gels (Figures 4.17 - A and B) exhibit highly compact, dense structures with minimal porosity, which contributes to a reduced water absorption capacity due to the collapse of the polymer network. Figure

4.17 - D shows porous structures collapsed during breaking which is confirmed by the observation of the walls of these structures. Meanwhile, the cellulose homopolymer hydrogels dried using the air-drying method after solvent exchange (Figures 4.17 - C) maintaining a more open and well-defined porous architecture. This preserved porous network confirmed the superiority of open drying as a method that mitigates structural damage and retains the absorption properties of the hydrogels.

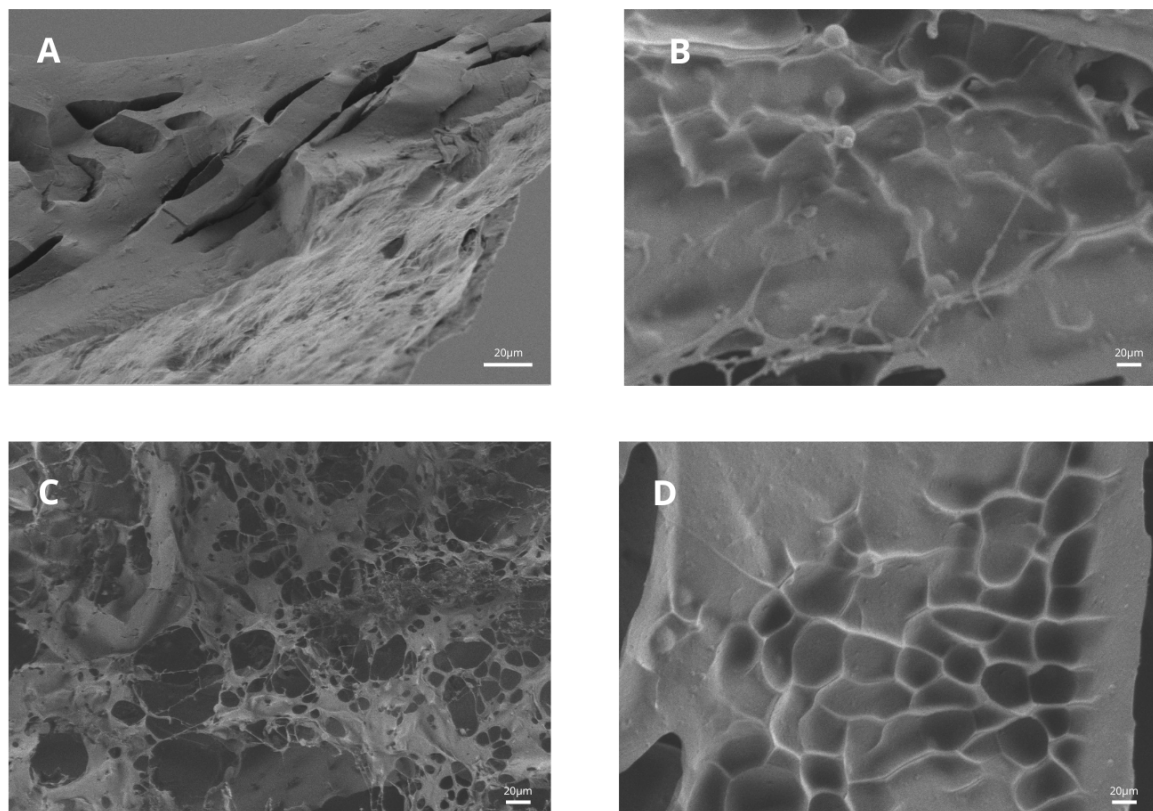


Figure 4.17: SEM images of cross-section of oven dried hydrogels: (a) cellulose hydrogel (control sample) (b) Cell_P1:M1, and air dried after solvent exchange with ethanol: (c) cellulose hydrogel and (d) Cell_P1:M1.

While the maximum swelling capacity of homopolymer hydrogels was unaffected by the drying method, the incorporation of cellulose introduced a significant sensitivity to the drying process. Oven drying, in particular, was detrimental to the copolymer hydrogels, leading to reduced water absorption capacity and gel fraction, implying that the denser and more compact structure induced by oven drying hinders the formation of an effective porous network, crucial for the functional performance of cellulose-based hydrogels.

Lastly, methanol is more toxic than ethanol and, when in contact with the skin, can cause irritation and inflammation [125]. Ethanol is a common sterilization product, which for proposed application could be a plus, and, besides that, the improvements in attributes were not considered significant between hydrogels with ethanol and methanol drying. For these reasons, open air-drying with solvent exchange for ethanol was the technique chosen for future testing with cellulose-based gels.

4.2.2.3 Monomers Ratio Effect in Cellulose-Based Hydrogels

After the drying method and crosslinker were selected, the concentration ratio of monomers was investigated in order to further optimize the hydrogel properties. Hydrogels were synthesized according to the protocols outlined in Table 4.9, this time using BAAM as the crosslinker and implementing open

air drying after solvent exchange with ethanol as drying method.

Table 4.9: Composition and formulation conditions of the hydrogels produced to analyze the effects of varying monomers concentrations. All hydrogels used 1 wt.% of BAAm as crosslinker and wt.% of initiator.

Sample ^a	CellM ^b	Cell:Mon Ratio (wt.%) ^c	Monomers (wt.%)		
			SPM	PAHEMA	META
Cell	5	0:100	0	0	0
Cell_S	5	50:50	50	0	0
Cell_P	5	50:50	0	50	0
Cell_M	5	50:50	0	0	50
Cell_S1:P1	5	50:50	25	25	0
Cell_P1:M1	5	50:50	0	25	25
Cell_S1:M1	5	50:50	25	0	25
Cell_S2:P1:M1	5	50:50	25	12.5	12.5
Cell_S1:P2:M1	5	50:50	12.5	25	12.5
Cell_S1:P1:M2	5	50:50	12.5	12.5	25
Cell_S1:P1:M1	5	50:50	16.7	16.7	16.7

^a Labeled according Cell_*ab:ab* format, with *a* indicating the monomers incorporated in hydrogels and *b* the ratio between the three monomers (S as SPM, P for PAHEMA, and M as in META).

^b Number of AGE equivalents in the cellulose derivative.

^c Cellulose and monomers content ratio in prepared gel.

The cellulose homopolymer showed 8.4 g/g of free swelling capacity, whereas hydrogels copolymerized with the other monomers attained 29.1 g/g, showing an improvement in swelling maximum capacity. This improvement was attributed to the introduction of hydrophilic groups into the polymer matrix, increasing the affinity for water.

The hydrogel presenting the greatest value of water absorption (29.1 g/g) was (Cell_S1:P1:M1) and this fact could be attributed to the synergistic effect of the three monomers used. The second greatest swelling value was obtained in the Cell_M (25.7 g/g), followed by Cell_S2:P1:M1 (22.2 g/g) (Figure 4.18 - A). In addition, hydrogels also exhibited good results in terms of gel content, reaching 89.1 wt.% compared with the cellulose homopolymer hydrogel which achieved 97.7 wt.% (Figure 4.18 - B), and thus suggesting an effective polymerization process.

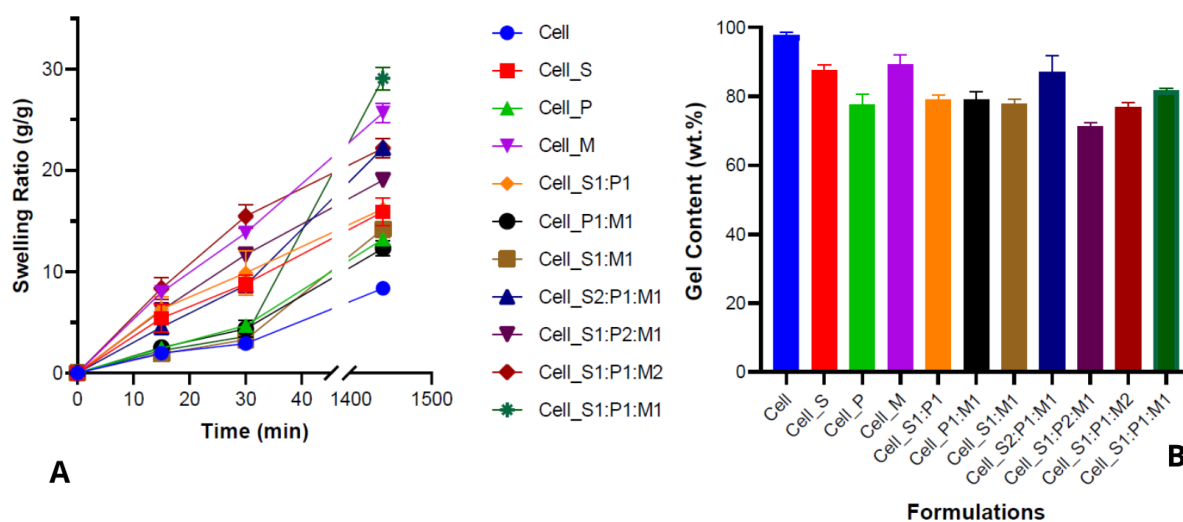


Figure 4.18: Influence of monomers ratio in (a) water swelling kinetics and (b) gel content. The assay was performed with hydrogels ($\varnothing = 20$ mm) dried in open air with solvent exchange with ethanol. For legend see Table 4.9

When comparing Figure 4.11 and Figure 4.18, it becomes evident that the selection of crosslinker and drying method has markedly improved both the absorption capacity and gel content of the hydrogels. In contrast to the previous analysis, where the minimum gel content was 53.7 wt.%, the current analysis achieved a significantly higher gel content of 71.3 wt.%. Similarly, the maximum swelling capacity has notably increased from a range of 2.5 g/g to 11.2 g/g to a range of 12.3 g/g to 29.1 g/g, highlighting the effectiveness of the new crosslinker and drying technique in optimizing hydrogel performance. Additionally, comparing Figure 4.7 and Figure 4.18, cellulose-based gels obtained from copolymerization with alternative monomers performed higher results than those with neutralized acrylic acid and acrylamide, with the same percentage of crosslinking agent. Thus, presenting a promising solution for the incorporation of these monomers with cellulose aiming personal care superabsorbent products.

The FTIR spectra (Figure 4.19) validated the copolymerization of cellulose with the monomers. The appearance of carbonyl (C=O) peaks at 1719 cm^{-1} and the amide I band at 1646 cm^{-1} in the hydrogels indicates the introduction of ester and amide functionalities [126], [127], [128]. It is worth mentioning that the typical stretching of C=C band that corresponds to the double bonds of cellulose, overlap with the amide I band from the monomers making it challenging to differentiate between the contributions from cellulose and the monomers. Despite this, the appearance of new peaks, alongside changes in the intensity and position of the bands, supports the occurrence of copolymerization.

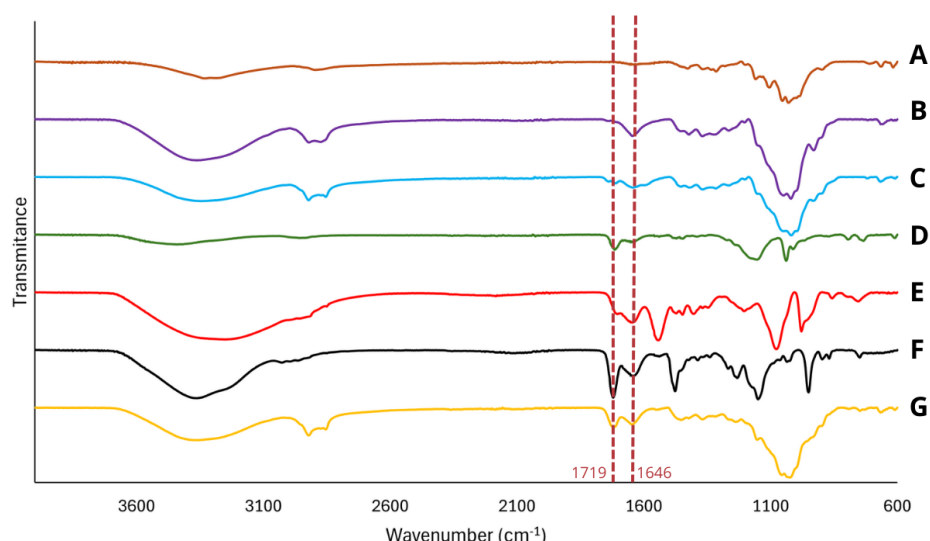


Figure 4.19: FTIR spectra of (a) cellulose powder, (b) Cell_5, (c) Cell_5_H (d) SPM hydrogel, (e) PAHEMA hydrogel, (f) META hydrogel and (g) Cell_S1:P1:M1 hydrogel.

4.2.2.4 Cellulose Degree of Substitution Effect

Considering the results from the previous task, formulation C_S1:P1:M1 alongside with C_S2:P1:M1 were selected to conduct the investigation of effect of the degree of modification for two primary reasons. Firstly, both achieved the higher overall swelling results, and, secondly allows for the investigation of the synergistic effect between the three chosen monomers. In this work, crosslinking density was evaluated by three different factors: (1) degree of substitution in cellulose derivatives, (2) crosslinking amount, and (3) initiator amount used. The hydrogel efficacy was systematically assessed in this investigation in relation to the impact of varying DS values, which ranged from 0.76 (Cell_3) to 1.21 (Cell_5) (Tables 4.1 and 4.10).

Table 4.10: Formulations and conditions of hydrogels for degree of substitution effect study. Hydrogels were produced with 1 wt.% of both BAAM and initiator.

Sample ^a	CellM ^b	Cell:Mon Ratio (wt.%) ^c	Monomers (wt.%)		
			SPM	PAHEMA	META
Cell_3	3	100:0	-	-	-
Cell_4	4	100:0	-	-	-
Cell_5	5	100:0	-	-	-
Cell_S2:P1:M1_3	3	50:50	25	12.5	12.5
Cell_S2:P1:M1_4	4	50:50	25	12.5	12.5
Cell_S2:P1:M1_5	5	50:50	25	12.5	12.5
Cell_S1:P1:M1_3	3	50:50	16.7	16.7	16.7
Cell_S1:P1:M1_4	4	50:50	16.7	16.7	16.7
Cell_S1:P1:M1_5	5	50:50	16.7	16.7	16.7

^a Samples were named following the format Cell_*ab:ab:ab*_d, where *a* represents the monomers (S as SPM, P for PAHEMA, and M as in META), *b* the ratio between monomers, and *c* the equivalents of AGE.

^b Number of AGE equivalents in the cellulose derivative.

^c Cellulose and monomers content ratio in prepared gel.

The degree of substitution in cellulose homopolymer hydrogels directly influences the crosslinking density of prepared hydrogels, and consequently, the absorption capacity and gel content (Figure 4.20). In the case of C_S1:P1:M1 and C_S2:P1:M1, both hydrogels showed superior efficacy using five AGE equivalents with swelling ratios reaching 29.1 g/g and 22.2 g/g, respectively. Meanwhile, for three equivalents of AGE, the swelling ratios only achieved values of 17.3 g/g and 14.6 g/g for the same formulations, respectively. In these formulations, the higher maximum swelling using higher DS may be attributed to the increased presence of linked sites in the cellulose matrix, which can be translated to a higher incorporation of the polymeric network.

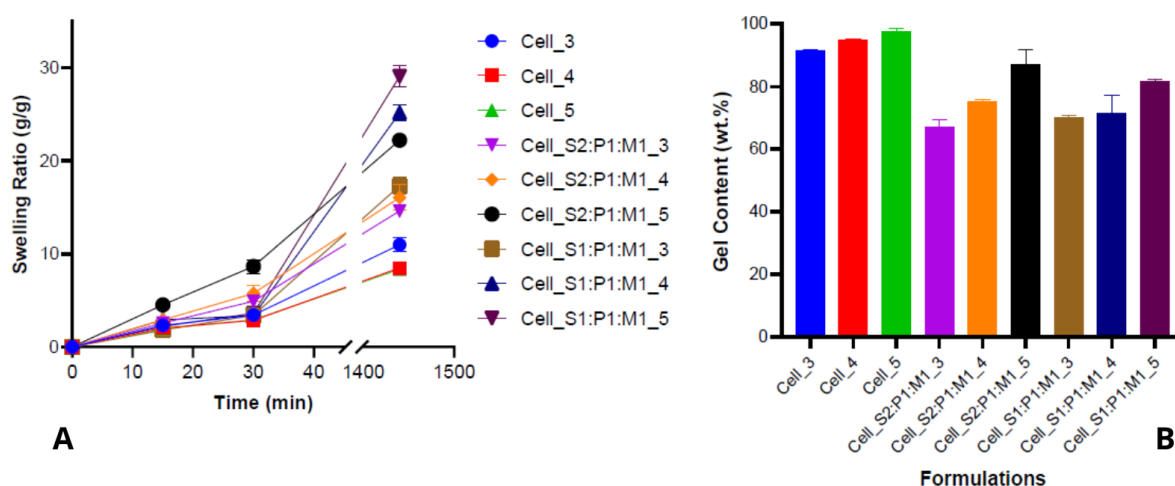


Figure 4.20: Cellulose-based hydrogels absorption behavior and (g) gel content with DS ranging from 0.76 to 1.21. Samples of $\varnothing = 20$ mm were submitted to swelling tests. See legend in Table 4.10.

The homopolymer of cellulose with a lower degree of substitution outperformed other cellulose controls, especially regarding the swelling ratio. The enhanced performance of the Cell_3 hydrogel, compared to Cell_4 and Cell_5, can be attributed to the lower amount of reactive sites, which led to a lower crosslinked network.

Moreover, the gel fraction displayed an upward trend with increasing DS, with the higher substituted derivatives yielding higher gel fractions. It points to the formation of a more resilient crosslinked network, possibly due to the higher concentration of reactive sites, which enhances the strength and stability of the gel structure. Results emphasize that while DS 0.76 provides a noticeable enhancement in swelling capacity over other cellulose homopolymer hydrogels it is at higher DS of cellulose derivatives values that the two formulations chosen accomplished the greatest outcomes, both in swelling and gel content. In that sense, further investigation studies were done on cellulose derivatives prepared with five AGE equivalents.

4.2.2.5 Crosslinker Quantity Effect in Cellulose-Based Hydrogels

The degree of crosslinking is a key factor in the swelling behavior of hydrogels. Highly crosslinked polymers tend to have a lower swelling ratio because the polymer structure becomes more compact, limiting the expansion of the network [23]. Therefore, to investigate whether reducing the crosslinking agent dosage would enhance hydrogels ability to expand and consequently result in higher swelling properties, tests were performed by adjusting the percentage between 0.5% and 0.1%, as detailed in Table 4.11.

Table 4.11: Hydrogels formulations produced to assess the crosslinker agent quantity effect. The initiator quantity was set at 1 wt.%.

Sample ^a	CellM ^b	Cell:Mon Ratio (wt.%) ^c	Monomers (wt.%)			BAAm (wt.%)
			SPM	PAHEMA	META	
Cell_S2:P1:M1_C0.10	5	50:50	25	12.5	12.5	0.10
Cell_S2:P1:M1_C0.25	5	50:50	25	12.5	12.5	0.25
Cell_S2:P1:M1_C0.50	5	50:50	25	12.5	12.5	0.50
Cell_S1:P1:M1_C0.10	5	50:50	16.7	16.7	16.7	0.10
Cell_S1:P1:M1_C0.25	5	50:50	16.7	16.7	16.7	0.25
Cell_S1:P1:M1_C0.50	5	50:50	16.7	16.7	16.7	0.50

^a Samples were named following the format Cell_*ab*:*ab*:*ab*_C*c*, where *a* represents the monomers, *b* indicates the ratio between monomers, and *c* the percentage of crosslinker agent.

^b Number of AGE equivalents in the cellulose derivative.

^c Cellulose and monomers content ratio in prepared gel.

Both formulations demonstrated similar behaviors, with an increase trend in swelling capacity and gel content following a higher amount of crosslinker (Figure 4.21). In opposition to original expectations, the swelling capacity did not rise when the crosslinker concentration was minimized.

Results suggest that the relationship between crosslinker content does not follow a linear pattern. While a higher crosslinker concentration leads to a denser framework that restricts swelling, a certain amount of crosslinker is necessary to maintain the structural integrity of the hydrogel and promote its water absorption. In the meantime, when the crosslinker content becomes too low, the network becomes too loose and unstable, leading to a decrease in the properties of hydrogels, namely swelling capacity. For such reason, the most promising quantity of crosslinking regarding both swelling and gel content

was 0.5 wt.% and was used for further investigations.

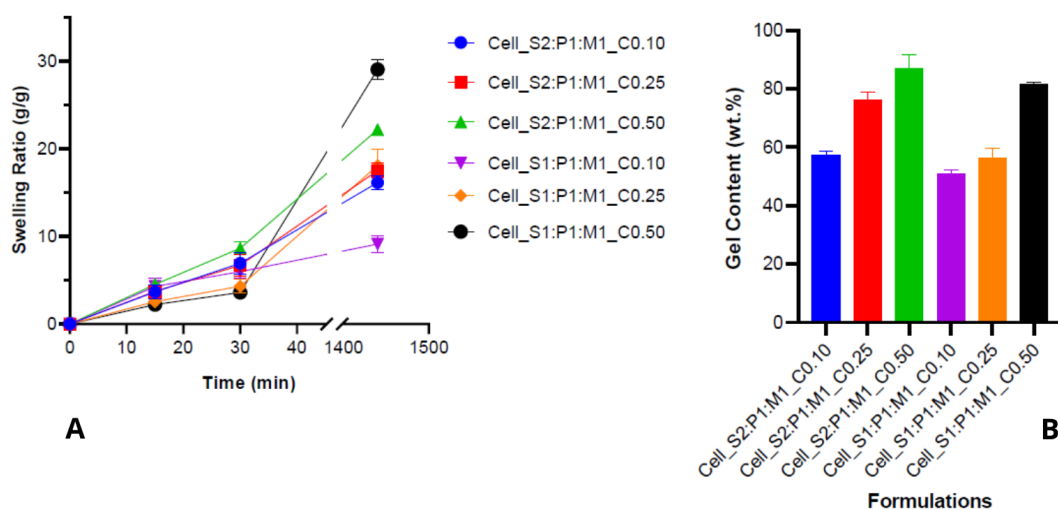


Figure 4.21: (a) Water absorption capacity of cellulose-based hydrogels ($\varnothing = 20$ mm) at 15 min, 30 min, and at 24 hours and (b) gel fraction with BAAM quantity varying from 0.1 to 0.5 wt.%. Legend in Table 4.11.

4.2.2.6 Initiator Quantity Effect in Cellulose-Based Hydrogels

Similarly to BAAM percentage, the quantity of initiator influences the crosslinking density of the polymeric network. In this way, to analyze the effects of initiator dosage on the hydrogels properties, all other reaction conditions were held constant and the 2-hydroxy-2-methylpropiophenone (HMP) quantity was decreased from 1 to 0.25 wt.%, as presented in Table 4.12.

Table 4.12: Formulation and reaction conditions used in the investigation of initiator dosage effects. Hydrogels were produced with 0.5 wt.% of BAAM.

Sample ^a	CellM ^b	Cell:Mon Ratio (wt.%) ^c	Monomers (wt.%)			Initiator (wt.%)
			SPM	PAHEMA	META	
Cell_S2:P1:M1_I1.00	5	50:50	25	12.5	12.5	1.00
Cell_S2:P1:M1_I0.75	5	50:50	25	12.5	12.5	0.75
Cell_S2:P1:M1_I0.50	5	50:50	25	12.5	12.5	0.50
Cell_S2:P1:M1_I0.25	5	50:50	25	12.5	12.5	0.25
Cell_S1:P1:M1_I1.00	5	50:50	16.7	16.7	16.7	1.00
Cell_S1:P1:M1_I0.75	5	50:50	16.7	16.7	16.7	0.75
Cell_S1:P1:M1_I0.50	5	50:50	16.7	16.7	16.7	0.50
Cell_S1:P1:M1_I0.25	5	50:50	16.7	16.7	16.7	0.25

^a Named following the format Cell_ *ab:ab:ab*_I_c, where *a* represents the monomers (S as SPM, P for PAHEMA, and M as in META), *b* indicates the ratio between monomers, and *c* the percentage of initiator present.

^b Number of AGE equivalents in the cellulose derivative.

^c Cellulose and monomers content ratio in prepared gel.

Results of the swelling and gel content are shown in Figure 4.22. The gel fraction presents an inverse relationship with the initiator dosage, with higher initiator concentrations resulting in a higher swelling capacity. Lower amount of initiator created less robust networks, as evidenced by the reduced gel fraction, which decreased drastically when initiator amount was reduced below 0.50 wt%.

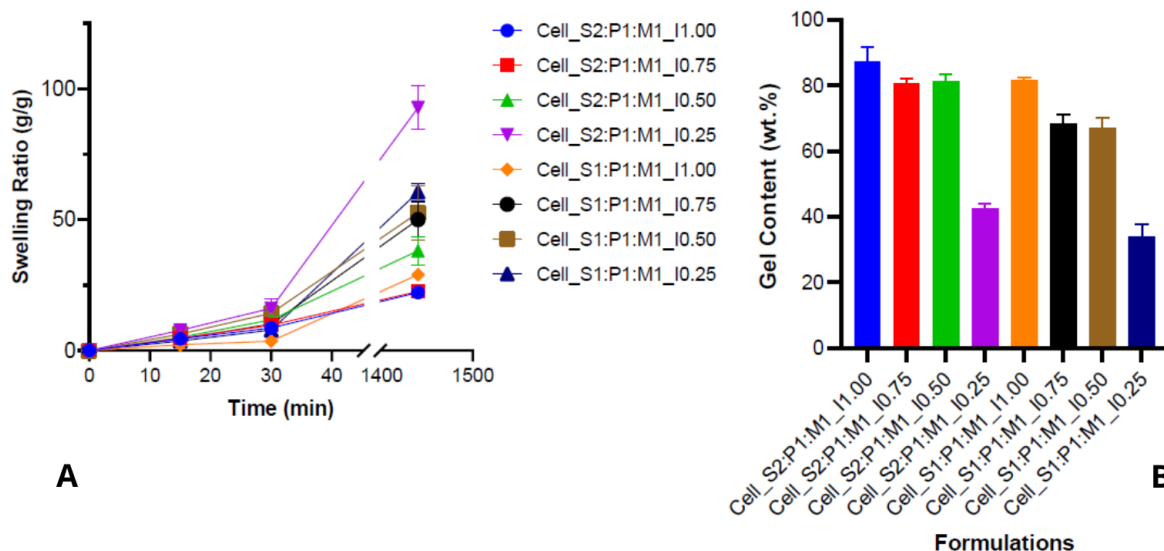


Figure 4.22: Influence of initiator dosage of hydrogels ($\varnothing = 20$ mm) in (a) water retention capacity at 15 min, 30 min and 24 hours and (b) gel content. Legend in Table 4.12.

The swelling capacity of the hydrogels increased significantly with the reduction in initiator dosage, particularly in C_S1:P1:M1_I0.25 (60,5 g/g) and C_S2:P1:M1_I0.25 (92,8 g/g). In contrast, with 1 wt.% of initiator, the same formulations resulted in swelling capacities of 22,2 g/g and 29,1 g/g, respectively. The gel content for C_S1:P1:M1_I0.50 and C_S2:P1:M1_I0.50 was 67.2% and 81.3%, respectively. Comparatively, hydrogels obtained values of 34.0% and 42.5% at 0.25 wt.% of initiator, which translates in nearly a 50% reduction in gel fraction (Figure 4.22 - B). At higher concentrations, the initiator promotes more active sites and a small polymer chains that with the same amount of crosslinker originates small size chains between crosslink points. On the other hand, reducing the initiator concentration results in fewer free radicals, leading to longer polymer chains and a bigger chains between crosslink points of the network that can absorb more water but lacks structural integrity, resulting in a lower gel fraction.

Considering this, the initiator concentration was set at 0.5 wt.% for subsequent studies on the cellulose:monomer ratio since personal care products required minimal quantity of residual reactants and undesired side reaction products released to the medium. Even though, regarding swelling, the Cell_S2:P1:M1_I0.25 and Cell_S1:P1:M1_I0.25 formulations performed better results in terms of maximum swelling capacity.

4.2.2.7 Cellulose:Monomers Ratio Effect

The relationship between the cellulose and monomers mass ratio used in hydrogels preparation and water absorbency values was studied by varying the ratio from 10:90 to 50:50 (Table 4.13). All the parameters were set according to the previous optimized results.

Table 4.13: Formulation and reaction conditions implemented for the study of cellulose: monomers ratio. Both crosslinker agent and initiator quantities were set at 0.5 wt.%.

Sample ^a	CellM ^b	Cell:Mon Ratio (wt.%) ^c	Monomers (wt.%)		
			SPM	PAHEMA	META
Cell_S2:P1:M1_10:90	5	10:90	25	12.5	12.5
Cell_S2:P1:M1_25:75	5	25:75	25	12.5	12.5
Cell_S2:P1:M1_50:50	5	50:50	25	12.5	12.5
Cell_S1:P1:M1_10:90	5	10:90	16.7	16.7	16.7
Cell_S1:P1:M1_25:75	5	25:75	16.7	16.7	16.7
Cell_S1:P1:M1_50:50	5	50:50	16.7	16.7	16.7

^a Named following the format Cell_ *ab:ab:ab_c*, where *a* represents the monomers (S as SPM, P for PAHEMA, and M as in META), *b* the ratio between monomers, and *c* the ratio between cellulose and monomers.

^b Number of AGE equivalents in the cellulose derivative.

^c Cellulose and monomers content ratio in prepared gel.

The maximum absorbency (102,3 g/g for Cell_S2:P1:M1_10:90) was obtained at lower concentrations of cellulose (Figure 4.23). This phenomenon happens due to an increased monomer content that introduces more hydrophilic groups into the polymer network that are capable of attracting and retaining water molecules, leading to greater swelling capacity. In contrast, as the cellulose content increases, the number of available hydrophilic sites may decrease, resulting in lower absorbency. Also, these outcomes can be due to the fact that cellulose possesses multiple binding sites in its structure, which results in a denser network. Meanwhile, gel content was decreased with lower concentrations of cellulose, suggesting that cellulose acts as backbone of the hydrogel network and is responsible for the hydrogel integrity and stability (Figure 4.23 - B). Not to mention, that the decrease in cellulose content probably will affect and reduce the biodegradability of prepared hydrogels once cellulose backbone is expected to be more prone to being biodegradable than the other monomers/polymers used. For the proposed application, both swelling and biodegradability are important features to take into account, and a balance should be achieved for practical applications.

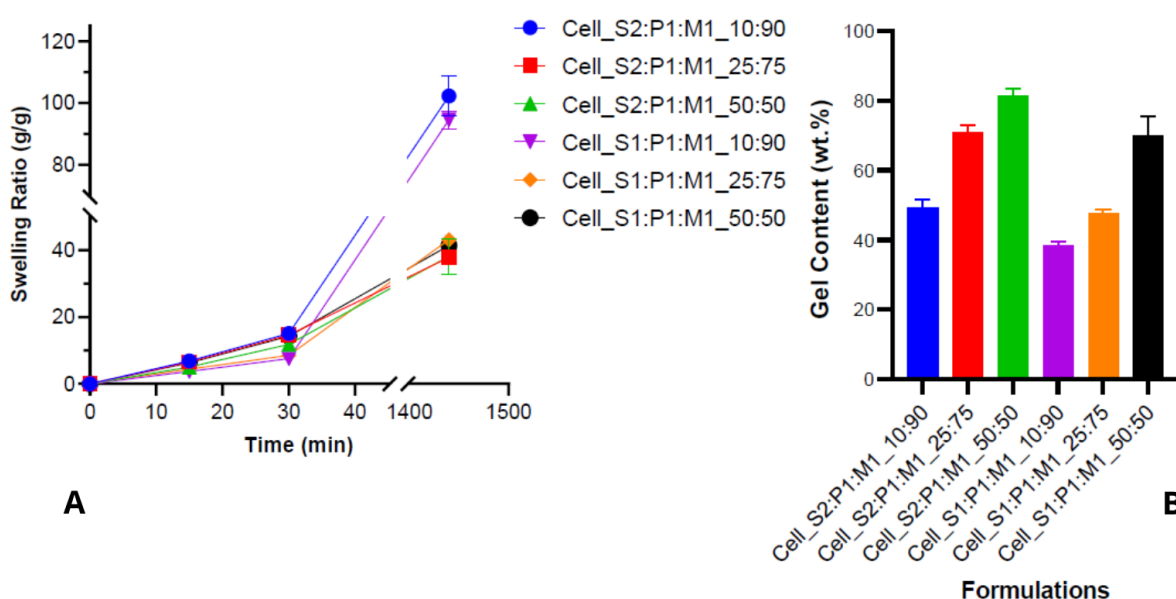


Figure 4.23: Hydrogels ($\varnothing = 20$ mm) with different cellulose:monomers ratio (a) water retention capacity at 15 min, 30 min and 24 hours and (b) gel content. For legend see Table 4.13

Overall, comparing Figure 4.18 and Figure 4.23 it is possible to verify that several parameters play an important role in the crosslinking density, and consequently, affect both water uptake and gel fraction. Initially, C_S1:P1:M1 and C_S2:P1:M1 only achieved values of 29.1 g/g and 22.2 g/g while the final maximum retention values were stated at 94,6 g/g and 102,3 g/g, respectively. By optimizing parameters, the hydrogels network structure was refined to allow for greater water absorption and retention, showcasing the importance of tuning hydrogels properties according to the desired application.

4.3 Most Promising Cellulose-Based Hydrogels

Regarding all findings, three formulations, as listed in Table 4.14, were chosen as the most promising for further investigation aiming practical applications.

Formulations with SPM:PAHEMA:META in a 2:1:1 ratio were chosen for characterization purposes. This decision relied on the fact that SPM evidenced the highest swelling capacity among the homopolymers, whereas PAHEMA stood out by its minimal swelling and gel content (as illustrated in Figure 4.14). On top of that, the most favorable absorption capacity results have been observed with this particular ratio of monomers (Figure 4.22 and 4.23) with Cell_S2:P1:M1_10:90 and Cell_S2:P1:M1_I0.25 as the formulations that demonstrated remarkably swelling capacities of 102.3 g/g and 92.8 g/g, respectively. In addition to these, the formulation Cell_S2:P1:M1 was also characterized, with the objective of evaluating the influence of cellulose and initiator quantity under consistent conditions. As positive and negative controls, isolated SAPs from diapers and homopolymer hydrogel of cellulose were used.

Table 4.14: Formulation and reaction conditions of cellulose-based hydrogels considered the most promising for personal care products and negative control.

Sample ^a	CellM ^b	Cell:Mon Ratio (wt.%) ^c	Monomers (wt.%)			BAAm (wt.%)	Initiator (wt.%)
			SPM	PAHEMA	META		
Cell_5_H	5	100:0	-	-	-	0.5	0.5
Cell_S2:P1:M1	5	50:50	25	12.5	12.5	0.5	0.5
Cell_S2:P1:M1_10:90	5	10:90	25	12.5	12.5	0.5	0.5
Cell_S2:P1:M1_I0.25	5	50:50	25	12.5	12.5	0.5	0.25

^a Named following the format Cell_*ab:ab:ab_c*, where *a* represents the monomers (S as SPM, P for PAHEMA, and M as in META), *b* the ratio between monomers, and *c* the variation parameter (I meaning initiator).

^b Number of AGE equivalents in the cellulose derivative.

^c Cellulose and monomers content ratio in prepared gel.

4.3.1 Detailed Characterization of Cellulose-Based Hydrogels

All previous assessments were conducted using circular shapes samples of hydrogels with a diameter of 20 mm. However, to more accurately simulate real conditions, various methods to break down the dried hydrogels samples into a powder form were examined. Hydrogels were prepared under three distinct conditions: (1) cryogenic fracture (CF), (2) coarsely hand broken (HB), and (3) grinding in a coffee grinder (CG). Figure 4.24 illustrates the swelling kinetics of the Cell_S2:P1:M1_10:90 hydrogel subjected to the three different powder form. SEM images of the surface of hydrogels prepared through different methods are shown in Figure 4.25.

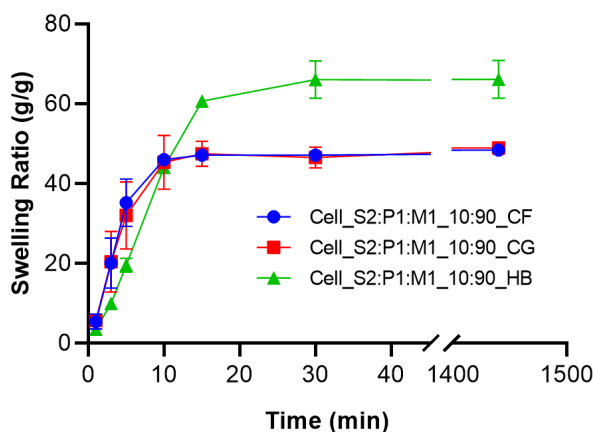


Figure 4.24: Swelling behavior of Cell_S2:P1:M1_10:90 hydrogel over time. Three preparation methods were compared: cryogenic fracture (CF), grinding in a coffee grinder (CG), and coarsely hand breaking (HB). The swelling ratio was measured at different time intervals up to maximum swelling.

In the initial 10 minutes, all three methods demonstrated a quick and similar swelling kinetics (Figure 4.24). However, after this period, there are clear differences in their performance. The CF and CG methods showed very similar swelling behavior, with equilibrium swelling ratios around 48 g/g. However, the manually broken hydrogel outperformed both CF and CG from 10 minutes onward, reaching 66,2 g/g. Despite that, none of the methods even came close to the maximum value previously obtained (102.3 g/g) (Figure 4.23).

Figure 4.24 evidence that the hydrogels with reduced particle sizes reached the equilibrium swelling within 15 minutes. In contrast, the hydrogels cut into circular shapes with a 20 mm diameter did not even reach their maximum swelling capacity by the 30-minute mark (Figure 4.23). In PCPs, a rapid absorption is crucial to quickly trap liquids and/or fluids, preventing leakage and ensuring the skin remains dry. In this sense, the smaller particles, with larger area-to-volume ratio, promoted faster water absorption, allowing the material to reach equilibrium quickly. Thus, preparation methods that produce smaller particles showed to be highly relevant for personal care products applications. Nonetheless, the results also suggest that certain methods may damage the honeycomb structure of hydrogels, with significant impact in the swelling performance.

Both cryogenically fractured (Figure 4.25 - B) and coffee grinder-prepared hydrogels (Figure 4.25 - C) clearly show surface damage, with fragmented and larger fissures evident in the SEM images. These processes are likely to apply substantial shearing forces, causing extensive fragmentation and further breakdown of the polymer network, which severely limits water retention. In contrast, hydrogels cut into 20 mm circular samples (Figure 4.25 - A) and manually broken hydrogels (Figure 4.25 - D) showed a more compact and less disrupted structure. The 20 mm hydrogels samples, maintained a smooth and intact surface morphology and achieved the highest swelling capacity (102.3 g/g), probably due to the preservation of their internal network, as cutting is a non-destructive method that does not exert significant mechanical stress on the polymer structure. On the other hand, HB-prepared hydrogels (Figure 4.25 - D) exhibited a more irregular and fragmented surface, indicating a relatively moderate disruption, that still compromised the hydrogels internal structure to a certain extent and results in a lower swelling capacity (66.2 g/g).

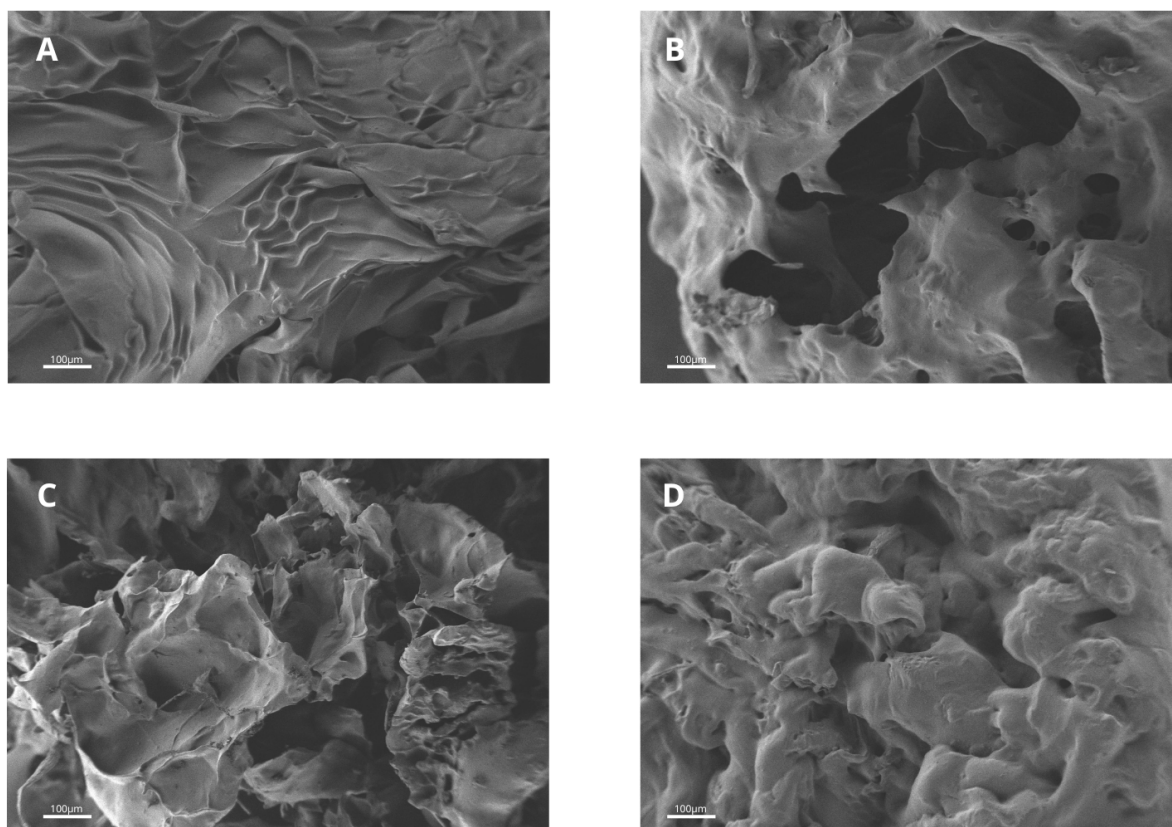


Figure 4.25: SEM images of hydrogel surfaces prepared under different conditions: (a) hydrogels cut into 20 mm circular samples, (b) cryogenically fractured hydrogels, (c) hydrogels ground in a coffee grinder, and (d) manually broken hydrogels.

The SEM images revealed a direct correlation between the hydrogels absorption capacity and their morphological structure. The introduction of significant structural disruptions of honeycomb structure caused severe reduction in water uptake. In contrast, non-destructive methods are likely to preserve the structure and result in maximal retention and absorption, however, led to slower absorption kinetics. Although manual breaking induces moderate structural disruption, it was selected as the preparation method because it shows a balance between maximum absorption capacity and promoting faster swelling kinetics.

4.3.1.1 Thermal Properties

Thermo gravimetric analysis (TGA) and derivative thermogravimetry (DTG) curves (Figure 4.26) provide insights about the thermal degradation behavior of materials [84]. The weight loss as a function of temperature in Figure 4.26 - A assesses the thermal stability of these materials and Figure 4.26 - B provides more detailed information on the rate of weight loss. Table 4.15 illustrates a summary of thermal properties of the samples evaluated by TGA.

All thermograms demonstrated small weight loss up to 110 °C due to evaporation of adsorbed water. In the cellulose powder TGA profile, fast pyrolysis ranged between 250 °C and 350 °C, corresponding to the typical dehydration and decomposition of the cellulose [129]. Meanwhile, although diaper absorbent main degradation step occurs at a higher temperature (around 500°C), it has lower degradation temperatures (T_{90} and T_{95}) (Table 4.15) which indicates an earlier onset of degradation that could be attributed to the volatilization of unreacted monomers, such as AA and AAm, whose boiling points typically range between 140 °C and 200 °C [130], [131].

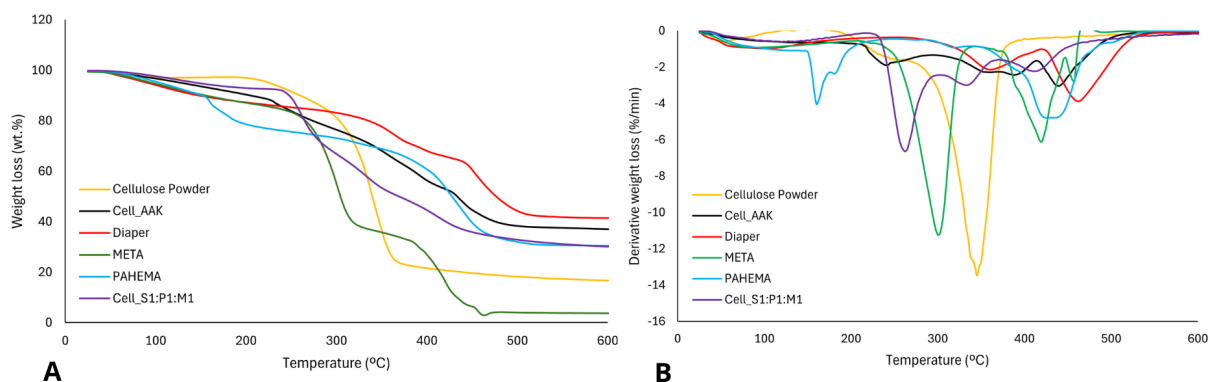


Figure 4.26: (a) TGA (b) DTG curves of samples in order to evaluate the thermal stability.

Cell_AAK_C0.5 exhibited a slightly delayed decomposition compared to cellulose powder and Cell_S1:P1:M1, with weight loss beginning around 275 °C and extending to 500 °C due to its composite nature. Further, Cell_AAK_C0.5 three-step profile had major weight loss located at 242.7 °C, 360.2 °C, and 439.6 °C temperatures which were attributed to decomposition of carboxyl groups, cellulose and main chain of the potassium acrylate, respectively. Comparing the DTG curves of Diaper and Cell_AAK_C0.5 in Figure 4.26 - B, both present peaks of decomposition between 350 °C and 500 °C that typically corresponds to decomposition of acrylic-based materials [132], [133], [134]. Thus, this evidence corroborates with the theory of diapers SAPs being acrylate-based polymers.

The sample Cell_S1:P1:M1 demonstrated significantly higher thermal stability compared to the other absorbent materials tested, with a 5 wt.% loss occurring at 145.9 °C. In contrast, the Diaper and Cell_AAK_C0.5 samples exhibited lower thermal stability, with 5 wt.% losses recorded at 91 °C and 127.7 °C, respectively. Peaks at 262.4 °C and 332.4 °C were identified as the removal of quaternary ammonium groups of META [135], and cellulose decomposition [132], [133]. Furthermore, the third stage probably corresponds to the decomposition of META [135], PAHEMA, and SPM backbone itself [136].

Table 4.15: Thermal properties of samples assessed by TGA.

Sample	TGA		
	T95 (°C) ^a	T90 (°C) ^b	W600 (%) ^c
Cellulose Powder	225.4	229.2	16.69
Diaper	91.0	147.5	41.46
Cell_AAK_C0.5	127.6	203.9	37.04
Cell_AAK_AAm_C0.5		d	
SPM		d	
META	95.5	154.7	3.76
PAHEMA	105.1	151.3	30.48
Cell_S1:P1:M1	145.9	247.5	30.08

^a Temperature of 95% remaining weight.

^b Temperature of 90% remaining weight.

^c Residual weight (wt.%) at 600 °C.

^d Results unable to obtain from TGA method.

Cellulose and META exhibit low residual masses of 16.7% and 3.8% at 600 °C, respectively. In contrast, diapers and Cell_AAK_C0.5 result in residues levels of 41.5% and 37.0%, respectively. Al-

though most used synthetic monomers offer main degradation step at a higher temperatures, the high residue levels translate into a substantial presence of inorganic or non-combustible components, which pose environmental challenges, namely in waste management and recycling [37], [38], [40].

4.3.1.2 Swelling and Holding Properties

The swelling kinetics of hydrogels and control samples were studied in four different fluids: deionized water, synthetic urine, pH 4 buffer, and pH 8 buffer, and the results are presented in Figure 3.2. Swelling behavior was evaluated in pH 4 and pH 8 buffers solution since these pHs correspond to the physiological extremes of urine pH [137].

In deionized water (Figure 3.2 - A), the differences between the prepared hydrogels and the positive control (hydrogel from diaper) were evident. The SAPs extracted from the diaper showed a significantly superior water absorbing capacity, reaching a value of 294.5 g/g. Among the hydrogels prepared, the formulation Cell_S2:P1:M1_10:90 emerged to be the most relevant, achieving a swelling ratio of 69.9 g/g, although it was still substantially lower than the diaper SAPs. Remaining hydrogels exhibited much lower swelling capacities, with ratios between 5–10 g/g.

Similar to deionized water, the diaper SAPs displayed the highest swelling ratio in synthetic urine (Figure 3.2 - B). Nevertheless, the hydrogels capacity to absorb fluid was significantly reduced by the presence of salts and ions with values ranging from 6.9 (cellulose homopolymer hydrogel) to 20.7 (diapers SAPs) g/g. Cell_S2:P1:M1_10:90 hydrogel remained the most promising among the prepared hydrogels, achieving a swelling ratio of 14.0 g/g while the other hydrogel formulations showed moderate swelling, with maximum ratios between 6.9–7.5 g/g.

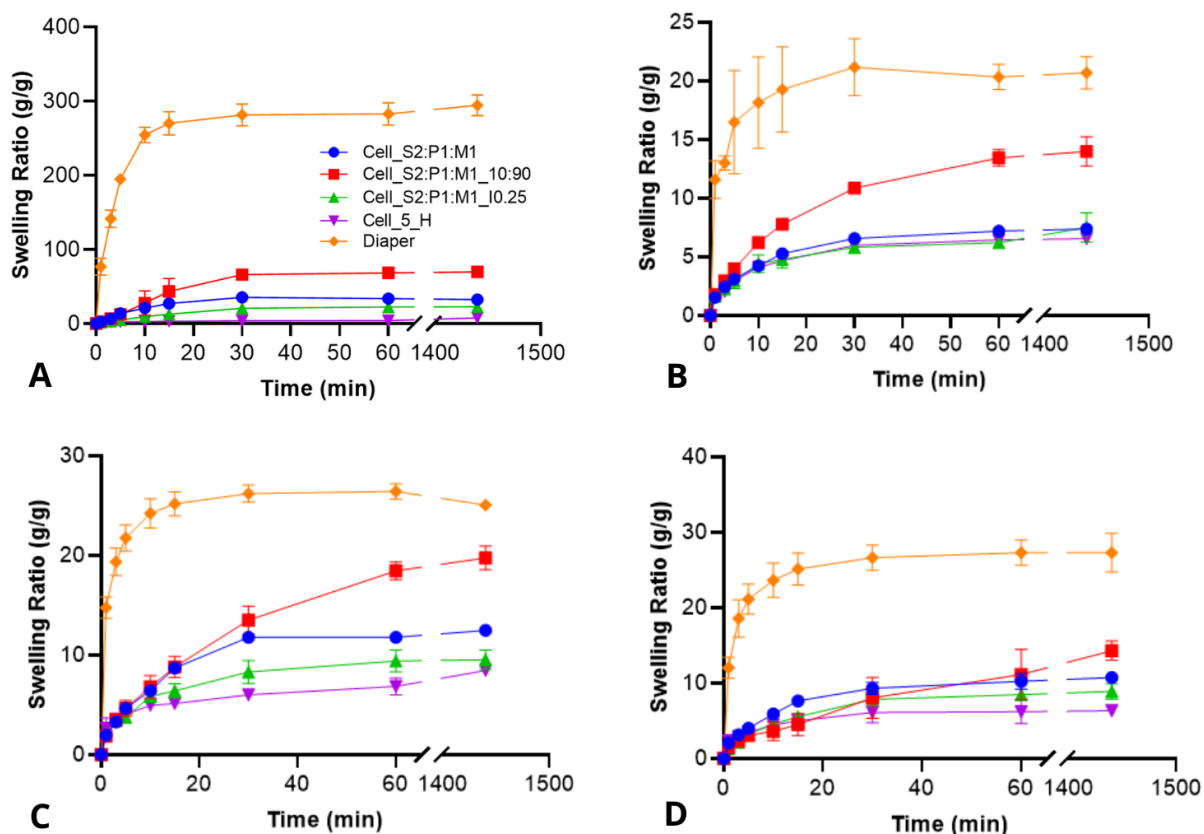


Figure 4.27: Swelling kinetics of most promising hydrogels for personal care products, as well as control samples, in (a) deionized water, (b) synthetic urine, (c) pH 4 buffer solution, and (d) pH 8 buffer solution. Legend in Table 4.14.

All samples exhibited higher absorption in buffer solutions compared to synthetic urine, likely due to the protonation of functional groups in the hydrogel, which enhances hydrophilicity and, thus, water uptake (Figures 3.2 - C and D) [92]. In pH 4 solution, the diaper SAPs exceeded a swelling ratio of 25.1 g/g, while Cell_S2:P1:M1_10:90 performed remarkably, achieving 19.8 g/g, which was closer to the SAPs diaper performance in the acidic environment than in any other medium tested. In comparison, the swelling behavior of the prepared hydrogels in pH 8 buffer was slightly lower than in pH 4 but still higher than in synthetic urine. However, the diaper SAPs showed improved performance in pH 8 compared to pH 4, reaching a swelling value of 27.3 g/g. Meanwhile, at pH 8, the Cell_S2:P1:M1_10:90 formulation managed to absorb 14.3 g/g.

Overall, the diaper SAPs demonstrated superior swelling and absorption rates across all fluids tested, which represents two important characteristics of SAPs design for PCPs. Among the hydrogels prepared, Cell_S2:P1:M1_10:90 consistently exhibited higher swelling ratios compared to the other formulations in all conditions. This data suggests that while the hydrogels, particularly Cell_S2:P1:M1_10:90, do not match the performance of commercial SAPs in deionized water, they show promise in synthetic urine, making them potential candidates for personal care applications. Furthermore, results from the hydrogels in this work showed better swelling capacities in water [138], [139], [140], [141] and synthetic urine/saline solution [139], [142], [143] than other cellulose-based superabsorbent products reported. Also, Cell_S2:P1:M1_10:90 achieved higher water swelling results than some commercially available diapers [92].

The retention capacity was evaluated (Figure 4.28) in both deionized water and synthetic urine over

an 8-hour period since absorbent hygiene products require rapid and high fluid absorption, alongside with good retention capacity [84]. All samples, except for Cell, showed a gradual decrease in water retention over time. The diaper SAPs experienced a faster decline than cellulose-based hydrogels, dropping to approximately 64.5% by the end of the 8-hour period. In contrast, the Cell_S2:P1:M1_10:90 hydrogel retained nearly 80% of its absorbed water after 8 hours, indicating its superior long-term water retention compared to the diaper SAPs. Furthermore, the remaining hydrogels also stated retention rates above 69% after 8 hours. The negative control of cellulose exhibited the poorest water retention, dropping below 20% by the 8-hour mark and suggesting weaker crosslinking or less efficient water-polymer interactions.

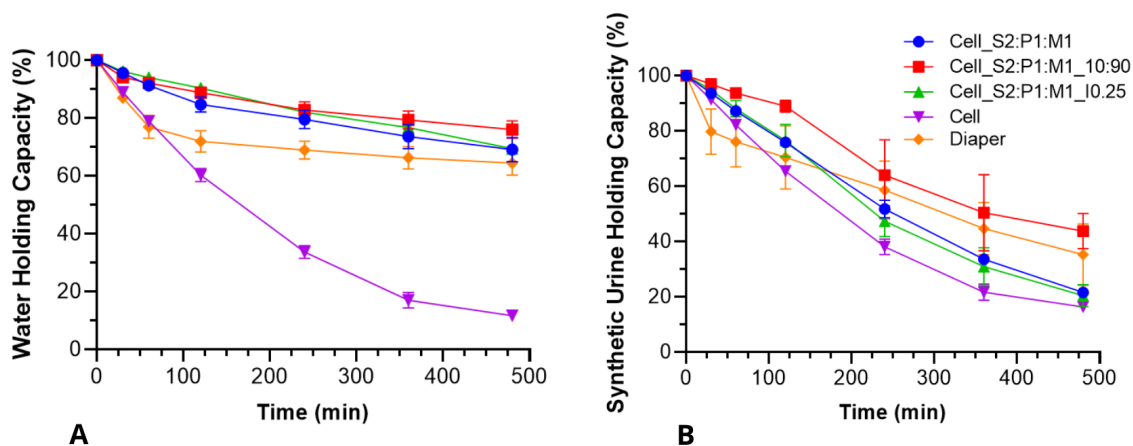


Figure 4.28: (a) Deionized water and (b) synthetic urine retention capacity of most promising samples and controls over an 8-hour period. Legend in Table 4.14.

Comparing Figure 4.28 - A and Figure 4.28 - B, it is evident that the retention capacity of all samples showed a more pronounced decrease in synthetic urine compared to deionized water, reflecting that the presence of salts and other dissolved ions can interfere with the polymer ability to hold absorbed fluid. The diaper SAPs displayed a significant drop in retention in the first 2 hours period falling to 70.4% while, the hydrogels exhibited more resilience in holding synthetic urine. Regarding the full time Cell_S2:P1:M1_10:90 had the greater performance retained around 43.8% after 8 hours while diaper SAPs only attained 35.7%. Diaper SAPs outperformed hydrogels in swelling capacity (Figure 3.2). However the hydrogels, especially the Cell_S2:P1:M1_10:90, exhibited superior long-term retention in both deionized water and synthetic urine making it more promising for applications requiring sustained fluid retention in personal care products. Cell_S2:P1:M1_10:90 performed greater water holding outcomes than the positive control, the diapers SAPs, and other cellulose-based superabsorbent products stated in the literature [141], [144].

The CRC and AUL method are used to ascertain the weight of liquid lost by swollen hydrogels after being saturated and centrifuged under controlled conditions and measure the strength of swollen hydrogels under certain pressure through the absorbency parameter, respectively [84], [92]. Results of FSC, CRC, and AUL of prepared hydrogels and controls samples in synthetic urine are represented in Figure 4.29.

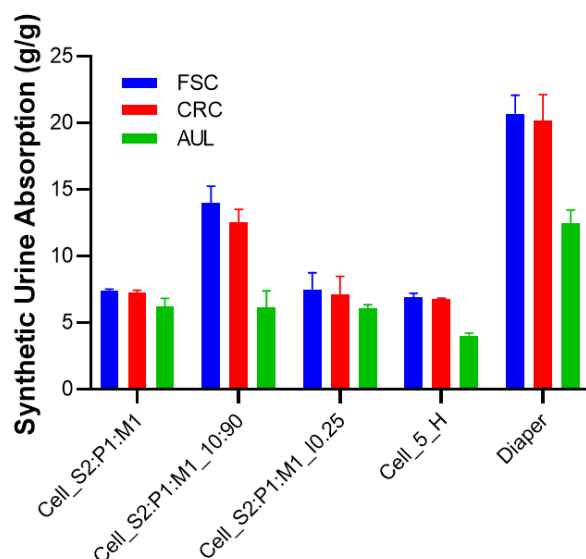


Figure 4.29: Free swelling capacity (FSC), absorbency under load (AUL), and centrifuge retention capacity (CRC) of most promising hydrogels and controls in synthetic urine. Legend in Table 4.14.

The highest CRC value was 20.17 g/g which is attributed to SAPs from diapers, and the most promising hydrogels values were 7.3, 12.5, and 7.1 g/g which were attributed to Cell_S2:P1:M1, Cell_S2:P1:M1_10:90, and Cell_S2:P1:M1_10:25, respectively. Comparing these CRC values to the FSC results, the stability of these hydrogels under centrifugation becomes evident since hydrogels are capable of maintaining a high percentage of their absorbed fluid, which translates into mechanical resilience and stability when fully saturated. As presented in Figure 4.29, the values for AUL test are significantly lower than for FSC and CRC for both hydrogels and controls. In synthetic urine, values ranged between 4.0 (cellulose homopolymer hydrogel) and 12.5 g/g (baby diaper SAP), with Cell_S2:P1:M1_10:90 lowering the swelling to 6.1 g/g which means it lacks mechanical strength and structure integrity, corroborating previous results of cellulose acting as the backbone of the hydrogel network. Nonetheless, it outperforms the AUL values of other cellulose-based polymers [143].

4.3.1.3 Biodegradability

The soil burial method is the most used method for assessing the biodegradability of hydrogels [145]. In this case, preliminary biodegradability tests using that method could not be performed due to the adhesion of the hydrogels to the soil (Figure 4.30), which hindered the accurate use of mass difference calculations.



Figure 4.30: Preliminary biodegradability tests showed visible hydrogel adhesion to the soil. This result prevented the measurement of the hydrogels biodegradability over a period of three weeks.

Alternative biodegradability tests can be used in hydrogels to overcome that drawback, like testing the hydrogel post-freeze-drying [84]. Additionally, quantifying the CO₂ efflux from soil-hydrogel incubations, measuring the biochemical oxygen demand of soil amended with hydrogel versus natural soil, monitoring the microbial biomass accumulation, and observing the changes in the hydrogel physical properties over time could be used to assess the biodegradability. Another method involves labeling the hydrogel with radioactive ¹⁴C to track the release of ¹⁴C in CO₂ or CH₄ during microbial metabolism of the polymer [145].

4.3.1.4 Biocompatibility

In vitro cytocompatibility of the developed hydrogels was determined by quantitative analysis using the MTS viability assay. NHDF fibroblast cells were cultured in the presence of the hydrogels for 3 and 7 days. The untreated cells (without mats) cultured on the surface of the wells served as control. The results of in vitro cytocompatibility are shown in Figure 4.31 as percentage of cell viability (%). According to ISO 10993-5:1999, materials with cell viability greater than 75% are considered non-cytotoxic.

Overall, the data showed that Diapers hydrogels exhibited a cytotoxic effect with cell viability less than 75% during the time interval. Particularly, cell viability for cultures with Cell_S2:P1:M1_10:90 hydrogels were $78.90 \pm 0.87\%$ (3 days) and $96.77 \pm 5.37\%$ (7 days), compared with the untreated cells, indicating that NHDF cells maintained their metabolic activity. Regarding Cell_S2:P1:M1, although at 3 days the viability was slightly lower than 75%, at 7 days the results showed a viability around 75%, demonstrating that both prepared hydrogels were non-citotoxic.

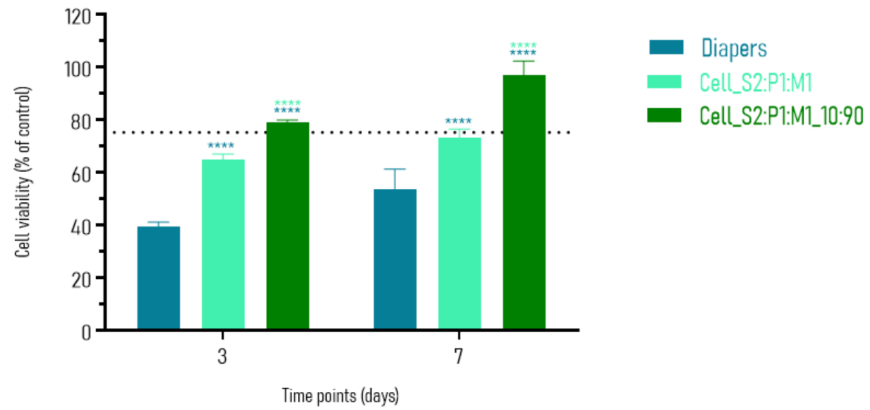


Figure 4.31: NHDF fibroblast viability in response to hydrogels and diaper samples over 3 and 7 days (MTS Assay). Legend in Table 4.14.

According to these findings, it can be concluded that the Cell_S2:P1:M1_10:90 hydrogels are cytocompatible with NHDF cells. These results were unexpected, as higher percentage of cellulose (Cell_S2:P1:M1) was anticipated to possess lower cytotoxicity effect. Nevertheless, both formulations presented higher cytocompatibility than diaper SAPs, proving that commercial diapers superabsorbent materials should be continuously studied and replaced by a more sustainable and biocompatible materials.

Chapter 5

Conclusion

5.1 Final Remarks

Absorbent hygiene products are vital for managing human fluids throughout different stages of life. As the global demand for these products continues to rise, especially in developed societies, their environmental impact has become a growing concern. Nowadays, most of these products are composed by synthetic polymers which present significant environmental and health challenges due to their limited biodegradability, potential cytotoxicity, and reliance on non-renewable resources. In this work, the development of cellulose-based hydrogels was performed for applications in personal care products. The main objective of the work has been reached: the production of cellulose-based hydrogels with enhanced properties, by taking advantage of cellulose biocompatibility, biodegradability, and hydrophilicity properties. Further, the most promising hydrogels considered were characterized and compared with SAPs isolated from diapers.

Several parameters influence hydrogels swelling properties that are crucial when designing SAPs, namely, crosslinking density, monomers ratio, and cellulose:monomers ratio. Also, the crosslinker, the drying method and preparation of hydrogels used for characterization purposes were observed to play an important role in these properties. BAAM and open air drying after solvent exchange for ethanol emerged as the most effective crosslinker agent and drying method, respectively, for the proposed application. For a detailed characterization, hydrogels were prepared in different forms to simulate real-life conditions, and it was observed that hydrogels handily-broken stroke a balance between maximum absorption capacity and faster swelling kinetics. Nevertheless, these results did not achieved higher swelling capacity compared to circular-shaped 2 cm cuted-hydrogels.

Cellulose-based hydrogels delivered promising results, in terms of swelling, thermal stability, biodegradability and biocompatibility. Regarding thermal properties, produced hydrogels showed lower residual weight at 600 °C and higher thermal stability, with T_{95} and T_{90} at higher temperatures, than absorbent material from diapers. The higher residual levels in diapers represent an environmental challenge in waste management and recycling.

Particularly, in swelling properties, Cell_S2:P1:M1_10:90 formulation showed greater holding capacity in synthetic urine than conventionally diapers SAPs. Concerning to free swelling capacity (in water, synthetic urine, pH 4, and pH 8) centrifuge retention capacity, and absorbance under load in synthetic urine the hydrogels produced did not outperformed diapers SAPs. Nonetheless, the results were considered promising, especially regarding FSC in synthetic urine, where the difference between Cell_S2:P1:M1_10:90 (14 g/g) and absorbent diapers material (20 g/g) was lower. Not to mention, hydrogels produced in this study outperformed other cellulose-based superabsorbent products already

reported, in terms of swelling properties.

Results from preliminary cytotoxicity tests confirmed Cell_S2:P1:M1_10:90 formulation as being biocompatible with cell viability greater than 75%, and for that reason it is considered non-cytotoxic by ISO 10993-5:1999. Meanwhile, diapers performed cell viability of less than 75% in the MTS assay, indicating potential concerns for skin compatibility and safety.

Optimizing the ratios used in hydrogels preparation led to an increase in swelling capacity to 102 g/g. However, achieving the desired balance between them and the provided properties of hydrogels will require more research and precise optimization. Also, the balance between biodegradability and industry benchmarks remains a challenge regarding practical and real applications, highlighting the need of continuous improvements. This dissertation presents valuable insights and contributions to the development and synthesis of cellulose-based hydrogels as well as the parameters that affect hydrogels properties and performance. Furthermore, represents an important step forward in the quest to replace petroleum-derived SAPs with environmentally friendly materials.

5.2 Future Work

Future research of cellulose-based hydrogel properties is needed. As this work has demonstrated, cellulose-based hydrogels show great promise in terms of biocompatibility and swelling properties. Additional cytotoxicity assays should be performed to confirm and validate the results of the biocompatibility of developed hydrogels. Further, alternative biodegradability tests should be performed to confirm the degradation of hydrogels over time.

It is recommended to improve performance in superabsorbent hydrogel formulations by exploring other cellulose derivatives like carboxymethyl cellulose and hydroxyethyl cellulose. Further studies about the use of BMEP as a crosslinking agent could be performed in order to enhance biodegradability, since studies have reported successful production of cellulose-based superabsorbent materials using this agent. Furthermore, incorporation of natural additives could also present a good alternative to achieve higher absorption capacities.

To overcome the structure damage on hydrogels and simulate real conditions, hydrogels can be prepared in emulsion, which results in a smaller particle size and improved structural integrity.

Finally, promising results from swelling tests in blood would extend the application of these hydrogels to feminine hygiene products and antimicrobial tests.

5.3 Work Limitations

Biodegradability and biocompatibility of hydrogels can be enhanced by cellulose. However, it reduces hydrogels swelling capacities and limits their ability to expand and absorb large quantities of fluids. Also, the optimization of hydrogels' properties presented challenges, regarding the balance between swelling capacity and gel fraction since the enhancement of one of these properties compromised the other, hindering the parameters optimization.

Bibliography

- [1] L. Arquillos *et al.*, “Edana sustainability report 2007-2008, absorbent hygiene products,” Accessed: 2023-12-11.
- [2] A. Bashari, A. Rohani, and M. Shakeri, “Cellulose-based hydrogels for personal care products,” *Polymers for Advanced Technologies*, vol. 29, 2018. DOI: <https://doi.org/10.1002/pat.4290>.
- [3] S. Wallmann *et al.*, “Edana - ahp waste to resource initiative report,” 2023, Accessed: 2023-12-11. [Online]. Available: <https://de.ramboll.com>.
- [4] M. Haque and M. Mondal, “Cellulose-based hydrogel for personal hygiene applications,” *Polymers and Polymeric Composites: A Reference Series*, M. Mondal, Ed., 2018. DOI: https://doi.org/10.1007/978-3-319-76573-0_44-1.
- [5] J. Patiño-Masó, F. Serra-Parareda, Q. Tarrés, P. Mutjé, F. X. Espinach, and M. Delgado-Aguilar, “Tempo-oxidized cellulose nanofibers: A potential bio-based superabsorbent for diaper production,” *Nanomaterials*, vol. 9, p. 1271, 2019, ISSN: 2079-677X. DOI: <https://doi.org/10.3390/nano9091271>.
- [6] S. M. F. Kabir, P. P. Sikdar, B. Haque, M. A. R. Bhuiyan, A. Ali, and M. N. Islam, “Cellulose-based hydrogel materials: Chemistry, properties and their prospective applications,” *Progress in Biomaterials*, vol. 7, no. 3, pp. 153–174, 2018, ISSN: 2090-0535. DOI: <https://doi.org/10.1007/s40204-018-0095-0>.
- [7] S. H. Zainal, N. H. Mohd, N. Suhaili, F. H. Anuar, A. M. Lazim, and R. Othaman, “Preparation of cellulose-based hydrogel: A review,” *Journal of Materials Research and Technology*, vol. 10, pp. 935–952, 2021. DOI: <https://doi.org/10.1016/j.jmrt.2020.12.012>.
- [8] P. D. Darbre, *Chapter 1 - Introduction to personal care products*, P. D. Darbre, Ed. Academic Press, 2023, pp. 3–31, ISBN: 978-0-323-99684-6. DOI: <https://doi.org/10.1016/B978-0-323-99684-6.00008-2>. [Online]. Available: <https://www.sciencedirect.com/science/article/pii/B9780323996846000082>.
- [9] M. Khalid and M. Abdollahi, “Environmental distribution of personal care products and their effects on human health,” *Iranian Journal of Pharmaceutical Research*, vol. 20, no. 1, pp. 216–253, 2021. DOI: <https://doi.org/10.22037/ijpr.2021.114891.15088>.
- [10] C. Lang *et al.*, “Personal care product use in pregnancy and the postpartum period: Implications for exposure assessment,” *International Journal of Environmental Research and Public Health*, vol. 13, p. 105, 2016. DOI: <https://doi.org/10.3390/ijerph13010105>.

- [11] M. Moreno-Lopez, F. Cordova-Buiza, C. Grillo Torres, and W. Auccahuasi, "Influencers and the purchase decision: A correlation in the personal care products sector," *European Conference on Innovation and Entrepreneurship*, vol. 18, pp. 651–659, 2023. DOI: <https://doi.org/10.34190/ecie.18.1.1352>.
- [12] J. Osuoha, B. Anyanwu, and C. Ejileugha, "Pharmaceuticals and personal care products as emerging contaminants: Need for combined treatment strategy," *Journal of Hazardous Materials Advances*, vol. 9, p. 100206, 2022. DOI: <https://doi.org/10.1016/j.hazadv.2022.100206>.
- [13] G. Carlucci, "New technologies for feminine hygiene products with reduced environmental impact," vol. 155, pp. 597–606, 2012. DOI: <https://doi.org/10.2495/SC120501>.
- [14] J. Bae, H. Kwon, and J. Kim, "Safety evaluation of absorbent hygiene pads: A review on assessment framework and test methods," *Sustainability*, vol. 10, no. 11, 2018, ISSN: 2071-1050. DOI: <https://doi.org/10.3390/su10114146>.
- [15] M. D. Onofrei and A. Filimon, "Cellulose-based hydrogels : Designing concepts , properties , and perspectives for biomedical and environmental applications," 2016.
- [16] W. Zhang *et al.*, "Factors affecting the properties of superabsorbent polymer hydrogels and methods to improve their performance: A review," *Journal of Materials Science*, vol. 56, pp. 1–20, 2021. DOI: <https://doi.org/10.1007/s10853-021-06306-1>.
- [17] X. Ma and G. Wen, "Development history and synthesis of super-absorbent polymers: A review," *Journal of Polymer Research*, vol. 27, 2020. DOI: <https://doi.org/10.1007/s10965-020-02097-2>.
- [18] F. L. Buchholz, "Superabsorbent polymers: An idea whose time has come," *Journal of Chemical Education*, vol. 73, no. 6, p. 512, 1996. DOI: <https://doi.org/10.1021/ed073p512>.
- [19] T.-C. Ho *et al.*, "Hydrogels: Properties and applications in biomedicine," *Molecules*, vol. 27, no. 9, 2022, ISSN: 1420-3049. DOI: <https://doi.org/10.3390/molecules27092902>.
- [20] S. Bashir *et al.*, "Fundamental concepts of hydrogels: Synthesis, properties, and their applications," *Polymers*, vol. 12, p. 2702, 2020. DOI: <https://doi.org/10.3390/polym12112702>.
- [21] F. Ullah, M. Othman, F. Javed, Z. Ahmad, and H. Md Akil, "Classification, processing and application of hydrogels: A review," *Materials Science & Engineering C: Materials for Biological Applications*, pp. 414–433, 2015. DOI: <https://doi.org/10.1016/j.msec.2015.07.053>.
- [22] G. Tang *et al.*, "Advances of naturally derived and synthetic hydrogels for intervertebral disk regeneration," *Frontiers in Bioengineering and Biotechnology*, vol. 8, 2020. DOI: <https://doi.org/10.3389/fbioe.2020.00745>.
- [23] M. Abdallah, "Development of hydrogels and study the effect of their mechanical properties on podocyte behaviors," Ph.D. dissertation, 2019.
- [24] H. Chamkouri, "A review of hydrogels, their properties and applications in medicine," *American Journal of Biomedical Sciences Research*, vol. 11, no. 6, pp. 485–493, 2021. DOI: <https://doi.org/10.34297/ajbsr.2021.11.001682>.
- [25] A. Jastram, T. Lindner, C. Luebbert, G. Sadowski, and U. Kragl, "Swelling and diffusion in polymerized ionic liquids-based hydrogels," *Polymers (Basel)*, vol. 13, no. 11, 2021. DOI: <https://doi.org/10.3390/polym13111834>.

- [26] L. Llanes, P. Dubessay, G. Pierre, C. Delattre, and P. Michaud, “Biosourced polysaccharide-based superabsorbents,” *Polysaccharides*, vol. 1, no. 1, pp. 51–79, 2020, ISSN: 2673-4176. DOI: <https://doi.org/10.3390/polysaccharides1010005>.
- [27] K. S. Anseth, C. N. Bowman, and L. Brannon-Peppas, “Mechanical properties of hydrogels and their experimental determination,” *Biomaterials*, vol. 17, no. 17, pp. 1647–1657, 1996, ISSN: 0142-9612. DOI: [https://doi.org/10.1016/0142-9612\(96\)87644-7](https://doi.org/10.1016/0142-9612(96)87644-7).
- [28] S. Mantha *et al.*, “Smart hydrogels in tissue engineering and regenerative medicine,” *Materials*, vol. 12, no. 20, 2019. DOI: <https://doi.org/10.3390/ma12203323>.
- [29] M. C. Catoira, L. Fusaro, D. Di Francesco, M. Ramella, and F. Boccafroschi, “Overview of natural hydrogels for regenerative medicine applications,” *Journal of Materials Science: Materials in Medicine*, vol. 30, no. 10, 2019. DOI: <https://doi.org/10.1007/s10856-019-6318-7>.
- [30] A. Sannino, C. Demitri, and M. Madaghiele, “Biodegradable cellulose-based hydrogels: Design and applications,” *Materials*, vol. 2, no. 2, pp. 353–373, 2009. DOI: <https://doi.org/10.3390/ma2020353>.
- [31] L. Zhao, Y. Zhou, J. Zhang, H. Liang, X. Chen, and H. Tan, “Natural polymer-based hydrogels: From polymer to biomedical applications,” *Pharmaceutics*, vol. 15, p. 2514, 2023. DOI: <https://doi.org/10.3390/pharmaceutics15102514>.
- [32] D. Jyoti and R. Sinha, “Physiological impact of personal care product constituents on non-target aquatic organisms,” *Science of the Total Environment*, vol. 905, 2023. DOI: <https://doi.org/10.1016/j.scitotenv.2023.167229>.
- [33] M. Ntekpe, E. Mbong, O. Mbong, E. Edem, N. Edem, and S. Hussain, “Disposable diapers: Impact of disposal methods on public health and the environment,” 2020.
- [34] A. Billon *et al.*, “Association of characteristics of tampon use with menstrual toxic shock syndrome in france,” *EClinicalMedicine*, vol. 21, 2020. DOI: <https://doi.org/10.1016/j.eclinm.2020.100308>.
- [35] J. Woo, S. Kim, H. Kim, K. S. Jeong, E. Kim, and E. Ha, “Systematic review on sanitary pads and female health,” *The Ewha Medical Journal*, vol. 42, p. 25, 2019. DOI: <https://doi.org/10.12771/emj.2019.42.3.25>.
- [36] J. Bender, J. Faergemann, and M. Sköld, “Skin health connected to the use of absorbent hygiene products: A review,” *Dermatology and Therapy*, vol. 7, pp. 319–330, 2017.
- [37] M. Velasco Perez, P. X. Sotelo Navarro, A. Vazquez Morillas, R. M. Espinosa Valdemar, and J. P. Hermoso Lopez Araiza, “Waste management and environmental impact of absorbent hygiene products: A review,” *Waste Management and Research*, vol. 39, no. 6, pp. 767–783, 2021. DOI: <https://doi.org/10.1177/0734242X20954271>.
- [38] F. Demichelis, C. Martina, D. Fino, T. Tommasi, and F. A. Deorsola, “Life cycle assessment of absorbent hygiene product waste: Evaluation and comparison of different end-of-life scenarios,” *Sustainable Production and Consumption*, vol. 38, pp. 356–371, 2023. DOI: <https://doi.org/10.1016/j.spc.2023.04.012>.
- [39] J. Plotka-Wasyłka *et al.*, “End-of-life management of single-use baby diapers: Analysis of technical, health and environment aspects,” *Science of The Total Environment*, vol. 836, p. 155 339, 2022, ISSN: 0048-9697. DOI: <https://doi.org/10.1016/j.scitotenv.2022.155339>.

- [40] K. Tsigkou *et al.*, “Used disposable nappies: Environmental burden or resource for biofuel production and material recovery?” *Resources, Conservation and Recycling*, vol. 185, p. 106493, 2022, ISSN: 0921-3449. DOI: <https://doi.org/10.1016/j.resconrec.2022.106493>.
- [41] M. J. Somers, J. F. Alfaro, and G. M. Lewis, “Feasibility of superabsorbent polymer recycling and reuse in disposable absorbent hygiene products,” *Journal of Cleaner Production*, vol. 313, p. 127686, 2021, ISSN: 0959-6526. DOI: <https://doi.org/10.1016/j.jclepro.2021.127686>.
- [42] S. Bhaladhare and D. Das, “Cellulose: A fascinating biopolymer for hydrogel synthesis,” *Journal of Materials Chemistry B*, vol. 10, 2022. DOI: <https://doi.org/10.1039/D1TB02848K>.
- [43] Y. Chen, H. Tang, Y. Liu, and H. Tan, “Preparation and study on the volume phase transition properties of novel carboxymethyl chitosan grafted polyampholyte superabsorbent polymers,” *Journal of the Taiwan Institute of Chemical Engineers*, vol. 59, pp. 569–577, 2016, ISSN: 1876-1070. DOI: <https://doi.org/10.1016/j.jtice.2015.09.011>.
- [44] J. S. Kim, D. H. Kim, and Y. S. Lee, “The influence of monomer composition and surface-crosslinking condition on biodegradation and gel strength of super absorbent polymer,” *Polymers*, vol. 13, no. 4, 2021, ISSN: 2073-4360.
- [45] L. Pérez-Álvarez, L. Ruiz-Rubio, E. Lizundia, and J. L. Vilas-Vilela, “Polysaccharide-based superabsorbents: Synthesis, properties, and applications,” in 2019, pp. 1393–1431. DOI: https://doi.org/10.1007/978-3-319-77830-3_46.
- [46] K. Guillén-Carvajal, B. Valdez-Salas, E. Beltrán-Partida, J. Salomón-Carlos, and N. Cheng, “Chitosan, gelatin, and collagen hydrogels for bone regeneration,” *Polymers*, vol. 15, 13 2023. DOI: <https://doi.org/10.3390/polym15132762>.
- [47] H. Zhang, D. Xu, Y. Zhang, M. Li, and R. Chai, “Silk fibroin hydrogels for biomedical applications,” *Smart Medicine*, vol. 1, 1 2022. DOI: <https://doi.org/10.1002/smmd.20220011>.
- [48] F. Abasalizadeh *et al.*, “Alginate-based hydrogels as drug delivery vehicles in cancer treatment and their applications in wound dressing and 3d bioprinting,” *Journal of Biological Engineering*, vol. 14, no. 1, 2020. DOI: <https://doi.org/10.1186/s13036-020-0227-7>.
- [49] M. Qamruzzaman, F. Ahmed, and M. I. H. Mondal, “An overview on starch-based sustainable hydrogels: Potential applications and aspects,” *Journal of Polymers and the Environment*, vol. 30, no. 1, pp. 19–50, 2022. DOI: <https://doi.org/10.1007/s10924-021-02180-9>.
- [50] R. Yegappan, V. Selvaprithiviraj, S. Amirthalingam, and R. Jayakumar, “Carrageenan based hydrogels for drug delivery, tissue engineering and wound healing,” *Carbohydrate Polymers*, vol. 198, pp. 385–400, 2018. DOI: <https://doi.org/10.1016/j.carbpol.2018.06.086>.
- [51] D. Klemm, B. Heublein, H. P. Fink, and A. Bohn, “Cellulose: Fascinating biopolymer and sustainable raw material,” *Angewandte Chemie - International Edition*, vol. 44, no. 22, pp. 3358–3393, 2005. DOI: <https://doi.org/10.1002/anie.200460587>.
- [52] R. Estela and J. Luis, “Hydrolysis of biomass mediated by cellulases for the production of sugars,” in *Sustainable Degradation of Lignocellulosic Biomass - Techniques, Applications and Commercialization*. InTech, 2013. DOI: <https://doi.org/10.5772/53719>.
- [53] T. Aziz *et al.*, “A review on the modification of cellulose and its applications,” *Polymers*, vol. 14, no. 15, p. 3206, 2022. DOI: <https://doi.org/10.3390/polym14153206>.

- [54] P. K. Gupta *et al.*, “An update on overview of cellulose, its structure and applications,” in *Cellulose*. InTechOpen, 2019. DOI: <https://doi.org/10.5772/intechopen.84727>.
- [55] S. Magalhães *et al.*, “Eco-friendly methods for extraction and modification of cellulose: An overview,” *Polymers*, vol. 15, no. 14, p. 3138, 2023. DOI: <https://doi.org/10.3390/polym15143138>.
- [56] M. O. Haque and M. I. H. Mondal, “Synthesis and characterization of cellulose-based eco-friendly hydrogels,” *Rajshahi University Journal of Science and Engineering*, vol. 44, pp. 45–53, 2016. DOI: <https://doi.org/10.3329/rujse.v44i0.30386>.
- [57] S. Gopi, P. Balakrishnan, D. Chandradhara, D. Poovathankandy, and S. Thomas, “General scenarios of cellulose and its use in the biomedical field,” *Materials Today Chemistry*, vol. 13, pp. 59–78, 2019, ISSN: 2468-5194. DOI: <https://doi.org/10.1016/j.mtchem.2019.04.012>.
- [58] D. E. Ciolacu and D. M. Suflet, *11 - Cellulose-Based Hydrogels for Medical/Pharmaceutical Applications*, V. Popa and I. Volf, Eds. Elsevier, 2018, pp. 401–439, ISBN: 978-0-444-63774-1. DOI: <https://doi.org/10.1016/B978-0-444-63774-1.00011-9>.
- [59] J. George and S. N., “Cellulose nanocrystals: Synthesis, functional properties, and applications,” *Nanotechnology, Science and Applications*, vol. 8, p. 45, 2015. DOI: <https://doi.org/10.2147/NSA.S64386>.
- [60] S.-Y. Park, J. O. Baker, M. E. Himmel, *et al.*, “Cellulose crystallinity index: Measurement techniques and their impact on interpreting cellulase performance,” *Biotechnology and Biofuels*, vol. 3, no. 10, 2010. DOI: <https://doi.org/10.1186/1754-6834-3-10>.
- [61] A. K. Singh, P. Itkor, and Y. S. Lee, “State-of-the-art insights and potential applications of cellulose-based hydrogels in food packaging: Advances towards sustainable trends,” *Gels*, vol. 9, no. 6, 2023, ISSN: 2310-2861.
- [62] J. Shuai and X. Wang, “Novel solvent systems for cellulose dissolution,” *BioResources*, vol. 16, no. 2, pp. 2192–2195, 2021. DOI: <https://doi.org/10.15376/biores.16.2.2192-2195>.
- [63] H. Jia and T. Michinobu, “Cellulose-based conductive gels and their applications,” *ChemNanoMat*, vol. 9, no. 5, e202300020, 2023. DOI: <https://doi.org/10.1002/cnma.202300020>. eprint: <https://aces.onlinelibrary.wiley.com/doi/pdf/10.1002/cnma.202300020>.
- [64] P. Zou *et al.*, “Advances in cellulose-based hydrogels for biomedical engineering: A review summary,” *Gels*, vol. 8, p. 364, 2022. DOI: <https://doi.org/10.3390/gels8060364>.
- [65] Q. Zhang *et al.*, “Adsorptivity of cationic cellulose nanocrystals for phosphate and its application in hyperphosphatemia therapy,” *Carbohydrate Polymers*, vol. 255, p. 117 335, 2020. DOI: <https://doi.org/10.1016/j.carbpol.2020.117335>.
- [66] M. M. Fiume *et al.*, “Safety assessment of nitrocellulose and collodion as used in cosmetics,” *International Journal of Toxicology*, vol. 35, 50S–59S, 2016, ISSN: 1091-5818. DOI: <https://doi.org/10.1177/1091581816651607>.
- [67] E. N. Bifari, S. B. Khan, K. A. Alamry, A. M. Asiri, and K. Akhtar, “Cellulose acetate based nanocomposites for biomedical applications: A review,” *Current Pharmaceutical Design*, vol. 22, no. 20, pp. 3007–3019, 2016, ISSN: 1381-6128. DOI: <https://doi.org/10.2174/13816128226661603161600>.

- [68] Y. Cheng, H. Qin, N. C. Acevedo, and X. Shi, "Development of methylcellulose-based sustained-release dosage by semisolid extrusion additive manufacturing in drug delivery system," *Journal of Biomedical Materials Research. Part B, Applied biomaterials*, vol. 109, no. 2, pp. 257–268, 2021, ISSN: 1091-5818. DOI: <https://doi.org/10.1002/jbm.b.34697>.
- [69] D. E. Ciolacu, R. Nicu, and F. Ciolacu, "Cellulose-based hydrogels as sustained drug-delivery systems," *Materials*, vol. 13, no. 22, pp. 1–37, 2020, ISSN: 2090-6756. DOI: <https://doi.org/10.3390/ma13225270>.
- [70] D. Wu, J. Cheng, X. Su, and Y. Feng, "Hydrophilic modification of methylcellulose to obtain thermoviscosifying polymers without macro-phase separation," *Carbohydrate Polymers*, vol. 260, 2021, ISSN: 0144-8617. DOI: <https://doi.org/10.1016/j.carbpol.2021.117792>.
- [71] S. Javanbakht and A. Shaabani, "Carboxymethyl cellulose-based oral delivery systems," *International Journal of Biological Macromolecules*, vol. 133, pp. 21–29, 2019, ISSN: 1097-0248. DOI: <https://doi.org/10.1016/j.ijbiomac.2019.04.079>.
- [72] P. D. Sawant, D. Luu, R. Ye, and R. M. Buchta, "Drug release from hydroethanolic gels. effect of drug's lipophilicity (logp), polymer-drug interactions and solvent lipophilicity," *International journal of pharmaceutics*, vol. 396, no. 1-2, pp. 45–52, 2010. DOI: <https://doi.org/10.1016/j.ijpharm.2010.06.008>.
- [73] G. A. Burdock, "Safety assessment of hydroxypropyl methylcellulose as a food ingredient," *Food and Chemical Toxicology*, vol. 45, no. 12, pp. 2341–2351, 2007, ISSN: 0278-6915. DOI: <https://doi.org/10.1016/j.fct.2007.07.011>.
- [74] S. J. Ban, C. W. Rico, I. C. Um, and M. Y. Kang, "Antihyperglycemic and antioxidative effects of hydroxyethyl methylcellulose (hemc) and hydroxypropyl methylcellulose (hpmc) in mice fed with a high fat diet," *International Journal of Molecular Sciences*, vol. 13, no. 3, pp. 3738–3750, 2012. DOI: <https://doi.org/10.3390/ijms13033738>.
- [75] F. H. A.-E. Kader, G. Said, M. M. El-Naggar, and B. A. Anees, "Characterization and electrical properties of methyl-2-hydroxyethyl cellulose doped with erbium nitrate salt," *Journal of Applied Polymer Science*, vol. 102, no. 3, pp. 2352–2361, 2006, ISSN: 1097-4628. DOI: <https://doi.org/10.1002/app.24482>.
- [76] W. Hu, Z. Wang, Y. Xiao, S. Zhang, and J. Wang, "Advances in crosslinking strategies of biomedical hydrogels," *Biomaterials Science*, vol. 7, no. 3, pp. 843–855, 2019, ISSN: 2050-4317. DOI: <https://doi.org/10.1039/c8bm01246f>.
- [77] A. Berradi, F. Aziz, M. E. Achaby, N. Ouazzani, and L. Mandi, "A comprehensive review of polysaccharide-based hydrogels as promising biomaterials," *Polymers*, vol. 15, no. 13, 2023, ISSN: 2073-4360. DOI: <https://doi.org/10.3390/polym15132908>.
- [78] B. R. Estevam, I. D. Perez, Â. M. Moraes, and L. V. Fregolente, "A review of the strategies used to produce different networks in cellulose-based hydrogels," *Materials Today Chemistry*, vol. 34, p. 101 803, 2023, ISSN: 2468-5194. DOI: <https://doi.org/10.1016/j.mtchem.2023.101803>.
- [79] M. Akter *et al.*, "Cellulose-based hydrogels for wastewater treatment: A concise review," *Gels*, vol. 7, no. 1, 2021, ISSN: 2310-2861. DOI: <https://doi.org/10.3390/gels7010030>.

- [80] R. Kundu, P. Mahada, B. Chhirang, and B. Das, "Cellulose hydrogels: Green and sustainable soft biomaterials," *Current Research in Green and Sustainable Chemistry*, vol. 5, p. 100252, 2022, ISSN: 2666-0865. DOI: <https://doi.org/10.1016/j.crgsc.2021.100252>.
- [81] N. Kayra and A. Aytakin, "Synthesis of cellulose-based hydrogels: Preparation, formation, mixture, and modification," in 2018, pp. 1–28, ISBN: 978-3-319-76573-0. DOI: https://doi.org/10.1007/978-3-319-76573-0_16-1.
- [82] M. A. Qureshi, N. Nishat, S. Jadoun, and M. Z. Ansari, "Polysaccharide based superabsorbent hydrogels and their methods of synthesis: A review," *Carbohydrate Polymer Technologies and Applications*, vol. 1, p. 100014, 2020, ISSN: 2666-8939. DOI: <https://doi.org/10.1016/j.carpta.2020.100014>.
- [83] C. Chang and L. Zhang, "Cellulose-based hydrogels: Present status and application prospects," *Carbohydrate Polymers*, vol. 84, no. 1, pp. 40–53, 2011, ISSN: 0144-8617. DOI: <https://doi.org/10.1016/j.carbpol.2010.12.023>.
- [84] R. Rebelo, B. Báguena, P. Pereira, R. Moreira, J. Coelho, and A. Serra, "Biocompatible cellulose-based superabsorbents for personal care products," *Journal of Polymers and the Environment*, pp. 1–16, 2024. DOI: <https://doi.org/10.1007/s10924-024-03315-4>.
- [85] R. Moreira, R. Rebelo, J. Coelho, and A. Serra, "Novel thermally regenerated flexible cellulose-based films," *European Journal of Wood and Wood Products*, pp. 1–14, 2024. DOI: <https://doi.org/10.1007/s00107-024-02126-7>.
- [86] A. Lourenço, J. Gamelas, T. Nunes, J. Amaral, P. Mutjé, and P. Ferreira, "Influence of tempoxidised cellulose nanofibrils on the properties of filler-containing papers," *Cellulose*, vol. 24, 2017. DOI: <https://doi.org/10.1007/s10570-016-1121-9>.
- [87] H. Qi, L. Zhang, Y. Zhou, N. Li, K. Fu, and Z. He, "Effects of temperature and molecular weight on dissolution of cellulose in NaOH/Urea aqueous solution," *Journal of Polymer Science Part B: Polymer Physics*, vol. 47, no. 2, pp. 161–170, 2009. DOI: <https://doi.org/10.1002/polb.21579>.
- [88] H. Qi, T. Liebert, and T. Heinze, "Homogenous synthesis of 3-allyloxy-2-hydroxypropyl-cellulose in naoh/urea aqueous system," *Cellulose*, vol. 19, no. 3, pp. 925–932, 2012. DOI: <https://doi.org/10.1007/s10570-012-9687-3>.
- [89] T. Fekete, J. Borsa, E. Takács, and L. Wojnarovits, "Synthesis and characterization of superabsorbent hydrogels based on hydroxyethylcellulose and acrylic acid," *Carbohydrate Polymers*, vol. 166, 2017. DOI: <https://doi.org/10.1016/j.carbpol.2017.02.108>.
- [90] E. Fu, S. Zhang, Y. Luan, Y. Zhang, S. Saghir, and Z. Xiao, "Novel superabsorbent polymer composites based on -cellulose and modified zeolite: Synthesis, characterization, water absorbency and water retention capacity," *Cellulose*, vol. 29, pp. 1–11, 2022. DOI: <https://doi.org/10.1007/s10570-021-04380-x>.
- [91] AAT Bioquest, *Aat bioquest*, Accessed: 2024-08-28, 2024. [Online]. Available: <https://www.aatbio.com/index.html>.
- [92] Y. Bachra, A. Grouli, F. Damiri, A. Bennamara, and M. Berrada, "A new approach for assessing the absorption of disposable baby diapers and superabsorbent polymers: A comparative study," *Results in Materials*, vol. , Volume 8, 2020. DOI: <https://doi.org/10.1016/j.rinma.2020.100156>.

- [93] R. Tong *et al.*, “Highly stretchable and compressible cellulose ionic hydrogels for flexible strain sensors,” *Biomacromolecules*, vol. 20, 2019. DOI: <https://doi.org/10.1021/acs.biomac.9b00322>.
- [94] E. Halligan *et al.*, “Synthesis and characterisation of hydrogels based on poly (n-vinylcaprolactam) with diethylene glycol diacrylate,” *Gels*, vol. 9, no. 6, 2023, ISSN: 2310-2861.
- [95] L. Nikolić, A. Zdravkovic, V. Nikolić, and S. Ilic-Stojanovic, “Synthetic hydrogels and their impact on health and environment,” in 2019, pp. 1363–1391, ISBN: 978-3-319-77829-7. DOI: https://doi.org/10.1007/978-3-319-77830-3_61.
- [96] A. Mallik *et al.*, “Benefits of renewable hydrogels over acrylate- and acrylamide-based hydrogels,” in 2019, pp. 197–243, ISBN: 978-3-319-77829-7. DOI: https://doi.org/10.1007/978-3-319-77830-3_10.
- [97] G. Sennakesavan, M. Mostakhdemin, L. Dkhar, A. Seyfoddin, and F. S.J., “Acrylic acid/acrylamide based hydrogels and its properties - a review,” *Polymer Degradation and Stability*, vol. 180, p. 109 308, 2020. DOI: <https://doi.org/10.1016/j.polyimdegradstab.2020.109308>.
- [98] F. Beland, P. Mellick, G. Olson, M. Mendoza, M. Marques, and D. Doerge, “Carcinogenicity of acrylamide in b6c3f(1) mice and f344/n rats from a 2-year drinking water exposure,” *Food and chemical toxicology : an international journal published for the British Industrial Biological Research Association*, vol. 51C, pp. 149–159, 2012. DOI: <https://doi.org/10.1016/j.fct.2012.09.017>.
- [99] P. Mohammadzadeh Pakdel and S. J. Peighambaroust, “A review on acrylic based hydrogels and their applications in wastewater treatment,” *Journal of environmental management*, vol. 217, pp. 123–143, 2018. DOI: <https://doi.org/10.1016/j.jenvman.2018.03.076>.
- [100] D. R. Barleany, R. Lestari, M. Yulvianti, T. Susanto, Shalina, and Erizal, “Acrylic acid neutralization for enhancing the production of grafted chitosan superabsorbent hydrogel,” *International Journal on Advanced Science, Engineering and Information Technology*, vol. 7, pp. 702–708, 2017.
- [101] Y. Situ, Y. Yang, C. Huang, S. Liang, X. Mao, and X. Chen, “Effects of several superabsorbent polymers on soil exchangeable cations and crop growth,” *Environmental Technology and Innovation*, vol. 30, p. 103 126, 2023, ISSN: 2352-1864. DOI: <https://doi.org/10.1016/j.eti.2023.103126>.
- [102] T. C. Industry, <https://www.tcichemicals.com/IN/en/p/A0139>, Accessed: 2024-09-01.
- [103] T. C. Industry, <https://www.tcichemicals.com/IN/en/p/A0141>, Accessed: 2024-09-01.
- [104] T. C. Industry, <https://www.tcichemicals.com/IN/en/p/P2276>, Accessed: 2024-09-01.
- [105] M. Biomedicals, <https://www.mpbio.com/eu/n-n-methylene-bis-acrylamide>, Accessed: 2024-09-01.
- [106] S. Alla, M. Sen, and A. W. El-Naggar, “Swelling and mechanical properties of superabsorbent hydrogels based on tara gum/acrylic acid synthesized by gamma radiation,” *Carbohydrate Polymers*, vol. 89, pp. 478–485, 2012. DOI: <https://doi.org/10.1016/j.carbpol.2012.03.031>.

- [107] T. Fekete, J. Borsa, E. Takács, and L. Wojnarovits, “Synthesis of cellulose-based superabsorbent hydrogels by high-energy irradiation in the presence of crosslinking agent,” *Radiation Physics and Chemistry*, vol. 118, 2015. DOI: <https://doi.org/10.1016/j.radphyschem.2015.02.023>.
- [108] W. Bankeeree, C. Samathayanon, S. Prasongsuk, P. Lotrakul, and S. Kiatkamjornwong, “Rapid degradation of superabsorbent poly(potassium acrylate) and its acrylamide copolymer via thermo-oxidation by hydrogen peroxide,” *Journal of Polymers and the Environment*, vol. 29, 2021. DOI: <https://doi.org/10.1007/s10924-021-02167-6>.
- [109] Z. Li *et al.*, “The effect of crosslinking degree of hydrogels on hydrogel adhesion,” *Gels*, vol. 8, p. 682, 2022. DOI: <https://doi.org/10.3390/gels8100682>.
- [110] Q. Wu *et al.*, “Multiple active sites cellulose-based adsorbent for the removal of low-level cu(ii), pb(ii) and cr(vi) via multiple cooperative mechanisms,” *Carbohydrate Polymers*, vol. 233, p. 115 860, 2020, ISSN: 0144-8617. DOI: <https://doi.org/10.1016/j.carbpol.2020.115860>.
- [111] K. Nalampang, N. Suebsanit, and R. Molloy, “Design and preparation of amps-based hydrogels for biomedical use as wound dressings,” vol. 34, 2006.
- [112] A. Goncalves, “Synthesis and characterization of high performance superabsorbent hydrogels using bis[2-(methacryloyloxy)ethyl] phosphate as crosslinker,” *Express Polymer Letters*, vol. 10, pp. 248–258, 2015. DOI: <https://doi.org/10.3144/expresspolymlett.2016.23>.
- [113] H.-Q. Mao, I. Kadiyala, Z. Zhao, W. Dang, A. Brown, and K. Leong, “Biodegradable poly(terephthalate-co-phosphate)s: Synthesis, characterization and drug-release properties,” *Journal of biomaterials science. Polymer edition*, vol. 16, pp. 135–61, 2005. DOI: <https://doi.org/10.1163/1568562053115426>.
- [114] W. Commons, *File:2-acrylamido-2-methylpropane sulfonic acid.png*, https://commons.wikimedia.org/wiki/File:2-Acrylamido-2-methylpropane_sulfonic_acid.png, Accessed: 2024-09-01, 2024.
- [115] TCI Chemicals, Accessed: 2024-09-01, 2024. [Online]. Available: <https://www.tcichemicals.com/BE/en/p/M1158>.
- [116] Sigma-Aldrich, *Product 695890*, Accessed: 2024-09-01, 2024. [Online]. Available: <https://www.sigmaaldrich.com/PT/en/product/aldrich/695890>.
- [117] Sigma-Aldrich, <https://www.sigmaaldrich.com/PT/en/product/aldrich/496758>, Accessed: 2024-09-01, 2024.
- [118] “Development of di-methacrylate quaternary ammonium monomers with antibacterial activity,” *Acta Biomaterialia*, vol. 129, pp. 138–147, 2021, ISSN: 1742-7061. DOI: <https://doi.org/10.1016/j.actbio.2021.05.012>.
- [119] Sigma-Aldrich, Accessed: 2024-09-01, 2024. [Online]. Available: <https://www.sigmaaldrich.com/PT/en/product/aldrich/408107>.
- [120] C. Ninciuleanu *et al.*, “The effects of monomer, crosslinking agent, and filler concentrations on the viscoelastic and swelling properties of poly(methacrylic acid) hydrogels: A comparison,” *Materials*, vol. 14, p. 2305, 2021. DOI: <https://doi.org/10.3390/ma14092305>.

- [121] C. Abreu, T. Rezende, A. Serra, A. Fonseca, R. Braslau, and J. Coelho, “Convenient and industrially viable internal plasticization of poly(vinyl chloride): Copolymerization of vinyl chloride and commercial monomers,” *Polymer*, vol. 267, p. 125 688, 2023. DOI: <https://doi.org/10.1016/j.polymer.2023.125688>.
- [122] M. P. Illa, C. Sharma, and M. Khandelwal, “Tuning the physiochemical properties of bacterial cellulose: Effect of drying conditions,” *Journal of Materials Science*, vol. 54, 2019. DOI: <https://doi.org/10.1007/s10853-019-03737-9>.
- [123] W. Mo, K. Chen, X. Yang, F. Kong, J. Liu, and B. Li, “Elucidating the hornification mechanism of cellulosic fibers during the process of thermal drying,” *Carbohydrate Polymers*, vol. 289, p. 119 434, 2022. DOI: <https://doi.org/10.1016/j.carbpol.2022.119434>.
- [124] M. Hashemzahi, B. Sjostrand, H. Håkansson, and G. Henriksson, “Degrees of hornification in softwood and hardwood kraft pulp during drying from different solvents,” *Cellulose*, vol. 31, 2024. DOI: <https://doi.org/10.1007/s10570-023-05657-z>.
- [125] A. Chan and T. Chan, “Methanol as an unlisted ingredient in supposedly alcohol-based hand rub can pose serious health risk,” *International Journal of Environmental Research and Public Health*, vol. 15, p. 1440, 2018. DOI: <https://doi.org/10.3390/ijerph15071440>.
- [126] S. C. Chua *et al.*, “Microwave radiation-induced grafting of 2-methacryloyloxyethyl trimethyl ammonium chloride onto lentil extract (le-g-dmc) as an emerging high-performance plant-based grafted coagulant,” *Scientific Reports*, vol. 10, p. 3959, 2020. DOI: <https://doi.org/10.1038/s41598-020-60119-x>.
- [127] B. Hussein, Z. Saad, I. N. Safi, and A. Saad, “Impact of phosphate ester addition on the cytotoxicity of heat cured denture base material,” *Materials Today: Proceedings*, vol. 42, 2021. DOI: <https://doi.org/10.1016/j.matpr.2020.12.254>.
- [128] T. Mai *et al.*, “Anionic polymer brushes for biomimetic calcium phosphate mineralization—a surface with application potential in biomaterials,” *Polymers*, vol. 10, no. 10, 2018, ISSN: 2073-4360. DOI: <https://doi.org/10.3390/polym10101165>. [Online]. Available: <https://www.mdpi.com/2073-4360/10/10/1165>.
- [129] L. Yeng, M. U. Wahit, and N. Othman, “Thermal and flexural properties of regenerated cellulose(rc)/poly(3-hydroxybutyrate)(phb)biocomposites,” *Jurnal Teknologi*, vol. 75, 2015. DOI: <https://doi.org/10.11113/jt.v75.5338>.
- [130] A. for Toxic Substances and D. R. (US), *Toxicological Profile for Acrylamide*. Atlanta (GA): Agency for Toxic Substances and Disease Registry (US), 2012, Accessed: 2024-09-13. [Online]. Available: <https://www.ncbi.nlm.nih.gov/books/NBK591431/>.
- [131] N. C. for Biotechnology Information (NCBI), *Acrylic acid*, <https://pubchem.ncbi.nlm.nih.gov/compound/Acrylic-acid>, Accessed: 2024-09-13, 2023.
- [132] J. Liu, Q. Li, Y. Su, Q. Yue, B. Gao, and R. Wang, “Synthesis of wheat straw cellulose-g-poly (potassium acrylate)/pva semi-ipns superabsorbent resin,” *Carbohydrate polymers*, vol. 94, pp. 539–46, 2013. DOI: <https://doi.org/10.1016/j.carbpol.2013.01.089>.
- [133] B. Zhao, H. Jiang, Z. Lin, S. Xu, J. Xie, and A. Zhang, “Preparation of acrylamide/acrylic acid cellulose hydrogels for the adsorption of heavy metal ions,” *Carbohydrate Polymers*, vol. 224, p. 115 022, 2019. DOI: <https://doi.org/10.1016/j.carbpol.2019.115022>.

- [134] M. Wiśniewska *et al.*, “Nanostructure of poly(acrylic acid) adsorption layer on the surface of activated carbon obtained from residue after supercritical extraction of hops,” *Nanoscale research letters*, vol. 12, p. 2, 2017. DOI: <https://doi.org/10.1186/s11671-016-1772-3>.
- [135] N. Shukla, R. Bhagat, and G. Madras, “Photo and thermal degradation of a cationic superabsorbent polymer,” *Polymer-Plastics Technology and Engineering*, vol. 52, 2013. DOI: <https://doi.org/10.1080/03602559.2012.719171>.
- [136] A. Hofman, M. Pedone, and M. Kamperman, “Protected poly(3-sulfopropyl methacrylate) copolymers: Synthesis, stability, and orthogonal deprotection,” *ACS Polymers Au*, 2021. DOI: <https://doi.org/10.1021/acspolymersau.1c00044>.
- [137] J. Simerville, W. Maxted, and J. Pahira, “Urinalysis: A comprehensive review,” *American family physician*, vol. 71, pp. 1153–62, 2005.
- [138] D. Ahmad, M. E. Wasli, C. Tan, Z. Musa, and S. Chin, “Eco-friendly cellulose-based hydrogels derived from wastepapers as a controlled-release fertilizer,” *Chemical and Biological Technologies in Agriculture*, vol. 10, 2023. DOI: <https://doi.org/10.1186/s40538-023-00407-6>.
- [139] C. Lacoste, J.-M. Lopez-Cuesta, and A. Bergeret, “Development of a biobased superabsorbent polymer from recycled cellulose for diapers applications,” *European Polymer Journal*, vol. 116, 2019. DOI: <https://doi.org/10.1016/j.eurpolymj.2019.03.013>.
- [140] Y. Bachra, A. Grouli, F. Damiri, X. Zhu, M. Talbi, and M. Berrada, “Synthesis, characterization, and swelling properties of a new highly absorbent hydrogel based on carboxymethyl guar gum reinforced with bentonite and silica particles for disposable hygiene products,” *ACS Omega*, vol. 7, pp. 39 002–39 018, 2022. DOI: <https://doi.org/10.1021/acsomega.2c04744>.
- [141] G. Reshma, R. R. S. Nair, and D. Menon, “Superabsorbent sodium carboxymethyl cellulose membranes based on a new cross-linker combination for female sanitary napkin applications,” *Carbohydrate Polymers*, vol. 248, p. 116 763, 2020. DOI: <https://doi.org/10.1016/j.carbpol.2020.116763>.
- [142] M. Nur Alam, M. S. Islam, and L. Christopher, “Sustainable production of cellulose-based hydrogels with superb absorbing potential in physiological saline,” *ACS Omega*, vol. 4, pp. 9419–9426, 2019. DOI: <https://doi.org/10.1021/acsomega.9b00651>.
- [143] S. Yadav, M. P. Illa, T. Rastogi, and C. Sharma, “High absorbency cellulose acetate electrospun nanofibers for feminine hygiene application,” *Applied Materials Today*, vol. 4, pp. 62–70, 2016. DOI: <https://doi.org/10.1016/j.apmt.2016.07.002>.
- [144] M.-T. Luo *et al.*, “Bacterial cellulose based superabsorbent production: A promising example for high value-added utilization of clay and biology resources,” *Carbohydrate Polymers*, vol. 208, 2018. DOI: <https://doi.org/10.1016/j.carbpol.2018.12.084>.
- [145] T. Adjuik, S. Nokes, and M. Montross, “Biodegradability of bio-based and synthetic hydrogels as sustainable soil amendments: A review,” *Journal of Applied Polymer Science*, vol. 140, 2023. DOI: <https://doi.org/10.1002/app.53655>.

Appendices

Appendix A

Method of Preparation of Hydrogels

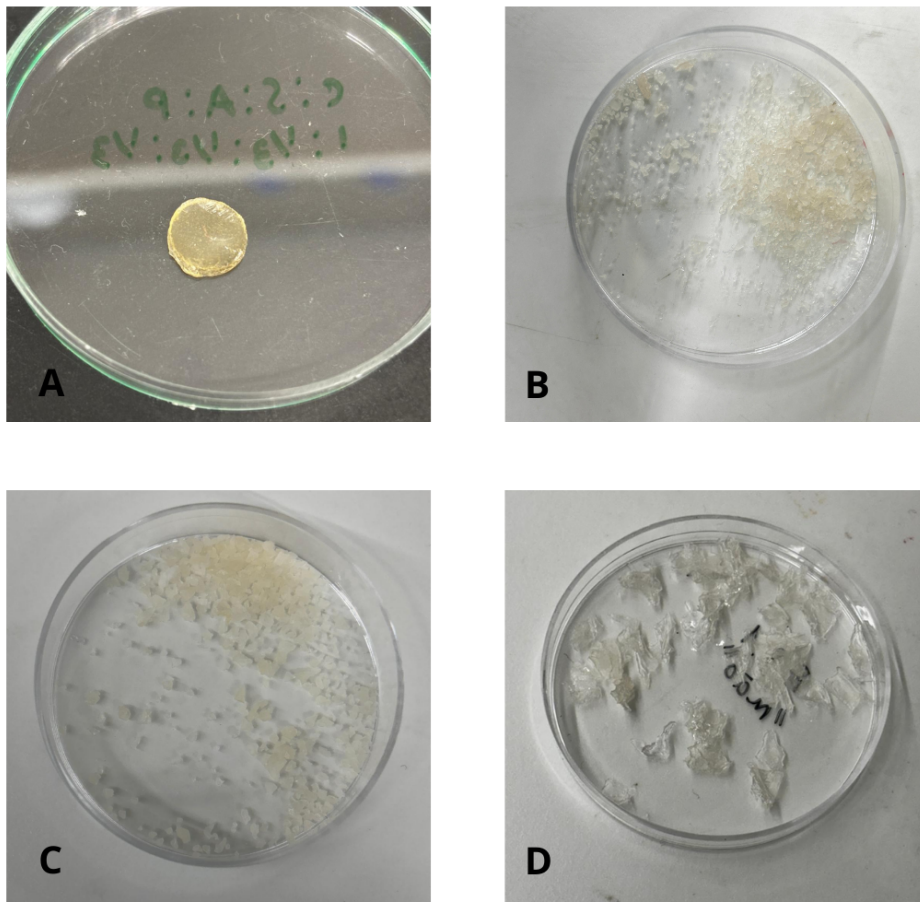


Figure A.1: Various hydrogel preparation methods for characterization purposes included: (a) cutting hydrogels into 20 mm diameter discs, (b) cryogenically fracturing the hydrogels, (c) grinding the hydrogels using a coffee grinder, and (d) manually breaking the hydrogels into coarse pieces.

Appendix B

Determination of Degree of Substitution

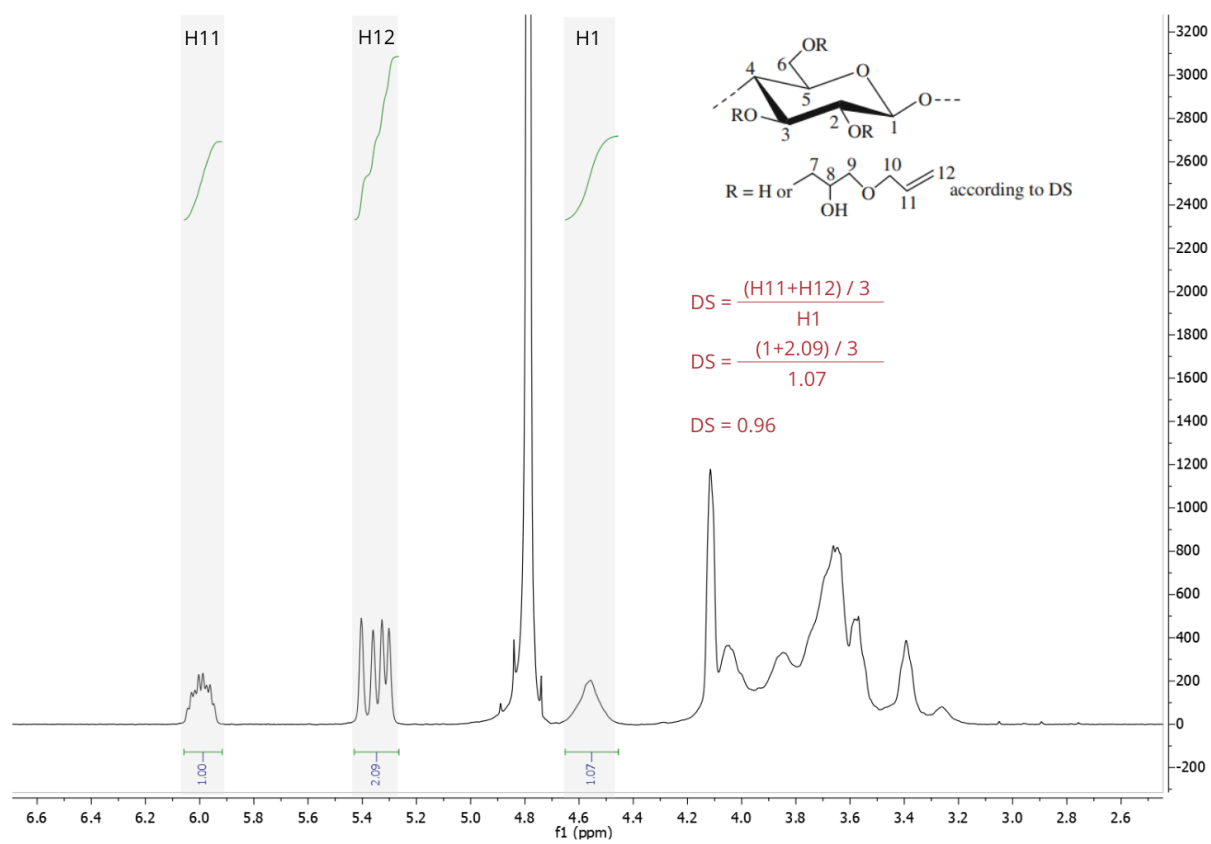


Figure B.1: Determination of degree of substitution through ^1H NMR method. Spectra of cellulose derivative prepared with 4 equivalents of AGE is used in this example.